INFORMATION TO USERS

This was produced from a copy of a document sent to us for microfilming. While the most advanced technological means to photograph and reproduce this document have been used, the quality is heavily dependent upon the quality of the material submitted.

The following explanation of techniques is provided to help you understand markings or notations which may appear on this reproduction.

1. The sign or "target" for pages apparently lacking from the document photographed is "Missing Page(s)". If it was possible to obtain the missing page(s) or section, they are spliced into the film along with adjacent pages. This may have necessitated cutting through an image and duplicating adjacent pages to assure you of complete continuity.

2. When an image on the film is obliterated with a round black mark it is an indication that the film inspector noticed either blurred copy because of movement during exposure, or duplicate copy. Unless we meant to delete copyrighted materials that should not have been filmed, you will find a good image of the page in the adjacent frame.

3. When a map, drawing or chart, etc., is part of the material being photographed the photographer has followed a definite method in "sectioning" the material. It is customary to begin filming at the upper left hand corner of a large sheet and to continue from left to right in equal sections with small overlaps. If necessary, sectioning is continued again—beginning below the first row and continuing on until complete.

4. For any illustrations that cannot be reproduced satisfactorily by xerography, photographic prints can be purchased at additional cost and tipped into your xerographic copy. Requests can be made to our Dissertations Customer Services Department.

5. Some pages in any document may have indistinct print. In all cases we have filmed the best available copy.

University
Microfilms
International

300 N. ZEEB ROAD, ANN ARBOR, MI 48106
18 BEDFORD ROW, LONDON WC1R 4EJ, ENGLAND

Downloaded from SHAREOK. Persistent Handle URL: https://hdl.handle.net/11244/4798

8101517

MARSH, HENRY ANTHONY, JR.

ELECTROCHEMICAL AND ENZYMATIC INVESTIGATIONS OF SOME BIOLOGICALLY IMPORTANT PURINES

The University of Oklahoma PH.D. 1980

University
Microfilms
International 300 N. Zeeb Road, Ann Arbor, MI 48106

PLEASE NOTE:

In all cases this material has been filmed in the best possible way from the available copy. Problems encountered with this document have been identified here with a check mark ✓.

1. Glossy photographs _____
2. Colored illustrations _____
3. Photographs with dark background _____
4. Illustrations are poor copy ✓
5. Print shows through as there is text on both sides of page _____
6. Indistinct, broken or small print on several pages _____
7. Tightly bound copy with print lost in spine _____
8. Computer printout pages with indistinct print _____
9. Page(s) _____ lacking when material received, and not available from school or author
10. Page(s) _____ seem to be missing in numbering only as text follows
11. Poor carbon copy _____
12. Not original copy, several pages with blurred type _____
13. Appendix pages are poor copy _____
14. Original copy with light type _____
15. Curling and wrinkled pages _____
16. Other _____

University Microfilms International

300 N. ZEEB RD., ANN ARBOR, MI 48106 (313) 761-4700

THE UNIVERSITY OF OKLAHOMA

GRADUATE COLLEGE

ELECTROCHEMICAL AND ENZYMATIC INVESTIGATIONS OF SOME BIOLOGICALLY IMPORTANT PURINES

A DISSERTATION

SUBMITTED TO THE GRADUATE FACULTY

in partial fulfillment of the requirements for the

degree of

DOCTOR OF PHILOSOPHY

By

Henry A. Marsh, Jr.

Norman, Oklahoma

1980

ELECTROCHEMICAL AND ENZYMATIC INVESTIGATIONS

OF SOME BIOLOGICALLY IMPORTANT PURINES

APPROVED BY

DISSERTATION COMMITTEE

ACKNOWLEDGEMENTS

Thanks go to Dr. Glenn Dryhurst for his scientific expertise, the suggesting of the problems studied herein, and his financial support in the form of research assistantships.

Financial assistance from the University of Oklahoma Chemistry Department in the form of teaching assistantships is gratefully acknowledged.

Special thanks go to James L. Owens for his patience in teaching me much of the art of electrochemistry. It must also be acknowledged that the work presented in Chapter 2 was performed jointly with Mr. Owens, and except for the double potential step work which is solely my own, the work in Chapter 2 belongs as much to Mr. Owens as to myself. Similar special thanks go to Michael T. Cleary for playing devil's advocate and serving as sounding board and advisor through much of my career here.

My appreciation also goes out for the friendship I found among the postdoc's and graduate students in Dr. Dryhurst's lab, especially to Arnold Conway, Deniz Ege-Serpkenci, and Lionel Karber.

My thanks to Dr. Eddie Carol Smith for his suggestions during initial attempts to study enzymatic reaction.

It is not possible to adequately thank the marvelous staff in the Department, but I do thank them, and especially Fred Dillon for

his patient and excellent repair work.

My thanks to Ms. Nancy Nielsen for her beautiful typing job.

I wish to thank my parents, Mr. & Mrs. Henry A. Marsh, for their loving support and encouragement throughout my academic career.

Finally, I would like to thank my wife, Patty, for her sacrifices, her understanding, and most of all her belief in me when I lacked belief in myself.

TABLE OF CONTENTS

Page

LIST OF TABLES vii

LIST OF ILLUSTRATIONS viii

Chapter

1. INTRODUCTION 1

2. ELECTROCHEMICAL OXIDATION OF URIC ACID AND XANTHINE

Introduction 11

Results 12

Discussion 35

Experimental 37

Summary 41

3. ENZYMATIC OXIDATION OF URIC ACID

Introduction 43

Results 43

Discussion 55

Experimental 57

Summary 60

4. ENZYMATIC AND ELECTROCHEMICAL OXIDATION OF GUANOSINE

Introduction 61

Results 61

Discussion 151

TABLE OF CONTENTS (continued)

Chapter		Page
	Experimental	153
	Summary	159
5.	REFERENCES	160

LIST OF TABLES

Table		Page
1.	Apparent first-order rate constants from double potential step chronoamperometry of uric acid	28
2.	Experimental n-values for electrochemical oxidation of uric acid and xanthine in a thin-layer cell at a gold minigrid electrode	29
3.	Observed first-order rate constants for reaction of the u.v.-absorbing intermediate formed on electrochemical oxidation of uric acid at gold minigrid electrode	34
4.	Observed first-order rate constants for reaction of the u.v.-absorbing intermediate formed on electrochemical oxidation of uric acid at a gold minigrid electrode	48
5.	Observed first-order rate constants for reaction of the u.v.-absorbing intermediate formed on oxidation of uric acid in the presence of type VIII peroxidase and H_2O_2 at pH 4.0 followed by pH adjustment	54
6.	Peak current ratios for electrooxidation peaks III_a, IV_a, and V_a of 0.5 m$\underline{M}$ guanosine at pH 7	69
7.	Peak current ratios for electrooxidation peaks I_a and II_a of 0.5 m$\underline{M}$ 8-hydroxyguanosine at pH 7	75
8.	Coulometric n-values of guanosine at pH 7	81
9.	Coulometric n-values of 8-hydroxyguanosine at pH 7	83
10.	Observed first-order rate constants for the electrochemical oxidation of guanosine and 8-hydroxyguanosine . . .	102
11.	Observed first-order rate constants for the enzymic oxidation of 8-hydroxyguanosine	106

LIST OF ILLUSTRATIONS

Figure		Page
1.	Cyclic voltammograms of 1 mM uric acid in pH 7.0 phosphate buffer at (A) RPGE, (B) SPGE, (C) gold foil electrode, and (D) RPGE, solution saturated with allopurinol	14
2.	Cyclic voltammograms of 1 mM uric acid in pH 7.0 phosphate buffer at a series of spectroscopic graphite electrodes . .	17
3.	Cyclic voltammograms of 1 mM xanthine in pH 7.0 phosphate buffer at a series of PGE and spectroscopic graphite electrodes	19
4.	Cyclic voltammograms of 1 mM uric acid pH 4-9 at (A) RPGE .	21
	(B) SPGE .	22
5.	Idealized double potential step chronoamperogram	23
6.	Experimental double potential step chronoamperometric R_I vs. T_F plot for 3 mM uric acid at pH 8	25
7.	Double potential step chronoamperometric R_I vs. $T_F/t_{1/2}$ plot for uric acid	27
8.	Spectrum of 10 mM uric acid solution electrolyzing at 0.9 V in phosphate buffer pH 7.0 at a gold minigrid electrode in a thin-layer cell	30
9.	(A) Variation of absorbance with time and (B) Kinetic plot of time versus log absorbance at 320 nm during electrooxidation of uric acid at pH 7 at a gold minigrid electrode	33
10.	Rapid scan spectrophotometry of uric acid in the presence of type VIII peroxidase and hydrogen peroxide	44
11.	Thin-layer spectroelectrochemical oxidation of uric acid at a gold minigrid electrode	45
12.	Rapid scan spectrophotometry of the u.v.-absorbing intermediate formed upon oxidation of uric acid with type VIII peroxidase and hydrogen peroxide	50

LIST OF ILLUSTRATIONS (continued)

Figure		Page
13.	Comparison of the spectrum of the u.v.-absorbing intermediates formed upon electrochemical and enzymatic oxidation of uric acid	52
14.	(A) Variation of absorbance with time and (B) Kinetic plot of time vs. log absorbance at 302 nm during enzymatic oxidation of uric acid by type VIII peroxidase and hydrogen peroxide	53
15.	Cyclic voltammogram of 0.5 mM guanosine in pH 7 phosphate buffer at a PGE	63
16.	Plot of peak current vs. concentration for guanosine at pH 7 and 5 mV sec^{-1} sweep rate	64
17.	Linear sweep voltammogram of 3 mM guanosine in pH 7 phosphate buffer at a rate of 5 mV sec^{-1}	66
18.	Plot of peak current function vs. $V^{1/2}$ for 0.5 mM guanosine in pH 7 phosphate buffer	67
19.	Cyclic voltammogram of 0.5 mM guanosine in pH 7 phosphate buffer at a sweep rate of 5 V sec^{-1}	68
20.	Cyclic voltammogram of 0.5 mM 8-hydroxyguanosine in pH 7 phosphate buffer at a PGE	71
21.	Cyclic voltammogram of a 0.5 mM 8-hydroxyguanosine solution at pH 7 and 200 mV sec^{-1} sweep rate	72
22.	Plot of peak current vs. concentration for 8-hydroxyguanosine in pH 7 phosphate buffer at a sweep rate of 5 mV sec^{-1}	73
23.	Linear sweep voltammogram of 0.25 mM 8-hydroxyguanosine solution at pH 7 and a sweep rate of 200 mV sec^{-1}	74
24.	Plot of peak current function vs. $V^{1/2}$ for 0.5 mM 8-hydroxyguanosine in pH 7 phosphate buffer	76
25.	Cyclic voltammograms of 0.5 mM 8-hydroxyguanosine in pH 7 phosphate buffer at sweep rates of 0.5 V sec^{-1} and 5.0 V sec^{-1}	77
26.	Liquid chromatogram of the products from the oxidation of a pH 7, 0.8 mM guanosine solution at 1.15 V (peak V_a)	84

LIST OF ILLUSTRATIONS (continued)

Figure — Page

27. Liquid chromatogram of the products from the oxidation of a pH 7, 0.8 mM guanosine solution at 0.96 V (peak IV_a) . . . 86

28. Liquid chromatogram of the products from the oxidation of a pH 7, 0.84 mM 8-hydroxyguanosine solution at 0.5 V (peak II_a) 87

29. Liquid chromatogram of the products from the oxidation of a pH 7, 0.84 mM 8-hydroxyguanosine solution at 1.0 V (peak III_a) 88

30. Liquid chromatogram of the products from the oxidation of a pH 7, 0.84 mM 8-hydroxyguanosine solution at 1.15 V (peak V_a of guanosine) 89

31. Spectrum of 1.0 mM guanosine solution in pH 7 phosphate buffer in a thin-layer cell with a RVC working electrode oxidized at 1.2 V until curve 2 92

32. Spectrum of 1.0 mM guanosine solution electrolyzing at 1.2 V in pH 7 phosphate buffer in a thin-layer cell 94

33. Spectrum of 1.0 mM 8-hydroxyguanosine solution in pH 7 phosphate buffer in a thin-layer cell electrolyzed at 0.7 V until curve 2 95

34. Spectrum of 1.0 mM 8-hydroxyguanosine solution electrolyzing at 0.7 V in pH 7 phosphate buffer in a thin-layer cell . . . 97

35. (A) Plot of absorbance vs. time (B) plot of time vs. log absorbance for fast and slow step (C) plot of time vs. log absorbance during electrooxidation of guanosine at pH 7 . . 99

36. (A) Plot of absorbance vs. time (B) plot of time vs. log absorbance for fast and slow step (C) plot of time vs. log absorbance for fast step during electrooxidation of 8-hydroxyguanosine at pH 7 101

37. Spectrum of 8-hydroxyguanosine at pH 7 being oxidized by the presence of hydrogen peroxide and type VIII peroxidase 104

38. (A) Plot of absorbance vs. time (B) plot of time vs. log absorbance for fast and slow step (C) time vs. log absorbance for fast step during enzymic oxidation of 8-hydroxyguanosine 107

LIST OF ILLUSTRATIONS (continued)

Figure Page

39. Cyclic voltammogram of 8-hydroxyguanosine during enzymic oxidation 109

40. Liquid chromatogram of the products from the oxidation at 1.15 V of a pH 7, 0.8 mM guanosine solution utilizing a coupled G-10, QAE A-25 system with H_2O eluant 110

41. Liquid chromatogram of products from the electrooxidation of a pH 7, 0.8 mM guanosine solution at 1.15 V (peak V_a) utilizing two G-10 columns with H_2O eluant 114

42. Liquid chromatogram of the material eluted under peak 3 of figure 41 utilizing two G-10 columns and H_2O as eluant . 116

43. Gas chromatogram of the silylated material eluted under peak 3 of figure 41 117

44. Mass spectrum of material appearing at 30.25 min in figure 43 118

45. Mass spectrum of material appearing at 23.15 min in figure 43 119

46. Liquid chromatogram of the products from the electro-oxidation at 1.15 V (peak V_a) of a pH 7, 0.8 mM guanosine utilizing two G-10 colums with H_2O eluant 122

47. Liquid chromatogram of the products from the electro-oxidation at 1.0 V (peak III_a) of a pH 7, 0.84 mM 8-hydroxyguanosine utilizing a G-10 column with 0.005 M pH 7 phosphate buffer as the eluant 124

48. Gas chromatogram of the material eluted under L.C. peaks 2, 3, and 4 of figure 47, after silylation 125

49. Mass spectrum of material occurring at 24.73 min in figure 48 126

50. Mass spectrum of material occurring at 25.45 min in figure 48 127

51. Mass spectrum of material eluting at 25.90 min in figure 48 128

52. Mass spectrum of material eluting at 26.25 min in figure 48 129

LIST OF ILLUSTRATIONS (continued)

Figure		Page
53.	Mass spectrum of authentic silylated d-ribose	130
54.	Mass spectrum of material eluting at 38.07 min in figure 48	131
55.	Mass spectrum of material eluting at 39.85 min in figure 48	133
56.	Gas chromatogram of the material eluting under L.C. peak 5 of figure 47, after silylation	134
57.	Liquid chromatogram of the products obtained from the oxidation of a pH 7, 0.84 mM 8-hydroxyguanosine solution at 1.0 V (peak III_a) utilizing a 35 cm G-10 column with H_2O eluant	135
58.	Gas chromatogram of the material eluting under L.C. peaks 5, 6, and 7 in figure 57, after silylation	137
59.	Mass spectrum of material eluting at 28.03 min in figure 58	138
60.	Gas chromatogram of the silylated material of thin-layer sample number three (TL #3)	140
61.	Mass spectrum of material eluting at 42.17 min in figure 60	141
62.	Mass spectrum of authentic silylated 8-hydroxyguanosine . .	142
63.	Mass spectrum of material eluting at 38.9 min in figure 60	143
64.	Gas chromatogram for the silylated material of TL #10 . . .	145
65.	Mass spectrum of material eluting at 39.38 min in figure 64	146
66.	Mass spectrum of material eluting at 40.73 min in the G.C. of silylated TL #13	148
67.	Mass spectrum of material eluting at 39.9 min in the G.C. of silylated TL #22'	149
68.	Mass spectrum of material eluting at 39.18 min in the G.C. of silylated TL #33	150

ELECTROCHEMICAL AND ENZYMATIC INVESTIGATIONS OF SOME BIOLOGICALLY IMPORTANT PURINES

CHAPTER 1

INTRODUCTION

Purines are a nearly ubiquitous component of biological systems. They occur in natural products such as human urine, blood, human and animal milk, cerebral spinal fluid, guano and other sources. They are commonly found as constituents of high molecular weight nucleic acids, although they are occasionally found as free bases. A number of purines, such as uric acid, xanthine, and hypoxanthine, were first discovered in animal tissues, body fluids, or excrement.[1-3]

Purine (I) was first named by Emil Fischer,[4] and he devised

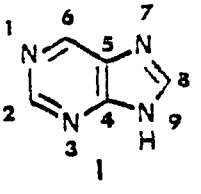

I

the numbering system most widely employed today.[5] The carbohydrate derivative in which the purine is linked to a sugar moiety through its N-9 position is called a nucleoside. Phosphate esters of the nucleo-

sides are known as nucleotides. The tri-phosphate adenine nucleotide (ATP) can hydrolyze with removal of a single molecule of phosphoric acid which causes a relatively large decrease in free energy. Purine nucleotides can form polymeric structures with pyrimidine nucleotides called nucleic acids. The nucleic acids are involved in protein synthesis, and the storage and transfer of genetic information.

Purines are nitrogen heterocyclic compounds having delocalized or mobile (π) electrons. The presence of delocalized (π) electrons makes these compounds good candidates for electrochemical study of their electron transfer reactions. Electrochemical studies can be utilized to determine the number of electrons involved in the electron transfer step, to detect intermediates formed after the electron transfer, mechanistic data, and much other useful information.[6,7]

Electrochemical techniques can be very useful in the study of biological systems. There are a number of similarities between enzymic and electrochemical reactions which make electrochemical studies appealing since parameters such as pH, temperature, buffer system, etc. can be varied much more readily in electrochemical studies than in <u>in vivo</u> studies. Some of the similarities are that both may occur at similar temperatures, both can occur at similar pH, both can occur in similar ionic strengths of an inert electrolyte, both may involve heterogeneous electron transfer process, and in both cases the molecule must be oriented in some specific manner for the electron transfer to take place.

Until recently a number of factors restricted the utility of electrochemical techniques in the study of oxidation processes of

biological molecules. One factor was the complexity of the oxidation processes as compared to the reduction processes for the same molecule, particularly in aqueous media. Several studies of purine reduction processes were performed in the 1930's and 1940's.[8-10] Although it was not until 1962 that Smith and Elving reported really thorough studies of some purine reduction processes.[11] Probably the greatest hindrance to oxidation studies of biological molecules was the lack of a suitable electrode. Metal electrodes suffer a range of problems from hydrogen sorption to poor potential limits (Adams has prepared a very useful description of several solid electrode materials[12]). Carbon electrodes are generally the most useful since they typically have large potential ranges in both the positive and negative direction.

In this study pyrolytic graphite electrodes (PGE)[13,14] will be the electrodes used, unless otherwise stated, since they have excellent potential limits[12,15] and are easily constructed.[16,17]

The usefulness of electrochemical studies can be seen by comparing electrochemical oxidations to various other oxidation processes such as enzymic and photochemical oxidations. The work in the present study is concerned mostly with three biologically significant purines: uric acid, xanthine, and guanosine. Accordingly, the following review will focus on these compounds.

The oxidation of uric acid in the presence of the enzyme uricase has been studied by several groups.[18,19] They reported two electrons are involved in the electron transfer step. They proposed that the attack occurred at the C4=C5 position resulting in a short-lived intermediate which they suggested was a carbonium ion. The

intermediate was proposed to be involved in further chemical reactions ultimately giving rise to allantoin.

The oxidation of uric acid by a number of peroxidase enzymes has also been investigated by several groups.[20-23] These studies revealed allantoin as the major product around neutral pH, and alloxan as the major product at low pH. In each case it was proposed that some unstable intermediate was the initial product and this intermediate species went on to form the observed products. Paul and Avi-Dor[22] suggested that the intermediate might be uric acid diimine (II) or

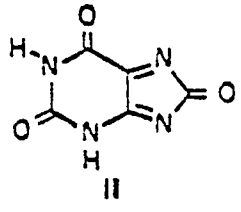

II

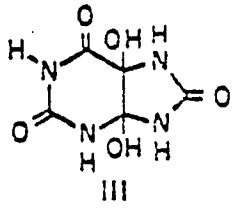

III

uric acid-4,5-diol (III). Similar results have been reported in other studies of the enzymic oxidation of uric acid.[24,25]

Only a few studies involving the photochemical or radiochemical oxidations of uric acid have been reported.[26-32] In these studies attack of the C4=C5 double bond to form a C-4 or C-5 hydroxy or hydroperoxide intermediate is proposed. Similar results were obtained for the photo- and radiochemical oxidations of xanthine.

Although there were some early investigations of the electrochemical oxidation of uric acid,[33,34] it was not until Struck and Elving's report[35] that the electrooxidation process was studied thoroughly. Struck and Elving proposed a scheme in which uric acid was oxidized

in a two electron process to an unstable dicarbonium ion (IV) which then reacts chemically to form the final products. Later though,

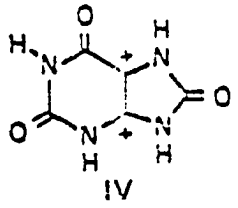

IV

a number of objections to this scheme were outlined by Dryhurst.[36,37] Electrochemical data indicates that protons are involved in the electron transfer step in the oxidation of uric acid, but Struck and Elving's scheme does not account for this. If a carbonium ion is formed it would seem more likely that the positive charge would be localized on surrounding nitrogen atoms instead of at C-4 and C-5 (IV). Finally, Struck and Elving suggested that at the potential where uric acid is oxidized to IV; that IV was further oxidized to parabanic acid. The likely hood of a dicarbonium ion readily giving up two more electrons seems remote.

Therefore, Dryhurst performed further electrooxidation studies on uric acid utilizing the PGE.[38] Equation 1 is the reaction scheme resulting from Dryhurst's investigations.[38,39] Uric acid (I, equation 1) is proposed to be electrooxidized in an initial $2\underline{e}$, $2H^+$ reaction to form an unstable uric acid diimine (II, equation 1). The diimine undergoes a two-step hydrolysis reaction to form uric acid imine alcohol (III, equation 1), and then uric acid-4,5-diol (IV). The diol species

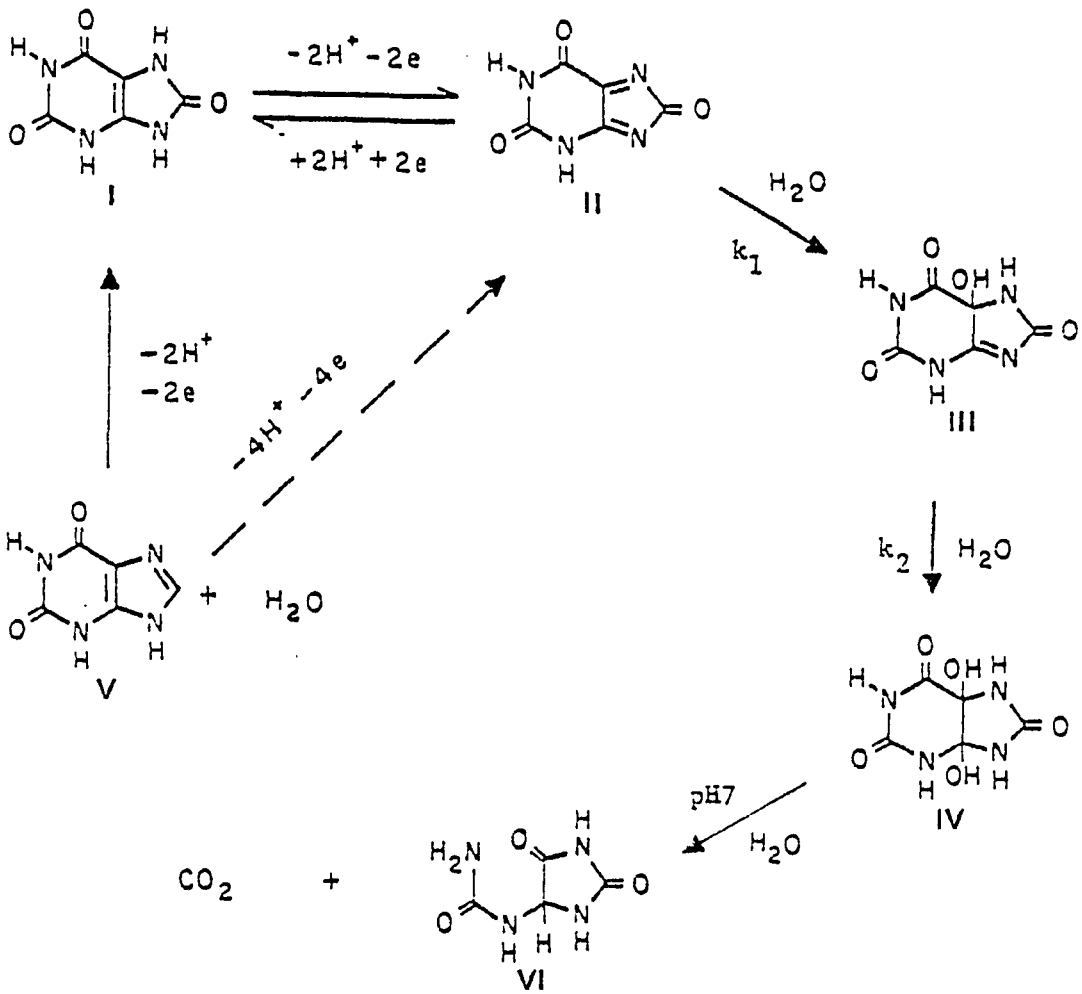

then decomposes to the ultimate products (allantoin around neutral pH or alloxan and urea at low pH).

Various electrochemical studies[38,39,40] have indicated the diimine is electroreducible and unstable. Other molecules having an imine bond such as methyl ketimine, thiamine, and pyridoxine are electroreducible.[41-48] Riboflavin which has a diimine structure very similar to the proposed intermediate is reduced at a potential of

-0.35 V in 1 N KCl. These studies have also suggested that the hydration of the diimine to the imine alcohol is relatively fast and the hydration of the imine alcohol to the diol relatively slow.

Xanthine (V, equation 1) is oxidized at the PGE *via* a single oxidation peak which occurs at a potential more positive than that of uric acid. Overall the oxidation is a $4\underline{e}/4H^+$ process, however, it has been proposed that the oxidation of xanthine proceeds via two $2\underline{e}/2H^+$ steps. The first step which is the oxidation to uric acid is the potential controlling reaction, and then uric acid is immediately oxidized to the diimine species (II, equation 1). The diimine then undergoes the same reactions proposed in equation 1 for uric acid. This view is supported by the fact that electrooxidation of xanthine gives the same products in approximately the same yields as the electrooxidation of uric acid.[36,40] It is further supported by the presence of a couple in the voltammetry at potentials matching those of uric acid (which appears only after xanthine has been oxidized).

Obviously then, there are several correlations between the electrochemical, photochemical, and biological oxidations of uric acid. Most workers have proposed an attack at the C4=C5 double bond. The most commonly proposed intermediates are unstable hydroxy or hydroperoxide intermediates. The products of the various oxidations are very similar. In the case of electrooxidation *versus* enzymic oxidation the effect of pH, the final products, and the yields are intriguingly similar. Thus, it would seem plausible that reaction schemes developed from electrochemical oxidation studies of biologically important purines might serve as a useful guide to interpreting enzymic oxidation

reactions.

The oxidation of guanosine has not been extensively studied under any conditions. Under photodynamic conditions Simon and Van Vanukis[49] found that guanosine reacts quite rapidly. In fact among disubstituted purines guanosine reacted the most rapidly.

Guanosine is electrochemically oxidized in aqueous solution at the pyrolytic graphite electrode (PGE) by way of four voltammetric oxidation peaks.[17] However, no products have been reported or reaction schemes proposed. Since little information is available concerning guanosine itself, it might be useful to look at the behavior of the parent compound guanine.[38] Guanine is oxidized *via* a single well-defined oxidation peak which occurs at potentials more negative than any of guanosine's four peaks. Equation 2 presents the reaction scheme proposed for the oxidation of guanine. It is proposed to be oxidized in an initial $2\underline{e}/2H^+$ process to 8-hydroxyguanine. 8-Hydroxyguanine should be much more easily oxidized than guanine so it is immediately further oxidized in a second $2\underline{e}/2H^+$ process to a diimine species. Thus, it has been proposed that guanine is oxidized in a $4\underline{e}/4H^+$ process resulting in a diimine species, a process analogous to the oxidation of xanthine. The diimine then undergoes a series of chemical reactions to yield carbon dioxide, guanidine (VIII), oxalyl-guanidine (V), and 2-oxy-4,5-dihydrooximidazole (VI). The 2-oxy-4,5-dihydroxyimidazole (VI) is then oxidized in a $2\underline{e}/2H^+$ process to give parabanic acid (IX). Close to 4.7 electrons are transferred during oxidation of guanine

1 M HOAc, which accounts for the four electrons involved in the primary electron-transfer process plus the extra electrons required

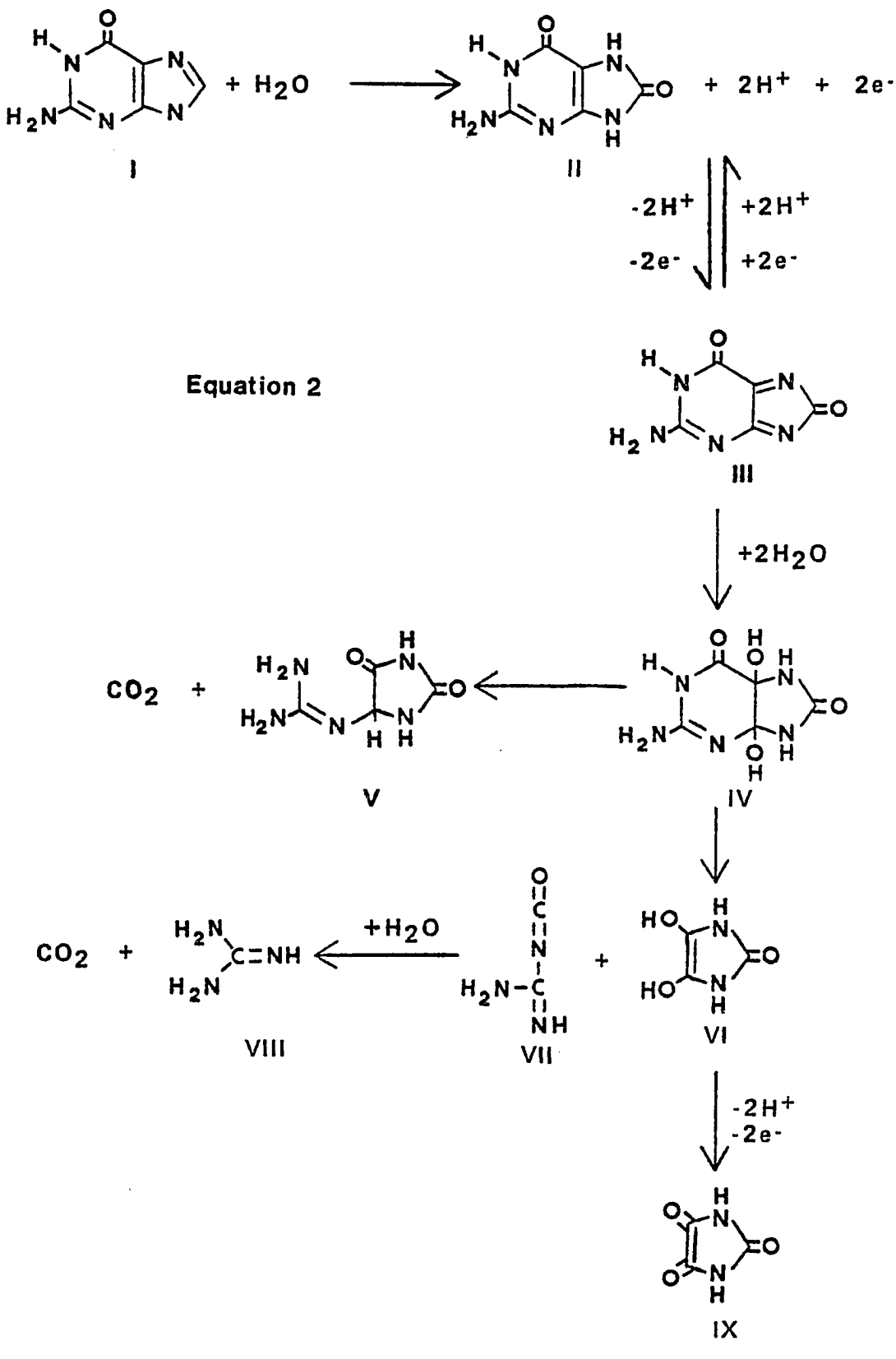
+ H2O
+ 2H+ + 2e-
I
II
-2H+
-2e-
+2H+
+2e-
Equation 2
III
+2H2O
CO2 +
V
IV
CO2 +
+H2O
VIII
VII
VI
-2H+
-2e-
IX

to oxidize 2-oxy-4,5-dihydroxyiidazole (VI) to parabanic acid (IX).

One should not expect guanosine to behave in exactly the same manner as guanine. However, knowledge of the reaction scheme of guanine does provide some useful guidelines for the investigation of guanosine.

The studies presented in the chapters to follow were undertaken with the overall goal of increasing our understanding of the oxidation of biologically important purines. Specifically, it was hoped to more clearly confirm the formation of the diimine and other intermediate species in the electrochemical and enzymatic oxidation of uric acid and xanthine. Further the same techniques were to be applied to a thorough study of the nucleoside guanosine.

ELECTROCHEMICAL OXIDATION OF URIC ACID AND XANTHINE AN INVESTIGATION BY CYCLIC VOLTAMMETRY, DOUBLE POTENTIAL STEP CHRONOAMPEROMETRY, AND THIN-LAYER SPECTROELECTROCHEMISTRY

CHAPTER 2

INTRODUCTION

In order to develop further experimental evidence for the reaction scheme proposed for the electrochemical oxidation of uric acid and xanthine in equation 1 of Chapter 1 it was decided to utilize the techniques of double potential step chronoamperometry and thin-layer spectroelectrochemistry. These two techniques had previously been successfully applied to the study of 5,6-diaminouracid (I).[50,51]

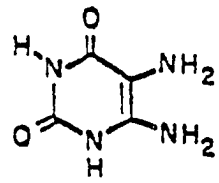

I

5,6-Diaminouracil is electrochemically oxidized in a $2\underline{e}/2H^+$ reaction to a diimine which undergoes a two-step hydrolysis to alloxan and ammonia in a process quite similar to that proposed for uric acid. Of particular interest was the fact that an unstable intermediate could be clearly observed by thin-layer spectroelectrochemistry.

It was hoped that by utilizing double potential step chronoamperometry it would be possible to demonstrate the formation of a diimine species (II, equation 1, Chapter 1) and to study the kinetics of its decay. Through the use of thin-layer spectroelectrochemical studies it was planned to observe and characterize the behavior of the proposed imine-alcohol species (III, equation 1, Chapter 1). In the course of these studies some additional cyclic voltammetry studies were performed.

RESULTS

Voltammetry of Uric Acid and Xanthine at Carbon and Gold Electrodes

Linear scan voltammetry utilizes a linearly changing d.c. voltage ramp applied to a working electrode. Simultaneous with the voltage scan the current at the working electrode is monitored. Cyclic voltammetry employs a triangular wave-form voltage applied to the electrode and again the current is recorded as a function of applied potential. Since voltammetry is performed at a stationary electrode in a quiet solution and the time interval between reverse sweeps is relatively short, the products of an oxidation are still in the vicinity of the electrode surface and thus, available for reduction on the

negative-going segment of the voltage sweep. Cyclic voltammetry can thus provide information on the reversibility of the electron transfer process. In addition, cyclic voltammetry is used for qualitative evaluation of electrode processes such as follow-up chemical reactions, or generation of intermediates, etc.

From earlier voltammetric studies of uric acid and xanthine[36] it is known that uric acid is oxidized at the PGE via a single $2e/2H^+$ process. The relationship between peak potential (E_p) and pH is given by the equation E_p = (0.76-0.069 pH)V from pH 1-12 at 5 mV sec^{-1} sweep rate. Figure 1A presents a voltammogram of uric acid in pH 7 phosphate buffer at a sweep rate of 200 mV sec^{-1} obtained using a rough PGE (RPGE, see Experimental). As noted in Chapter 1 prior studies[36] have proposed that peak I_a in the voltammetry of uric acid is the 2e oxidation of uric acid to uric acid diimine. Electroreduction peak I_c is the quasi-reversible reduction of the diimine to urid acid, and peak II_c is due to the reduction of the imine-alcohol (see equation 1, Chapter 1).

When using a smooth PGE (SPGE, see Experimental) peak I_c is not apparent at a sweep rate of 200 mV sec^{-1} (see figure 1B). At the SPGE peak I_c is not readily observable until sweep rates $\geq$1 V sec^{-1} are utilized. When a gold foil electrode is employed oxidation peak I_a is well defined (see figure 1C), but peak I_c is not present. In fact, peak I_c could not be observed at the gold foil electrode until sweep rates $\geq$20 V sec^{-1} were employed.

It appears from the discussion above that the roughness of the electrode surface has a pronounced effect on the height of the diimine reduction peak I_c. Previous work has indicated that at the

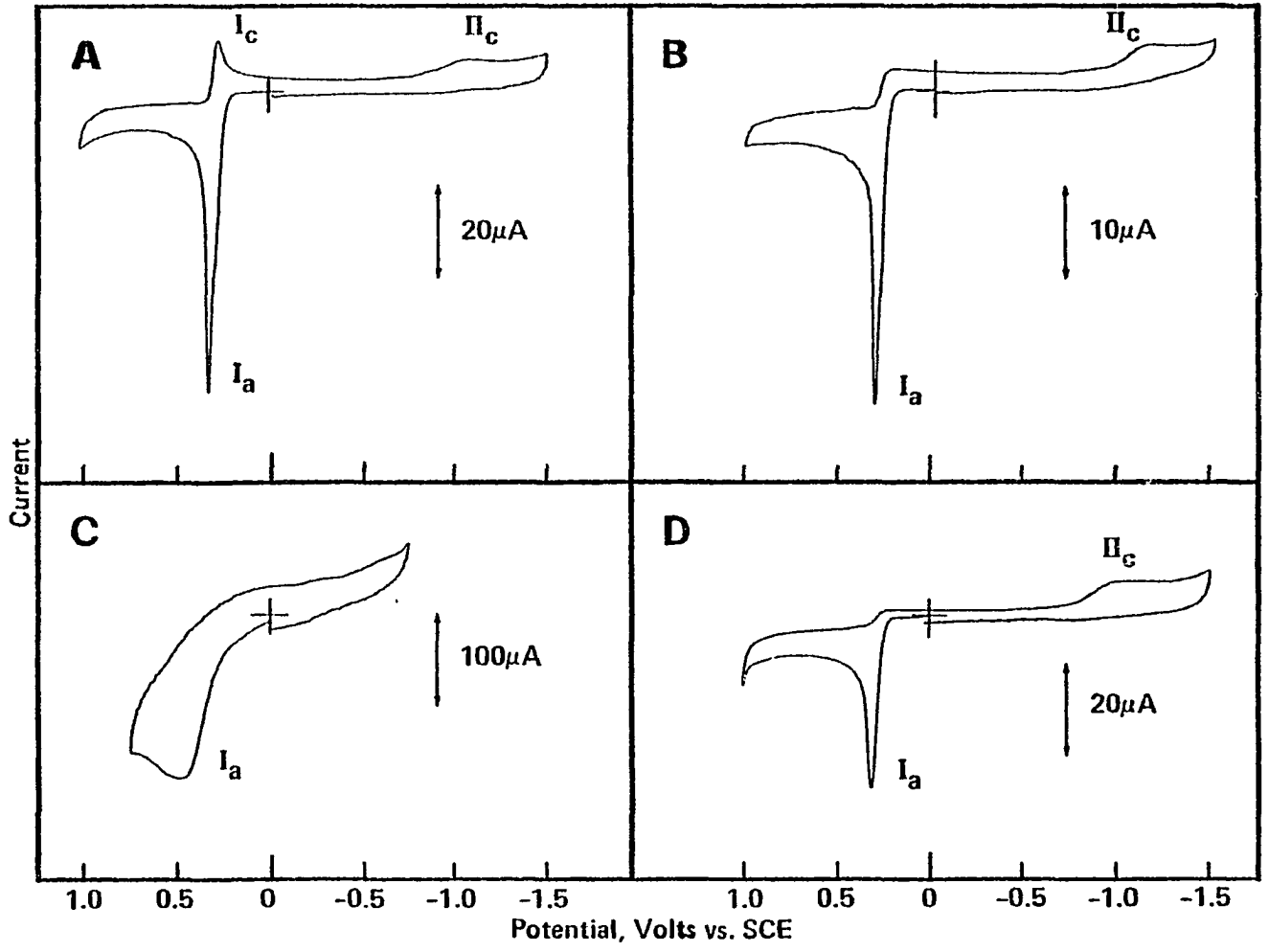

Figure 1. Cyclic voltammograms of 1 mM uric acid in pH 7.0 phosphate buffer at (A) RPGE, (B) SPGE, (C) gold foil electrode and (D) RPGE, solution saturated with allopurinol. The starting potential is indicated by (+); initial sweep always towards positive potentials. Sweep rate: 200 mV s^{-1}. Geometric area for PGE's 0.03 cm^2; for gold electrode 0.28 cm^2.

RPGE uric acid is strongly adsorbed.[52] The fact that the observed peak current for uric acid at the RPGE (see figure 1A) is significantly large than at a SPGE (see figure 1B) of the same geometric area further supports the view that uric acid is strongly adsorbed. Peak I_c appears at the RPGE, but not at the SPGE at 200 mV sec^{-1} sweep rate. This indicates that at the RPGE the diimine is adsorbed and is in some way stabilized by the adsorption.

It has been reported than in the presence of allopurinol (1H-pyrazolo[3,4-d]-pyrimidin-4-ol, II) the adsorption of uric acid is greatly decreased.[52] It would not be surprising then if in the

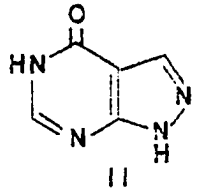

II

presence of allopurinol the adsorption of the diimine were decreased. Based on the earlier work it would then be expected that in the presence of allopurinol peak I_c of uric acid would be diminished at the RPGE at 200 mV sec^{-1} sweep rate. Indeed that was the case, in figure 1D is a voltammogram at 200 mV sec^{-1} of a uric acid solution in pH 7 buffer which has been saturated with allopurinol. Peak I_c is not apparent, and indeed was not observed until sweep rates of ca. 10 V sec^{-1} were employed.

Another reduction peak (II_c) is observed in the cyclic voltam-

metry of uric acid at the PGE (figure 1A,B,D). Peak II_c is observed at all sweep rates. As mentioned in the discussion of equation 1 of Chapter 1 peak II_c has been proposed to be due to the reduction of the imine-alcohol species. There is no reason, on the basis of the work reported here, to believe that the latter explanation of peak II_c is not correct. Oxidation peak II_c of uric acid is not observed at the gold foil electrode because the potential range of a gold foil electrode does not extend to sufficiently negative potentials. Peak II_c was not well defined under any of the conditons reported in this study.

Utilizing a number of different spectroscopic graphite electrodes for voltammetry of uric acid yields more support for the view that the diimine species is stabilized by being adsorbed. Figure 2A is a cyclic voltammogram of uric acid obtained at a rough spectroscopic graphite electrode (see Experimental). Obviously peak I_c is very large even though the sweep rate is only 200 mV sec^{-1}. When using a rough wax-impregnated spectroscopic graphite electrode (WISGE, see Experimental) it was necessary to sweep at rates $\geq$1 V sec^{-1} in order to observe peak I_c (see figure 2B). At a sweep rate of 1 V sec^{-1} peak I_c could not be observed when the working electrode was a smooth WISGE (figure 2C). It was necessary to utilize sweep rates approaching 50 V sec^{-1} to obtain a significant peak I_c (figure 2D) at the smooth WISGE. The rough spectroscopic graphite has a very open, porous structure which means a very large surface area. Due to the large surface area the degree of adsorption is increased, the diimine intermediate is stabilized and peak I_c is very large. A WISGE

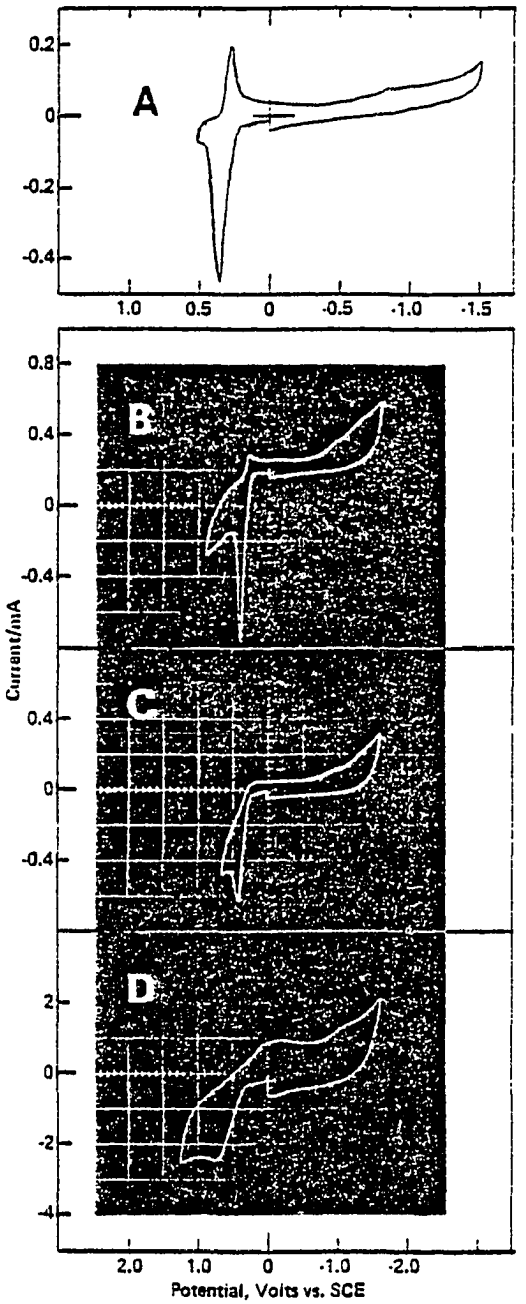

Figure 2. Cyclic voltammogram of 1 mM uric acid in phosphate buffer pH 7.0 at (A) rough spectroscopic graphite electrode at 200 mV s^{-1}, (B) rough WISGE at 1 V s^{-1}, (C) smooth WISGE at 1 V s^{-1} and (D) smooth WISGE at 50 V s^{-1}. Geometric area of spectroscopic graphite electrode 0.16 cm^2, WISGE 0.28 cm^2.

has had all internal pores filled with wax and thus even the rough WISGE has much less surface area than the rough spectroscopic graphite electrode. Therefore, peak I_c is much smaller at the rough WISGE. The smooth WISGE had been polished to a mirror-like surface and has even fewer adsorption sites. For that reason peak I_c was even smaller at the smooth WISGE. The fact that as the electrode surface became smoother the peak current for oxidation peak I_a became smaller supports the idea that the amount of adsorption decreased with increasing electrode smoothness.

The E_p *versus* pH relationship for xanthine from pH 1-12 is given by $E_p = (1.07-0.060\ pH)V$.[36,37] Peak II_a of figure 3A is the primary 4*e* oxidation of xanthine. As discussed earlier and shown in equation 1 of Chapter 1 xanthine is proposed to be oxidized to the same diimine species as uric acid. Peaks I_c and II_c correspond to the same processes in the voltammetry of xanthine as they did in the voltammetry of uric acid. Peak I_a which appears on the second positive sweep in the voltammetry of xanthine is due to the electrooxidation of uric acid formed in the peak I_c process. The cyclic voltammetry of xanthine at different PGE and spectroscopic graphite electrodes (figure 3) behaves exactly the same as the cyclic voltammetry of uric acid. That is under circumstances where adsorption is minimized peaks I_a and I_c do not appear at slow sweep rates, but they can be observed at fast sweep rates.

Thus the voltammetry of uric acid and xanthine indicates the peak current for peak I_c is directly dependent upon the roughness of the electrode surface. This implies that the diimine species formed

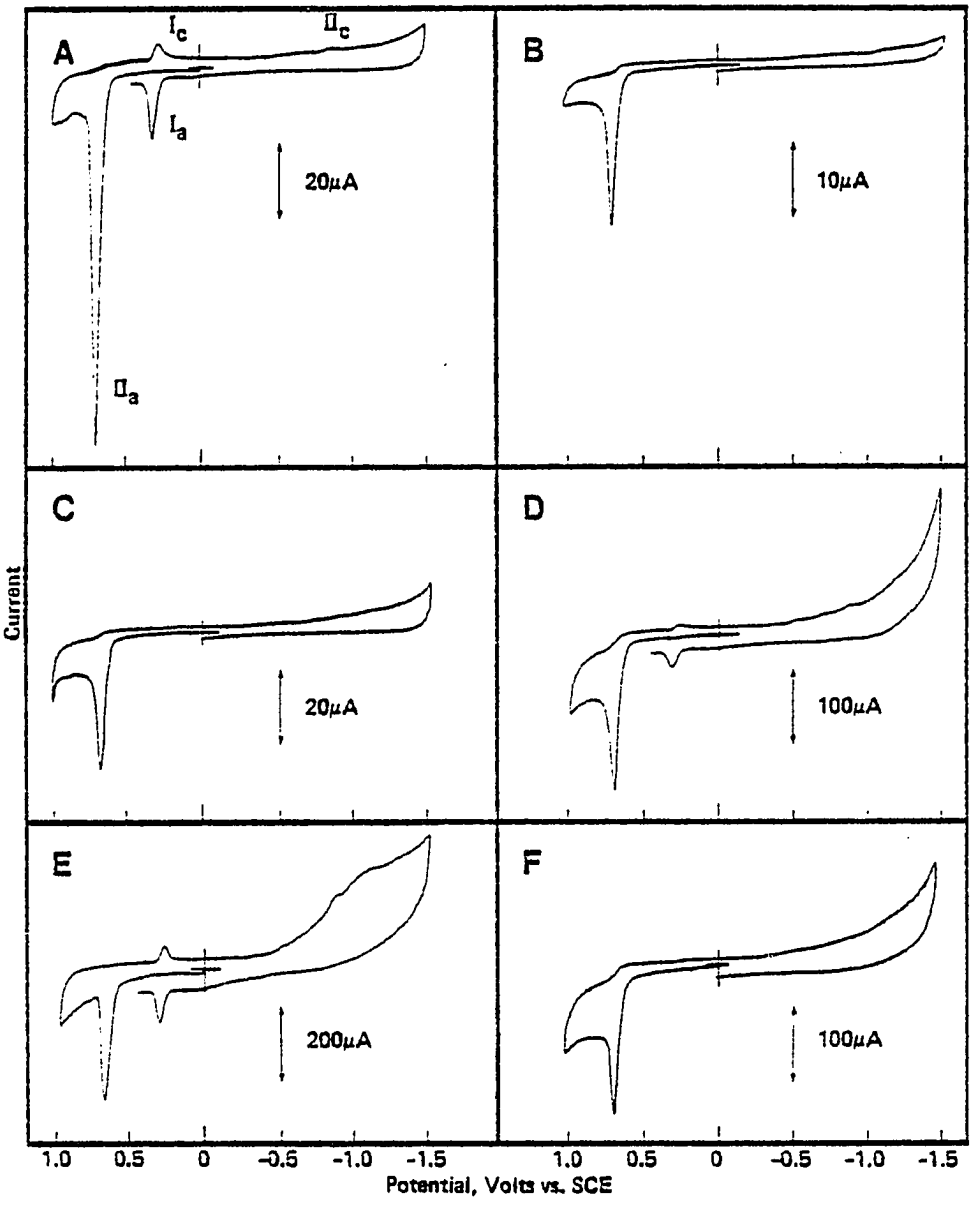

Figure 3. Cyclic voltammograms of 1 mM xanthine in pH 7.0 phosphate buffer at (A) RPGE, (B) SPGE, (C) RPGE, solution saturated with allopurinol, (D) rough WISGE, (E) rough spectroscopic graphite electrode, and (F) smooth WISGE. Geometric area of PGE's 0.03 cm^2, geometric area of WISGE's 0.28 cm^2, geometric area of spectroscopic graphite electrode 0.16 cm^2. Sweep rate: 200 mV s^{-1}.

upon electrooxidation of uric acid or xanthine is stabilized by being adsorbed and that the rate of hydration of the diimine in solution is quite fast.

The cyclic voltammetry of uric acid at a number of pH values and 200 mV sec^{-1} at the RPGE is shown in figure 4A and at the SPGE in figure 4B. Obviously peak I_c is not observed at the SPGE under the conditions, and is most pronounced at approximately neutral pH at the RPGE. This suggests that the species responsible for reduction peak I_c is most stable at pH 7-8. Xanthine behaved essentially the same at the various pH values.

Double potential step chronoamperometry

In view of the fact that peak I_c as observed by cyclic voltammetry of uric acid is always smaller than peak I_a except at very high sweep rates it may be concluded that the primary electrooxidation product, the diimine (II, equation 1, Chapter 1) undergoes a rapid follow-up chemical reaction presumably forming an imine-alcohol. The kinetics of this process were studied using double potential step chronoamperometry after the method of Bard.[53] In double potential step chronoamperometry beginning at an initial potential (E_i) where no electrochemical reaction occurs a potential (E_p) is applied which is 100-200 millivolts more positive than the oxidation peak of interest. At a certain time (T_F, see figure 5) the potential is returned to E_i. As the potential is varied the current is monitored as a function of time. An idealized diagram of the response is shown in figure 5. At time T_F one measures the forward current (I_F) and at $2T_F$ one measures

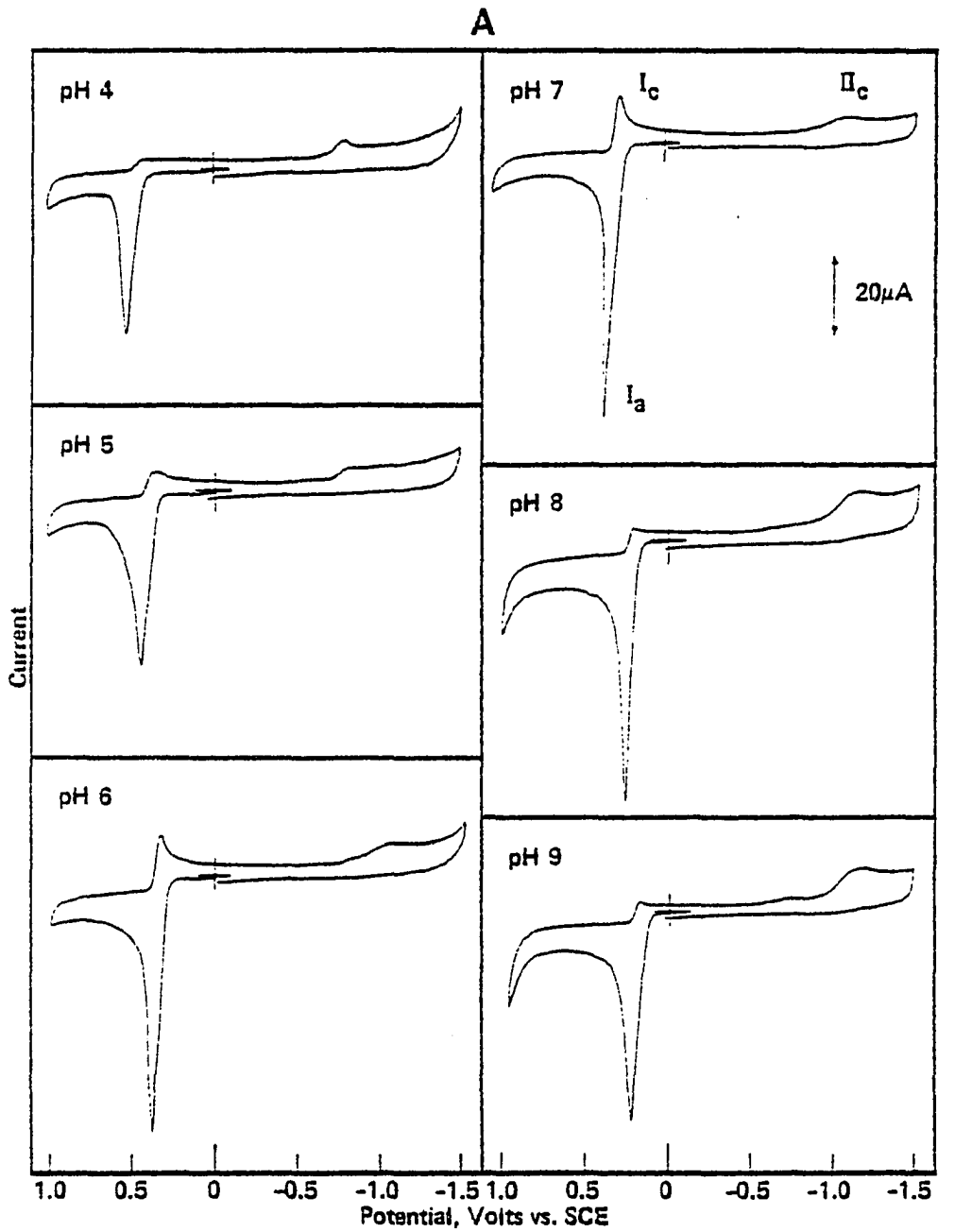

Figure 4. Cyclic voltammograms of 1 mM uric acid in phosphate buffer at RPGE at 200 mV s^{-1} sweep rate between pH 4 and 9.

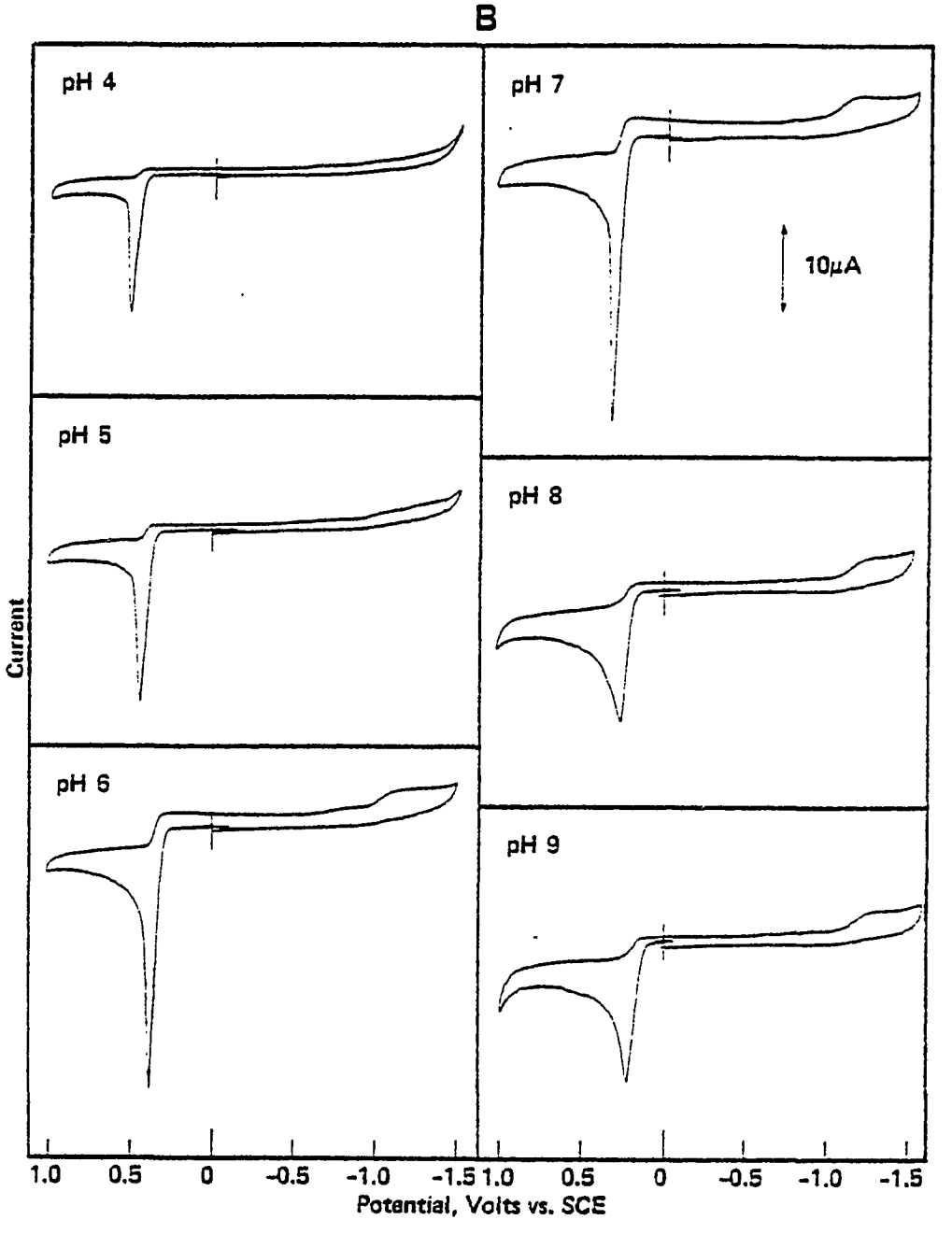

Figure 4. Cyclic voltammograms of 1 mM uric acid in phosphate buffer at SPGE at 200 mV s^{-1} sweep rate between pH 4 and 9.

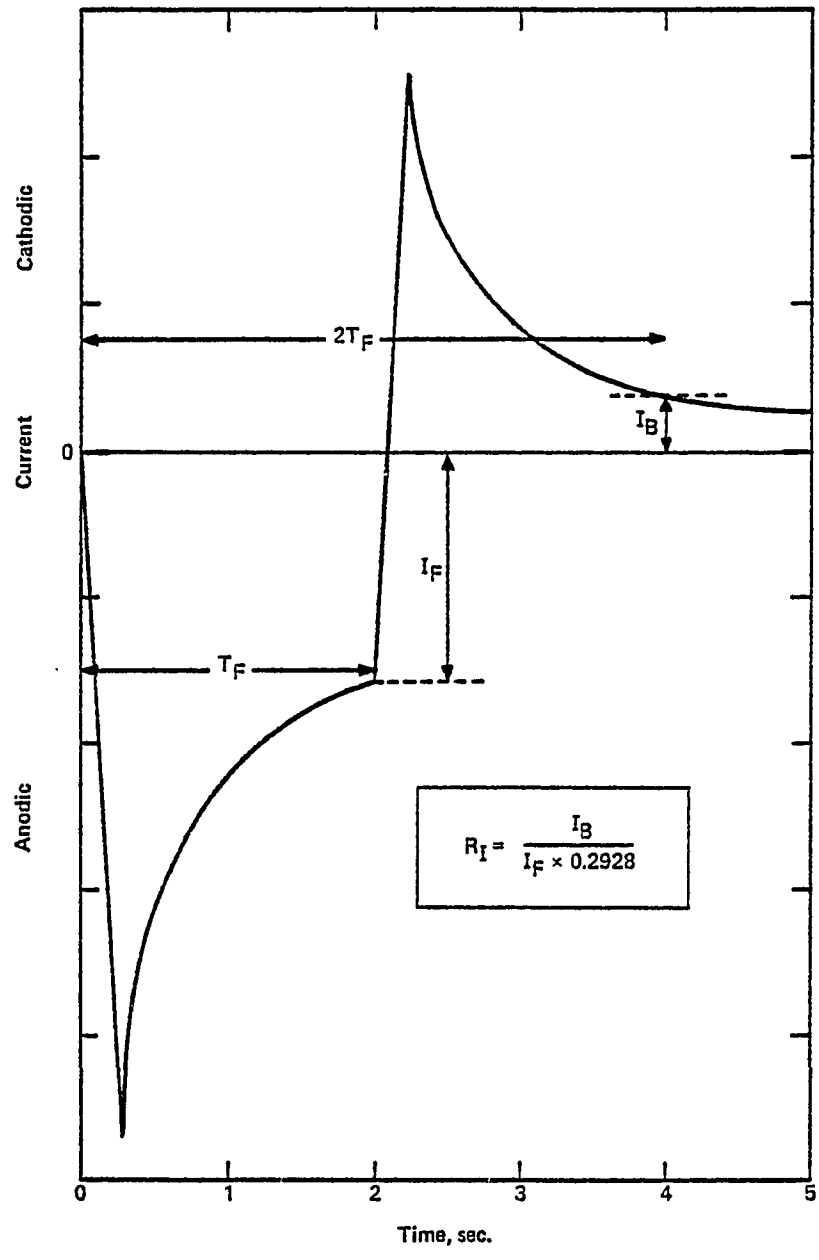

Figure 5. Double potential step chronoamperogram illustrating the measurement of I_F, current at time T_F, and I_B, current at time $2T_F$. T_F is the time of potential reversal.

the back current (I_B). For a process with no kinetic perterbations I_B/I_F is equal to 0.2928. One can then define a normalized current ratio (R_I) as $R_I = I_B/I_F x 0.2928$. If T_F is significantly shorter than the half life of the species being studied, then R_I will approach a value of one. That is the system appears unperterbed. At long time R_I will approach zero. By performing this experiment at a number of different T_F values one can then plot R_I vs. T_F. A typical plot for uric acid is shown in figure 6. When R_I is equal to 0.5 one obtains a value called $t_{1/2}$. Using $t_{1/2}$ values one can normalize double potential step experiments done at different pH's and/or concentrations by plotting R_I vs. $T_F/t_{1/2}$. Normalized $T_F/t_{1/2}$ plots may be compared to each other or more importantly can be compared to theoretical plots for the various types of mechanisms (i.e., first-order e.c., second-order, etc.). Once the mechanism is known the proper equation for calculating the rate constant (k) may be selected. For a first-order e.c. mechanism $k = 0.406/t_{1/2}$.

Initial experiments using the RPGE were unsuccessful. The chronoamperometric curves were quite irreproducible, apparently due to significant adsorption effects. Attempts to reduce the adsorption by saturating the solution with allopurinol were also unsuccessful. The reproducibility was reasonably good with the allopurinol present, and R_I vs. $T_F/t_{1/2}$ curves matched theoretical first-order e.c. curves reasonably well. However, comparing experimental peak current functions to theoretical peak current indicated significant adsorption was still occurring thereby invalidating any rate constants. Voltammetric studies indicated the smooth WISGE would be a much better electrode

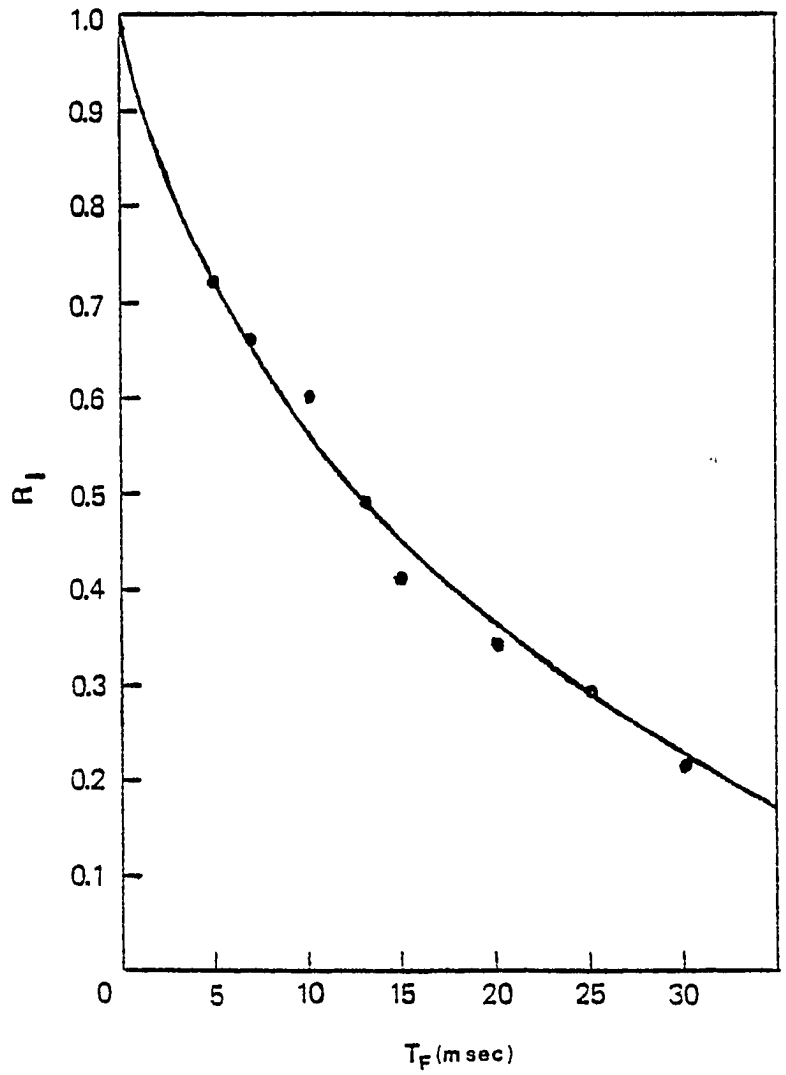

Figure 6. Experimental double potential step chronoamperometric results for the electrochemical oxidation of 3 mM uric acid in pH 8 phosphate buffer at a stationary smooth WISGE (0.066 cm^2). The value of $t_{1/2}$ was 12.6 msec.

for double potential step chronoamperometric studies since much less adsorption appeared to occur. Results with the smooth WISGE were much better, but still must be accepted cautiously since at some pH values the reproducibility was not too good. In figure 7 the various experimental R_I *vs.* $T_F/t_{1/2}$ values are plotted along with the theoretical R_I *vs.* $T_F/t_{1/2}$ plot for a first-order e.c. reaction.

Table 1 shows the rate constants observed over the pH range 6-10. The most reliable data appears to be that obtained at pH 8. At pH 8 the reproducibility and the agreement with the theoretical curve are both quite good. A rate constant of 32.5 sec^{-1} was obtained at pH 8. This is quite fast and is consistent with voltammetric studies at the smooth WISGE. The rest of the data indicates the diimine is both acid and base catalyzed. Whether the rate constants are completely accurate or not the results clearly indicate the diimine is very unstable, but is most stable at approximately pH 8. This information is consistent with voltammetric studies, but yields a more precise picture of the behavior of the diimine.

Thin-layer spectroelectrochemical studies

For the thin-layer spectroelectrochemical studies performed upon uric acid and xanthine a gold minigrid electrode, similar to that described by Heineman, *et al.*[54,55] and a Harrick rapid scan spectrophotometer were utilized. In order to demonstrate that the same electrochemical reaction occurred at a gold electrode as at a graphite electrode for uric acid and xanthine a series of voltammetric and coulometric experiments were carried out at gold electrodes.

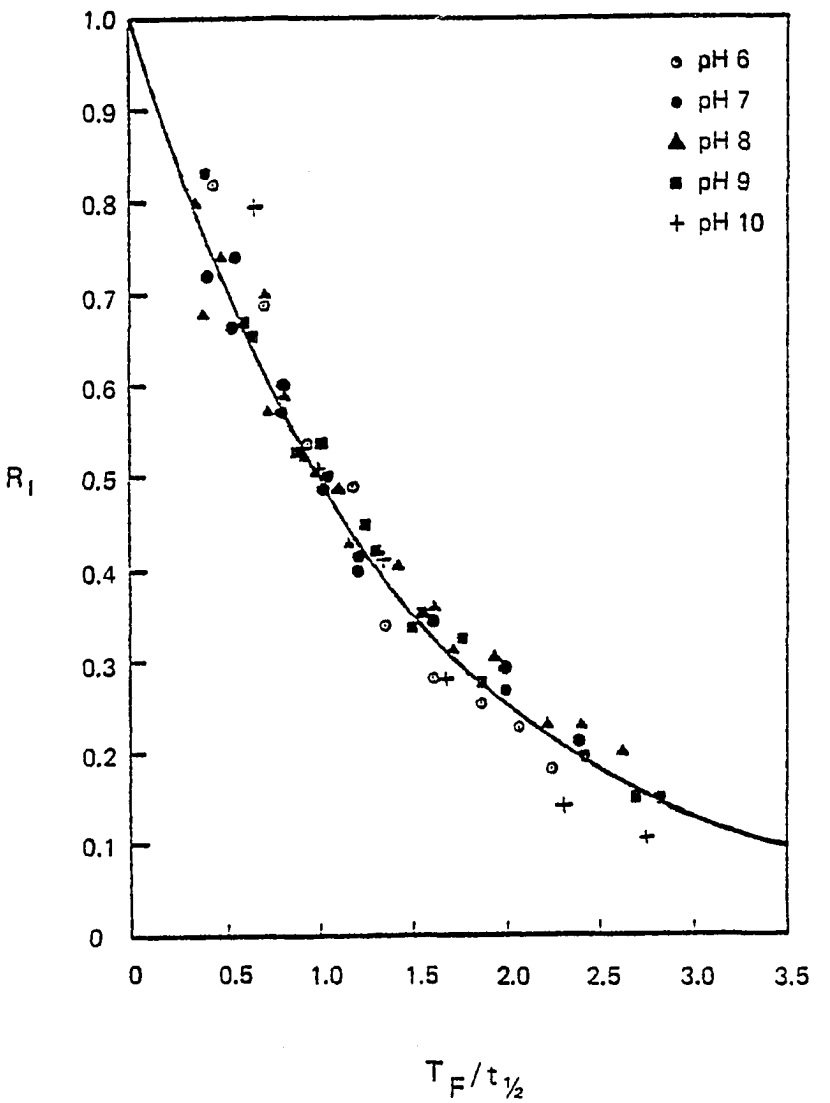

Figure 7. Experimental double potential step chronoamperometric results for the electrochemical oxidation of uric acid at a stationary smooth WISGE (0.066 cm^2). Uric acid concentrations ranged from 0.3 mM-3 mM. The line is the theoretical relationship expected for a first-order e.c. mechanism.

Table 1

Apparent first-order rate constants from double potential step chronoamperometry of uric acid

Initial concentration of uric acid/mM	pH	k_{obs}/s^{-1}
1.0	6	92.3
0.30	7	88.3
0.80		68.8
3.00		81.2
0.3	8	32.5
3.0		32.5
1.0	9	52.4
3.0		49.2
1.0	10	135.3

The E_p *versus* pH equation for uric acid at 5 mV sec^{-1} from pH 4-9 is E_p = (1.03-0.086 pH)V, and for xanthine under the same conditions the relationship is E_p = (1.15-0.06 pH)V. Peak I_a of uric acid shows quite clearly at the gold electrode and peak I_c can be observed at sweep rates $\geq$20 V sec^{-1} (figure 1C). Voltammetry of xanthine at the gold electrode, even though peak II_a could be observed, was not useful because at the potential where peak II_a occurs gold oxides are formed. The gold oxides cause a large reduction peak on the reverse negative sweep which totally obscures peak I_c of xanthine.

Coulometric n-values for uric acid and xanthine were determined

in the thin-layer cell. The values obtained are presented in Table 2

Table 2

Experimental n-values observed for electrochemical oxidation of uric acid and xanthine in a thin-layer cell at a gold minigrid electrode

Compound	pH	Initial Concentration, mM	Controlled Potential/V vs. SCE	n-Value[a]
Uric acid	7	5	0.9	1.8
Uric acid	8	5	0.8	1.9
Uric acid	9	1	0.8	1.6
Xanthine	8	1.5	1.2	3.7

[a]By graphical integration of current-time curve.

and are obviously the same as those obtained with macroscale coulometric experiments at the PGE. Thus, the voltammetric and coulometric experiments both indicate that the electrode reaction for uric acid and xanthine at the gold and graphite electrodes is the same.

A typical u.v. spectrum obtained prior to electrolysis of uric acid at pH 7 in a thin-layer spectroelectrochemical cell is shown in curve 1 of figure 8. The absorbance maximum for uric acid is located at 287 nm. Applying a potential of 0.9 V the uric acid peak at 287 nm decreases with time and a broad absorbance grows in at 304 nm (pH 6-9). After reaching a maximum the 304 nm peak then decreases. The above

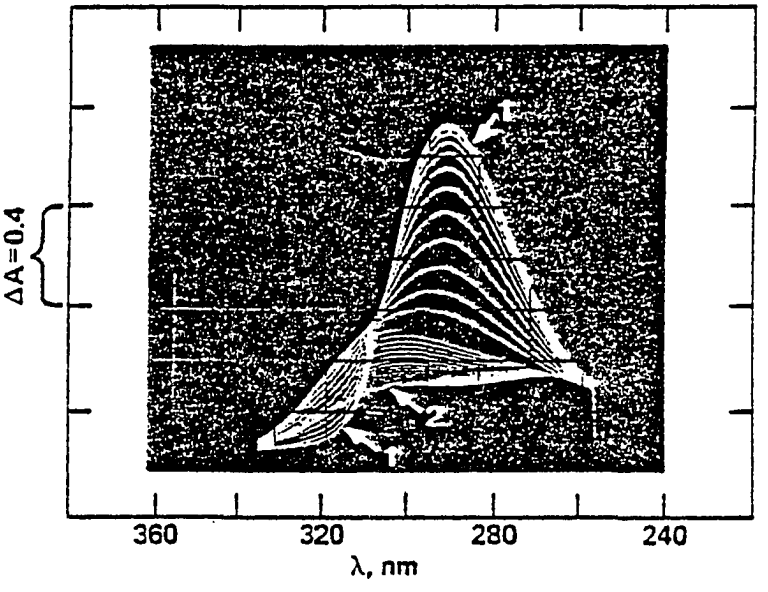

Figure 8. Spectrum of 10 mM uric acid solution electrolyzing at 0.9 V in phosphate buffer pH 7.0 at a gold minigrid electrode in a thin-layer cell. Curve (1) is uric acid spectrum before electrolysis. Repetetive scans (260 nm to 340 nm) of 9.5 s are shown. Trace (2) is the spectrum of the exhaustively electrolyzed solution.

behavior indicates that when uric acid is electrooxidized an unstable intermediate which absorbs at longer wavelengths is generated.

Curve 2 of figure 8 is the spectrum of a fully electrolyzed uric acid solution which has also been given time for the unstable intermediate to fully decay. The spectrum of a 10 mM allantoin solution (the final product of electrooxidation of uric acid at pH 7[36,38]) is identical to curve 2, figure 8. Thin-layer spectroelectrochemical studies of uric acid from 1-10 mM at pH 7 utilizing potentials from 0.4-1.0 V yielded results essentially the same as those in figure 8. It should be noted, however, that when utilizing potentials negative of the peak potential of uric acid the rate of oxidation was significantly slower. The spectra of uric acid at pH 8 and 9 were no different than that obtained at pH 7 (figure 8). The absorbance due to the intermediate became much smaller below pH 7 and thus difficult to study. At pH 5 or below no absorbance other than that of uric acid could be observed even using very fast sweep rates. Apparently the unstable intermediate formed by the electrooxidation of uric acid absorbs differently below pH 7 or is significantly less stable. Below pH 7 uric acid is noticeably less soluble, thus introducing another obstacle to thin-layer spectroelectrochemical studies at low pH.

As was the case with the voltammetry the thin-layer spectroelectrochemical studies of xanthine were virtually identical in behavior to that of uric acid. In both cases an unstable intermediate appears at 304 nm. Because of the lower solubility of xanthine the spectra are not as good as those for uric acid. Below pH 7 xanthine was insufficiently soluble to allow any useful thin-layer spectroelectro-

chemical studies. Between pH 7 and 9 the appearance and decay of the unstable, u.v. absorbing intermediate formed upon electrochemical oxidation of xanthine was not dependent upon the applied potential employed. The appearance of the spectrum after xanthine had been completely electrolyzed and the unstable intermediate allowed time to fully disappear was identical to the spectrum of allantoin under the same conditions.

Kinetic measurements

The kinetic behavior of the disappearance of the intermediate observed at 304 nm upon electrooxidation of uric acid and xanthine was studied by thin-layer spectroelectrochemistry. During the electrooxidation of uric acid or xanthine at the gold minigrid electrode the absorbance at 320 nm was monitored as a function of time. 320 nm was chosen because there was minimal overlap between the intermediate peak and the uric acid or xanthine peak. A typical absorbance versus time for uric acid at pH 7 is shown in figure 9B. The linearity of the plot shows clearly that the decomposition reaction of the intermediate observed at 304 nm follows first-order kinetics.

Table 3 shows the values obtained for the rate constant of the intermediate formed upon electrooxidation of uric acid from pH 7-9. It is clear from Table 3 that the observed rate constant is not concentration dependent. The change observed with pH is believed due to changes in buffer composition and does not necessarily indicate that the reaction is acid catalyzed. Therefore the apparent rate constant for the decomposition reaction of the intermediate observed

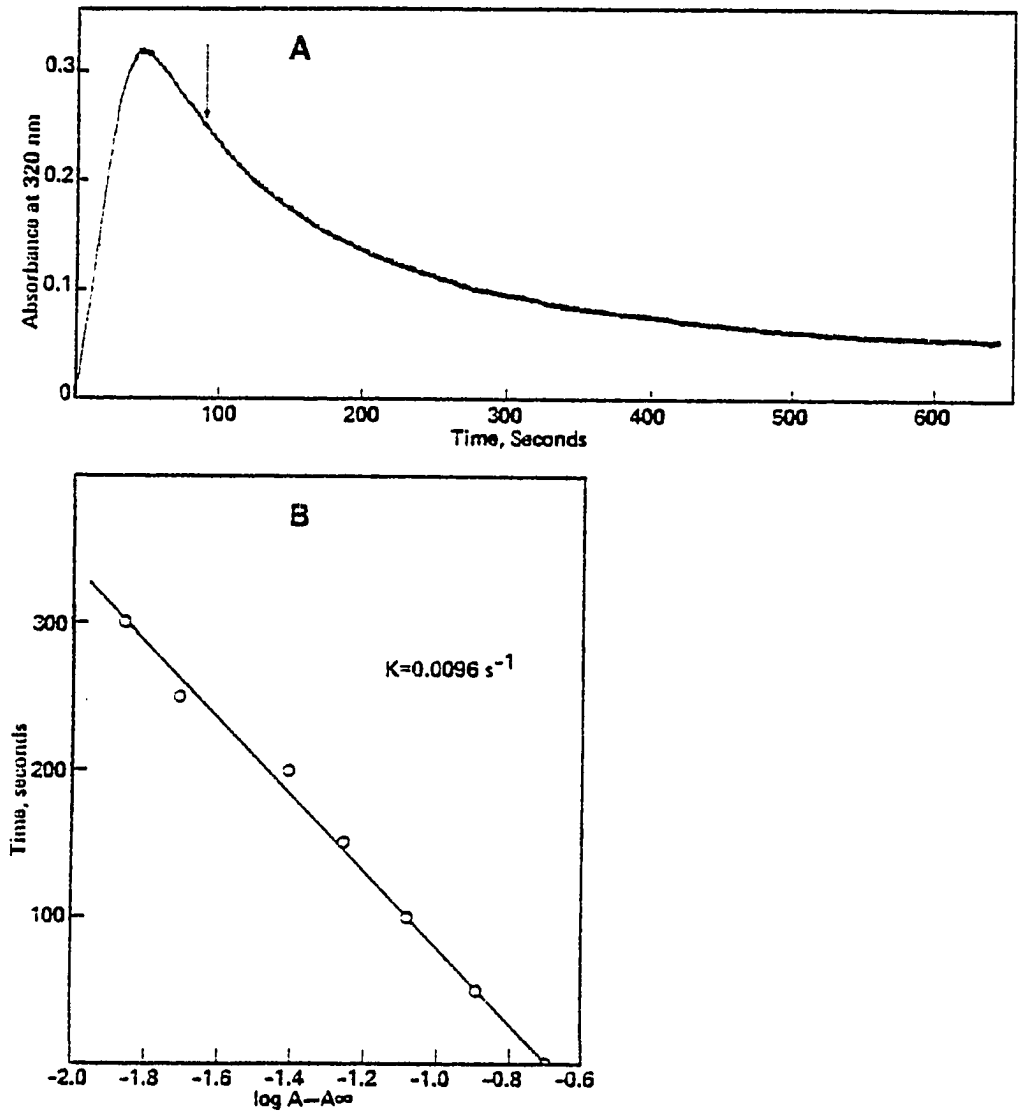

Figure 9. (A) Variation of the absorbance with time observed on electrochemical oxidation of 5 mM uric acid in phosphate buffer pH 7.0 at a gold minigrid electrode (0.9 V) in a thin-layer cell. (B) Kinetic plot of time versus log absorbance at 320 nm. Absorbance data were taken from curve (A) setting time = 0 at the point where the concentration of uric acid was at or very near to zero, i.e., at arrow in (A).

Table 3

Observed first-order rate constants for reaction of the u.v.-absorbing intermediate formed on electrochemical oxidation of uric acid at gold minigrid electrode

Initial Concentration of uric acid/mM	pH[a]	k_{obs}/s^{-1}
1.0	7	0.010
5.0		0.009
10.0		0.008
1.0	8	0.009
5.0		0.006
10.0		0.007
1.0	9	0.007
5.0		0.004
10.0		0.006

[a]Phosphate buffers containing K_2SO_4, all having an ionic strength of 0.5.

at 304 nm is 0.008±0.002 sec^{-1}.

In the case of xanthine the observed first-order rate constant over the pH range of 7-9 is 0.006±0.003 sec^{-1}. Because of the fact that the first-order rate constants of uric acid and xanthine are similar, the λ_{max} of their u.v.-absorbing intermediates are identical (304 nm, pH 7-9), and the final product for both is allantoin. The logical conclusion to draw is that the mechanism of the electro-

oxidation of uric acid and xanthine is the same.

DISCUSSION

Thus from the results presented above it seems that at graphite and gold electrodes uric acid and xanthine are initially oxidized to a species with a half-life $\leq$23 msec. The observation of peak I_c in the cyclic voltammetry of both compounds indicates that the short-lived product is reducible. This study supports the view put forth in previous reports[36,38] that the initial product of the electrooxidation of uric acid and xanthine is the diimine (II, equation 1, Chapter 1). At sweep rates around 200 mV sec^{-1} peak I_c could be observed only at electrodes with a rough surface. At a gold electrode or a highly polished graphite electrode the reduction of the diimine could be observed only at fast sweep rates ($\geq$20 V sec^{-1}). It seems then that the diimine species is quite unstable in homogeneous solution, but is stabilized when adsorbed at an electrode surface. Rough graphite electrodes seem to have a larger number of adsorption sites compared to the smooth electrodes and thus more of the diimine is stabilized and peak I_c is larger. Double potential step chronoamperometry indicates the hydrolysis of the electrogenerated diimine to the uric acid imine-alcohol (III, equation 1, Chapter 1) is a first-order reaction with an apparent rate constant of 32.5 sec^{-1} at pH 8. This hydrolysis also appears to be acid and base catalyzed.

An intermediate is observed at 304 nm in the thin-layer spectroelectrochemical studies of uric acid and xanthine. The decomposition reaction of this u.v.-absorbing intermediate is a first-order process having an observed rate constant of 0.008 sec^{-1} from pH 7-9. Clearly, from the rate constants the u.v.-absorbing intermediate is not the diimine species responsible for voltammetric peak I_c. It appears then that the intermediate observed at 304 nm in the thin-layer spectroelectrochemistry of uric acid and xanthine is the imine-alcohol and the decay observed is due to the hydration reaction of the imine-alcohol to form uric acid-4,5-diol (IV, equation 1, Chapter 1). The rate of hydration is independent of the solution pH between pH 7-9.

As indicated earlier voltammetric peak II_c of uric acid and xanthine is observed at both fast and slow potential sweep rates. The information available indicates the hydration of the diimine to the imine-alcohol is quite rapid, and the hydration of the imine-alcohol to uric acid-4,5-diol is rather slow.

The studies presented here provide new insights into the mechanism of the electrochemical oxidation of xanthine and uric acid. In addition, the techniques utilized in these studies, thin-layer spectroelectrochemistry, cyclic voltammetry at various electrodes, and double potential step chronoamperometry should be extremely useful in studies of other biologically important molecules.

EXPERIMENTAL

Chemicals

Uric acid was supplied by Eastman Chemicals, allopurinol by Calbiochem, and xanthine by Nutritional Biochemicals.

Buffer solutions were prepared from reagent grade chemicals with an ionic strength of 1.0 M (0.5 M upon 1:1 dilution with deionized water). The buffers were constituted as follows: pH 1-3, H_3PO_4 and KH_2HPO_4; pH 6-8, NaOH and KH_2PO_4; pH 11-12, $Na_2HPO_4 \cdot 7H_2O$ and NaOH. All buffers contained K_2SO_4 as an ionic strength buffer.

Apparatus

Linear sweep voltammetry and cyclic voltammetry were carried out with an instrument based on conventional operational amplifier design.[56] Double potential step chronoamperometry utilized a Princeton Applied Research Corporation Model 175 universal programmer.

For all voltammetric studies a three compartment cell utilizing a saturated calomel reference electrode (SCE) and a platinum foil counter electrode were employed. All potentials are referred to the SCE at 25°C.

The spectrometer used for all absorbance measurements was a Harrick Rapid Scan Spectrometer (RSS) and signal processing module (Harrick Scientific Co., Ossining, N.Y.). On the sample side of the spectrometer compartment was placed the thin-layer cell, sample cup, reference electrode, counter electrode, and the required electrical connections. An identical thin-layer cell containing only the appropriate buffer and requiring no electrical connections was placed in

the reference beam of the RSS.

Voltammograms, chronoamperograms, absorbance versus time curves, and RSS spectra were recorded on either a Hewlett-Packard Model 7001A XY recorder or a Tektronix Model 5031 dual beam storage oscilloscope equipped with a Tektronix Model C-70 camera.

The thin-layer spectroelectrochemical cells utilized a gold minigrid (Buckbee Mears Co., St. Paul, Minn.) as the optically transparent working electrode and was similar to those reported by Murray et al.[54] and Heinieman.[55] The transmittance of the gold minigrid was ca. 50%. The construction of the cell has been reported elsewhere.[51,54,55] The thickness of the cells in this study ranged from 0.009-0.010 cm. All thin-layer electrochemical studies were carried out at room temperature (25±2°C).

Controlled potentials applied to the thin-layer cell were maintained with a Wenking Model LT73 potentiostat.

The gold foil electrode utilized for voltammetric studies was constructed by glueing a 1 cm^2 piece of gold foil with Duro Super Glue 3 (Woodhill Chemical Sales Corp., Cleveland, Ohio) to the end of a 6 mm o.d. glass tube. Next the gold foil not stretched across the end of the glass tube was folded firmly against the glass tube and sealed with epoxy resin (Epoxi-Patch, Dexter Corp., Olean, N.Y.). The epoxy coating was painted with three coats of Carboline K-63 white paint (Carboline Co., St. Louis, Mo.) to protect it from chromic acid cleaning solutions. In order to make electrical contact with the gold the glass tube was packed very firmly with carbon paste (3 g Ultra Carbon UCP-1-M, Ultra Carbon Corp., Bay City, Mich.; in 2 ml Nujol). Then a copper

wire was inserted into the carbon paste with enough left protruding to attach electrical leads. It was necessary to carry out a pretreatment process before using the gold foil electrode.[57] First, the electrode is placed in a solution of concentrated chromic acid for 2 min and then thoroughly rinsed with water. Next the electrode is placed in the sample solution and a -0.5 V applied for 2 minutes. The electrode is then tapped to remove bubbles and a voltammogram run immediately.

Two types of pyrolytic graphite electrodes were used in these studies. The rough PGE which consists of a 2 mm x 10 mm rod of pyrolytic graphite sealed in a 2 mm i.d. glass tube with epoxy resin (construction details have been presented elsewhere[17]). The surface of the RPGE was renewed by polishing on a 600-grit silicon carbide paper (Buehler, Inc., Evanston, Ill.) attached to a metallographic polishing wheel. The resurfaced graphite was then thoroughly washed with deionized water. The body of the electrode was then dried completely and the excess water removed by lightly brushing the electrode surface with a soft paper tissue.

The smooth pyrolytic graphite electrode (SPGE) was similar to the RPGE in construction. Except for the SPGE a few millimeters of the graphite rod was allowed to protrude from the end of the glass tubing, and then completely covered with epoxy resin. A graphite surface was exposed by cleaving the epoxy coated, protruding graphite rod with a razor blade or similar sharp implement. The exposed tip was already relatively smooth, but was further polished on an alumina (<0.1 μm, Grade B Gamma Alumina, Fisher Scientific) impregnated felt cloth. The surface of this electrode had the appearance of a metallic

mirror and was considerably less rough than the RPGE.

There were three types of spectroscopic graphite electrodes utilized in these studies. A rod of pure spectroscopic graphite (Ultra Carbon, Bay City, Mich.) was used. After using this particular electrode it was necessary to grind away approximately 6 mm of the electrode due to sample penetration into its extremely porous matrix. A rough wax impregnated spectroscopic graphite electrode (rough WISGE) was utilized and was resurfaced in the same manner as the RPGE (see above). A smooth WISGE was prepared by polishing the electrode on an alumina-impregnated felt pad.

Procedures

Typically 1 mM solutions of uric acid or xanthine were prepared for voltammetric studies. Concentration ranges from 0.3 mM to 10 mM were employed for double potential step chronoamperometric and RSS studies.

In the thin-layer spectroelectrochemical studies the sample solution was placed in a 5 ml, half-cylinder glass cup. A platinum foil counter electrode shaped to fit the contour of the cup was also placed in the glass cup. The open end of the thin-layer cell was then lowered approximately 3 mm into the solution. Vacuum was used to pull fresh solution into the cell, after which capillary action retained the solution in the cell. The light beam was positioned as nearly as possible in the center of the working electrode for both the sample and reference thin-layer cells. The wavelength region of 260-340 nm was monitored in these studies, although in preliminary

studies much broader ranges encompassing much of the visible region were also scanned. Because the oxidation of xanthine occurs at potentials somewhat greater than 1.0 V over the pH range 5-9,[36,37] it was necessary to apply a potential of -0.5 V for 3 minutes before each run.[57] If this was not done the rate of electrooxidation was severely slowed by the presence of gold oxides on the electrode surface.

In the double potential step chronoamperometric studies a cyclic voltammogram was run before each study to determine E_i and E_f (figure 5). In the studies undertaken for this work typical values of E_i and E_f, respectively, are -0.1 V and 0.85 V. Although, values of E_i from 0 to -0.4 V were tried and [illegible] from 0.75 to 1 V were investigated. The [illegible] every run, but was simply ta[illegible]

I[illegible]orded. Backgrou[illegible]except that n[illegible]

[illegible]pectro-elect[illegible]hrono-amperc[illegible]mployed to inves[illegible] The proposal th[illegible]ácid and xanthine is a d[illegible]ed. This diimine is very rapidly hydr[illegible]alcohol in a first-order process. Despite the low stability shown by the diimine in

studies much broader ranges encompassing much of the visible region were also scanned. Because the oxidation of xanthine occurs at potentials somewhat greater than 1.0 V over the pH range 5-9,[36,37] it was necessary to apply a potential of -0.5 V for 3 minutes before each run.[57] If this was not done the rate of electrooxidation was severely slowed by the presence of gold oxides on the electrode surface.

In the double potential step chronoamperometric studies a cyclic voltammogram was run before each study to determine E_i and E_f (figure 5). In the studies undertaken for this work typical values of E_i and E_f, respectively, are -0.1 V and 0.85 V. Although, values of E_i from 0 to -0.4 V were tried and E_f values ranging from 0.75 to 1 V were investigated. The electrode was not resurfaced after every run, but was simply tapped to disperse the electrical double layer.

In all cases at least three replicate runs were recorded. Background runs were also carried out in exactly the same way except that no uric acid or xanthine was included.

SUMMARY

A number of electrochemical methods such as thin-layer spectroelectrochemistry, cyclic voltammetry, and double potential step chronoamperometry at various graphite and gold electrodes have been employed to investigate the electrooxidation of uric acid and xanthine. The proposal that the primary electrooxidation product of uric acid and xanthine is a diimine species has been strongly supported. This diimine is very rapidly hydrated in solution to an imine-alcohol in a first-order process. Despite the low stability shown by the diimine in

solution, its voltammetric reduction peak can be observed at rather low sweep rates at a rough graphite electrode. This is apparently due to the diimine being adsorbed and stabilized by the adsorption. The hydration reaction of the diimine to form the imine-alcohol can be observed as the growth and decay of a u.v.-absorbing intermediate in the thin-layer spectroelectrochemical studies.

ENZYMATIC OXIDATION OF URIC ACID

CHAPTER 3

INTRODUCTION

An underlying rationale for the studies of the electrochemical oxidation of biologically important purines is that such studies can lead to information bearing on the reaction routes and mechanisms of biological oxidation reactions.[58] Following the studies in Chapter 2 we possessed a good deal of information regarding the electrochemical oxidation of uric acid. It was natural, therefore, to attempt to compare the electrochemical oxidation to a biological oxidation. A system utilizing horseradish peroxidase (HRP) and hydrogen peroxide was chosen to carry out the oxidation. This system was chosen because it was known to oxidize uric acid to the same products as the electrochemical oxidation and some similar intermediates had been proposed.[38,39]

RESULTS

RSS Studies

The initial studies of the enzymatic and electrochemical oxidation of uric acid were carried out at pH 7.0 using rapid scan spectrophotometry. Typical spectra obtained at pH 7.0 utilizing each of the two methods of oxidation are shown in figures 10 and 11.

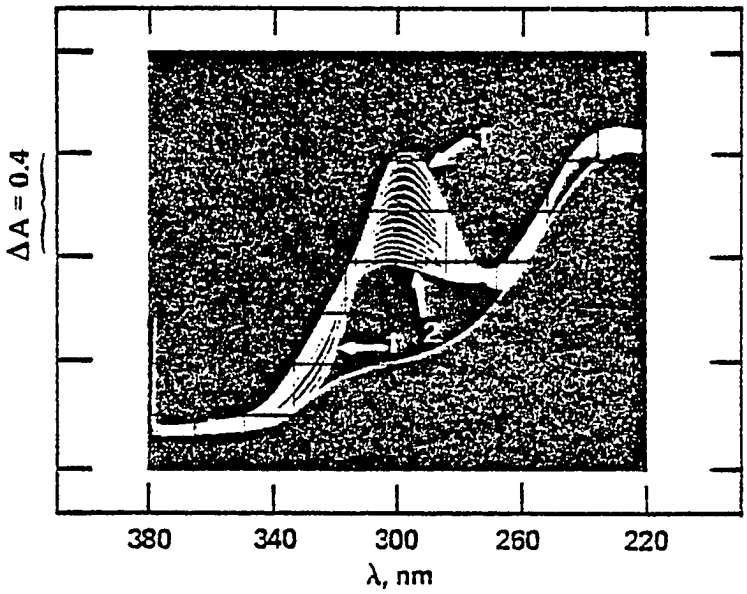

Figure 10. Rapid scan spectrophotometry of uric acid (100 μM) in the presence of type VIII peroxidase (0.17 μM) and H_2O_2 (200 μM) in phosphate buffer pH 7.0 having an ionic strength of 1.0 M. Curve 1 is the spectrum before initiation of the oxidation. Curve 2 is the spectrum after 5 minutes oxidation.

Repetitive scans of 19 seconds

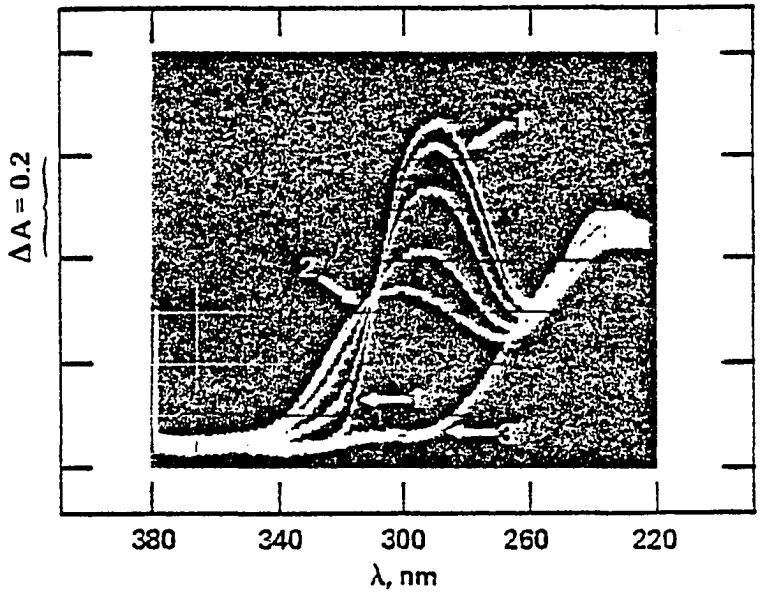

Figure 11. Thin-layer spectroelectrochemical oxidation of uric acid (5 mM) at a gold minigrid electrode at 0.9 V in phosphate buffer pH 7.0 having an ionic strength of 1.0 M. Curve 1 is the spectrum before initiation of the oxidation. Curve 2 is the spectrum when 90% of the uric acid has been oxidized.

Repetitive sweeps of 9.4 seconds.

Curve 1 in the latter figures corresponds to the spectrum of uric acid (λ_{max} = 287 nm) before initiation of any oxidation. Upon initiation of the oxidation, either enzymatically or under thin-layer spectroelectrochemical conditions the u.v. peak of uric acid decreases and correspondingly, a new peak grows in at longer wavelengths. Curve 2 in figure 10 is the spectrum observed about 5 minutes after initiation of the enzymatic oxidation. The absorbance between 350 and 320 nm has clearly increased over that observed for the initial uric acid solution. In figure 11 the effect is much more apparent. Thus, curve 2 in figure 11 is the spectrum observed about 30 seconds after initiation of the electrooxidation of uric acid. In this case the absorbance between 350-320 nm has increased compared to that observed before electrooxidation. However, the λ_{max} of the new absorbing species clearly occurs at 302-304 nm. With increasing time the growing absorbance observed at 350-320 nm increases as the uric acid peak decreases, reaches a maximal value (corresponding to about curve 2 in figure 11) and then decreases. Clearly, the species responsible for the increased absorbance at 350-320 nm must be an unstable intermediate formed in the enzymatic and electrochemical oxidation of uric acid. After complete enzymatic or electrochemical oxidation of uric acid, i.e., after the intermediate species has completely disappeared, the spectrum of the solution corresponds exactly to that of allantoin, the known electrochemical[59] and enzymatic product.[22,23]

The r.s.s. curves shown in figure 10 for the peroxidase oxidation are not as well defined as those shown for the electro-

chemical oxidation shown in figure 11. This is because the peroxidase catalyzed oxidation of uric acid is quite slow at pH 7.0. For example, at pH 7.0 in phosphate buffer having an ionic strength of 1.0 M the observed first-order rate constant for oxidation of uric acid under the conditions described in figure 10 is 0.0032 sec^{-1}. This value is significantly smaller than the observed rate constant at pH 4 under otherwise identical conditions (0.0092 sec^{-1}). Thus, the rate of oxidation of uric acid at pH 7.0 is quite slow and, as will be shown subsequently, the rate of disappearance of the u.v.-absorbing intermediate is not greatly different from the rate of oxidation of uric acid. Thus at pH 7, under the conditions outlined above, it is not possible to observe the spectrum of the intermediate species without there also being significant quantities of absorbing uric acid present in the solution. The rate of peroxidase-catalyzed oxidation of uric acid may be increased by increasing the enzyme concentration. However, the cost of the enzyme precluded extensive studies at very high peroxidase concentrations.

Kinetic measurements

In order to characterize the u.v-absorbing intermediate formed on electrochemical oxidation of uric acid, thin-layer spectroelectrochemical studies were carried out between pH 7.0 and 9.3. Below pH 7.0 the molar absorptivity of the intermediate species decreased very significantly such that it could not be monitored. Between pH 7.0 and 9.3 the u.v.-absorbing intermediate had a λ_{max} of 302-304 nm, i.e., λ_{max} was essentially independent of pH. The kinetics

of disappearance of the u.v.-absorbing intermediate was studied by applying a constant potential to an optically transparent gold minigrid electrode in a thin-layer spectroelectrochemical cell and monitoring the absorbance of the intermediate species at a wavelength where uric acid exhibited minimal absorbance (e.g., 320 nm). When the absorbance at the latter wavelength reached its maximal value, the electrolysis was terminated and the $A_{320\ nm}$ versus time decay was recorded. Analysis of these A versus time curves indicated that the disappearance of the u.v.-absorbing intermediate followed first-order kinetics. Some typical first-order rate constants are presented in Table 4. It should be noted that the observed rate constants

Table 4

Observed first-order rate constants for reaction of the u.v.-absorbing intermediate formed on electrochemical oxidation of uric acid at a gold minigrid electrode

Initial Concentration of Uric Acid/mM	pH[a]	k_{obs}/s^{-1}
5	7.0	0.0040
5	8.0	0.0030
5	9.3	0.0035
		Mean: 0.0035±0.0005

[a]Phosphate buffers, see Experimental for details of buffer composition.

reported in Table 4 are somewhat smaller than those (0.008 sec^{-1} between pH 7 and 9) reported previously.[59] The latter values were obtained in a different buffer system (phosphate plus K_2SO_4) having an ionic strength of 0.5 M. This suggests that the rate of disappearance of the u.v.-absorbing intermediate is affected by ionic strength and/or the buffer constituents. However, no systematic investigation of this effect has been carried out.

Attempts to study the kinetics of disappearance of the u.v.-absorbing intermediate observed on peroxidase/H_2O_2 oxidation of uric acid at pH 7 and above were not meaningful because the oxidation of uric acid is so slow that the absorbance versus time curves reflect a combination of the rate of oxidation of uric acid and the reaction of the intermediate species. In order to circumvent this problem two experimental approaches were employed. The first method used involved performing the enzymatic oxidation at pH 4.0 where the peroxidase catalyzed oxidation of uric acid occurs most rapidly.[22] Then, when $\geq$95% of the uric acid was oxidized the pH was rapidly adjusted to 7 or higher, where the intermediate species absorbs strongly, and the kinetics of reaction of the intermediate could be easily followed by a spectrophotometric method. This method will be referred to as the pH-step method. A typical rapid scan spectral response using the pH-step method is shown in figure 12. Thus, after rapid peroxidase catalyzed oxidation of uric acid at pH 4.0 then, on adjusting the pH to 7.0, the spectrum of the intermediate is essentially identical to that observed for the intermediate obtained upon electrochemical oxidation of uric acid, i.e., $\lambda_{max} \approx 302$ nm (see figure

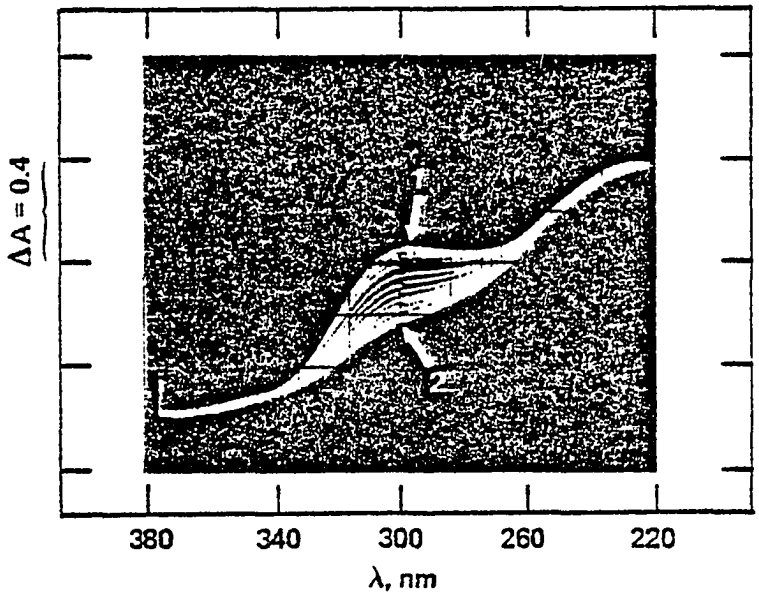

Figure 12. Rapid scan spectrophotometry of the absorbing intermediate formed upon oxidation of uric acid (200 μM) with type VIII peroxidase (0.34 μM) and H_2O_2 (400 μM) at pH 4.0. Following oxidation of uric acid the pH is adjusted to 7.0. Curve 1 is the initial spectrum, curve 2 that obtained about 11 minutes later.

Repetitive scans of 47 seconds.

11). That the spectrum of the u.v.-absorbing intermediate formed upon enzymatic oxidation of uric acid is the same as that formed by electrochemical oxidation is shown more clearly in figure 13. The kinetics of disappearance of the u.v.-absorbing intermediate observed upon peroxidase oxidation of uric acid using the pH-step method described were studied by monitoring the absorbance of the intermediate at 302 nm as a function of time (figure 14A). A typical rate plot for such an experiment is presented in figure 14B. Clearly, the plot of log $A-A_{\infty}$ versus time is linear indicating that the reaction of the absorbing intermediate species follows first-order kinetics. Values of the observed first-order solution rate constants for reaction of the u.v.-absorbing intermediate obtained using the pH-step method between pH 7 and 9.3 are presented in Table 5. Obviously, between pH 7 and 9.3 the value of the observed first-order rate constant ($0.0035\ sec^{-1}$) for reaction of the u.v.-absorbing intermediate formed enzymatically is identical to that formed electrochemically (see Table 4). The fact that the observed rate constant is independent of pH, at least between pH 7 and 9.3, indicates that the reaction of the intermediate is probably not base catalyzed over this pH range. The data presented in Table 5 also support the conclusion that the reaction of the intermediate is independent of the enzyme and uric acid concentration. The rate of oxidation of uric acid is, however, directly dependent on the enzyme concentration.

Attempts to measure the reaction kinetics for the u.v.-absorbing intermediate below pH 7 were difficult because the molar absorptivity of the intermediate significantly decreases. In addition, thin-layer

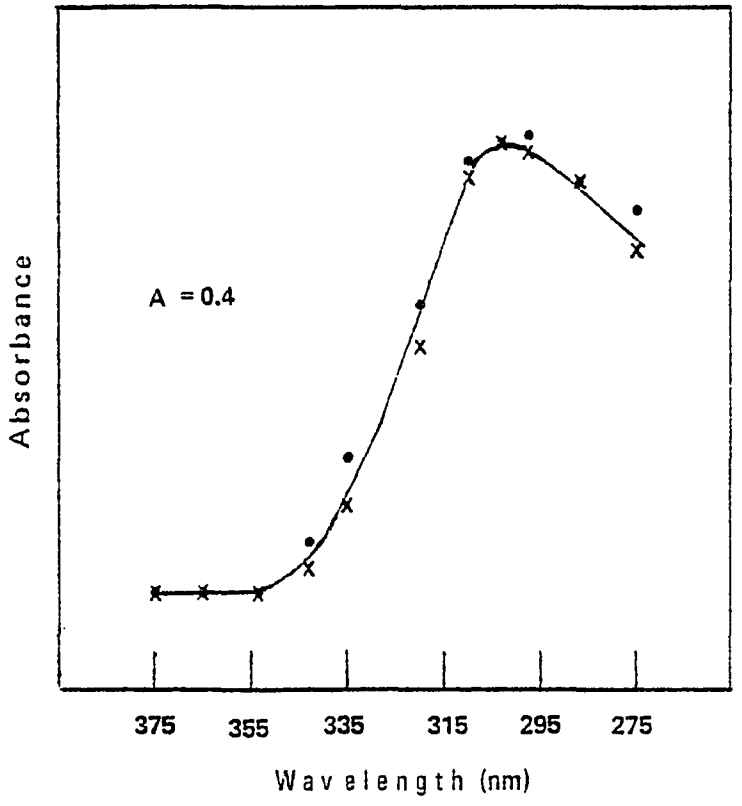

Figure 13. Comparison of the spectrum of the u.v.-absorbing intermediate formed upon electrochemical (X) and enzymatic (·) oxidation of uric acid. The enzymatic data points were obtained when uric acid (100 μM) was oxidized in the presence of type VIII peroxidase (0.17 μM) and H_2O_2 (200 μM) in phosphate buffer pH 7.0, ionic strength 1.0 M 5 min after initiation of the oxidation in a 1.0 cm cell. The electrochemical points were obtained when uric acid (5 mM) was oxidized at 0.9 V in a thin-layer cell (0.009 cm thick) at a gold minigrid electrode at a time when ≥90% of the uric acid was oxidized. The absorbance values obtained in the latter experiment were all multiplied by a constant factor of 2.24 to obtain the best fit to the enzymatic data points.

Figure 14. (A) Variation of the absorbance with time observed for the intermediate formed upon oxidation of uric acid (200 μM) with type VIII peroxidase (0.34 μM) and H_2O_2 (400 μM) at pH 4 followed by adjustment of the pH to 7.0.
(B) Kinetic plot of time versus log absorbance at 302 nm.

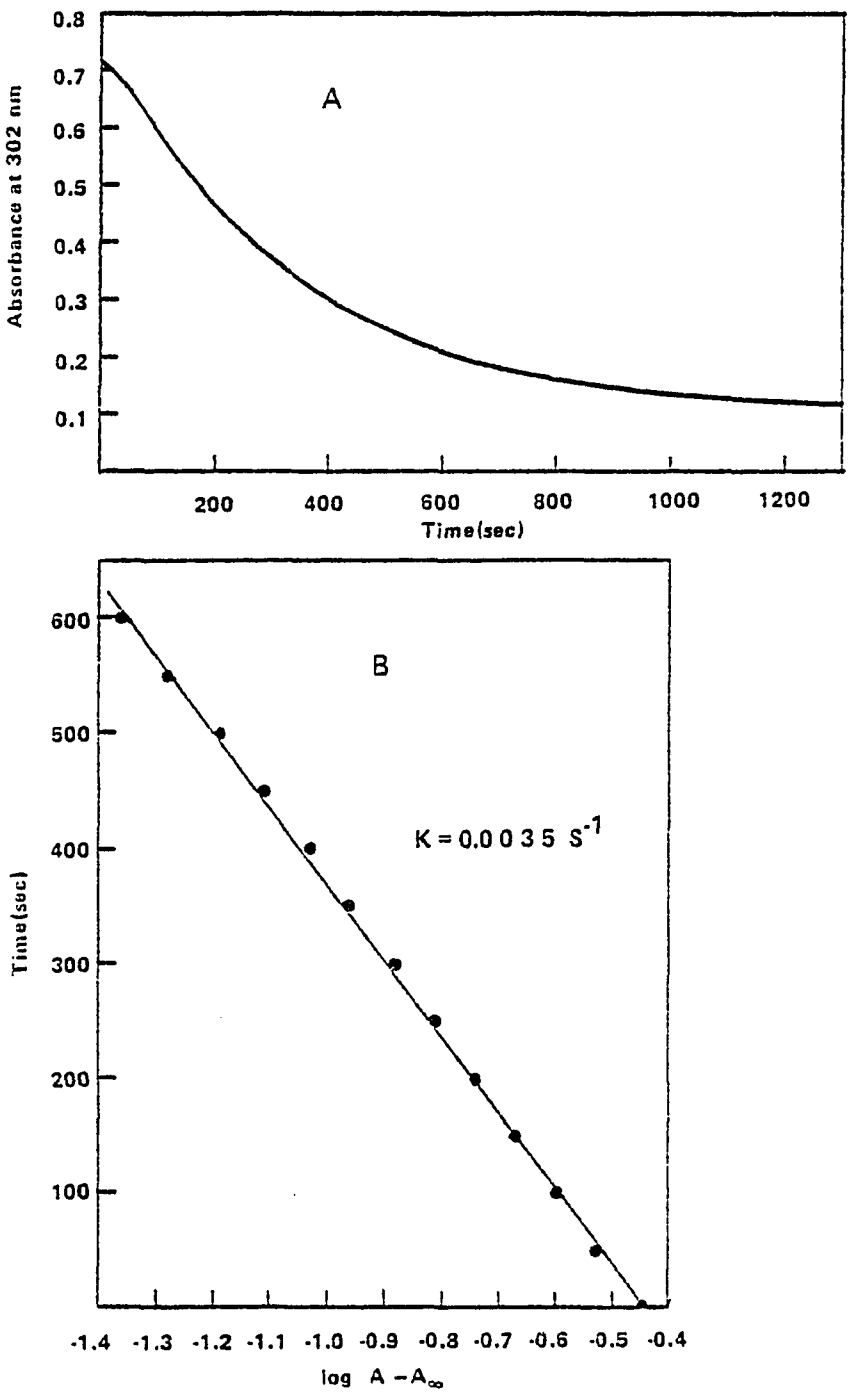

Table 5

Observed first-order rate constants for reaction of the u.v.-absorbing intermediate formed on oxidation of uric acid in the presence of type VIII peroxidase and H_2O_2 at pH 4.0 followed by pH adjustment

Initial Concentration of uric acid/μM	pH	HRP Concentration/μM	H_2O_2 Concentration/μM	k_{obs}/s^{-1}
20	7.0	0.17	200	0.0039
100	7.0	0.17	200	0.0039
200	7.0	0.17	200	0.0035
100	7.0	0.34	200	0.0037
100	7.0	0.034	200	0.0036
20	8.0	0.17	200	0.0036
100	8.0	0.17	200	0.0030
200	8.0	0.17	200	0.0032
20	9.27	0.17	200	0.0033
100	9.27	0.17	200	0.0032
200	9.27	0.17	200	0.0032
			Mean:	0.0035±0.0004

spectroelectrochemical studies which, because of the very thin reaction cell used, require rather high uric acid concentrations (≥2 mM) to produce measurable concentrations of the intermediate, become very difficult below pH 7 owing to the low solubility of uric acid. However, using the pH-step enzymatic method, the approximate first-order rate constant for reaction of the intermediate at pH 6.0 was ca. 0.006 sec^{-1} and at pH 4.8 0.0095 sec^{-1}. These values are much less reliable than those obtained at pH 7-9.3, but they do suggest

that the reaction of the intermediate might be somewhat acid catalyzed below pH 7.

In order that the conditions of the enzymatic oxidation parallel more closely the electrochemical oxidation of uric acid, it was decided to attempt to oxidize uric acid at pH 7 with type VIII peroxidase and, when a significant quantity of the u.v-absorbing intermediate had been formed, to terminate the oxidation reaction so that the decay of the intermediate could be observed without interference from the continuing oxidation of uric acid. It was found that the most successful method of doing this was to terminate the oxidation of uric acid by addition of a large excess of the enzyme catalase. The latter enzyme rapidly removes H_2O_2 from the reaction mixture. Using catalase to terminate the reaction of uric acid, H_2O_2, and peroxidase at pH 7.0 in this fashion (see Experimental for details) it was found that the u.v.-absorbing intermediate gave an observed first-order rate constant of 0.0035 sec^{-1}. If the oxidation of uric acid with peroxidase and H_2O_2 was carried out at pH 4.0 and then, when the uric acid was virtually all oxidized, the pH adjusted to 7.0 with a buffer solution containing catalase, the observed intermediate was 0.0034 sec^{-1}.

DISCUSSION

The studies reported here indicate that when uric acid is oxidized either electrochemically or with type VIII horseradish peroxidase an intermediate is formed which exhibits a well-defined u.v-absorption peak with λ_{max} = 302-304 nm between pH 7-9.3. This

intermediate species decays in a first-order process with an apparent rate constant of 3.5×10^{-3} sec^{-1} between pH 7 and 9.3. After complete oxidation the final spectrum corresponds to allantoin regardless of whether the oxidation is carried out electrochemically or enzymatically. The evidence, therefore, strongly supports the view that the same u.v.-absorbing intermediate is generated by both electrochemical and peroxidase catalyzed oxidation of uric acid.

In Chapter 2 it was demonstrated that under electrochemical conditions at gold or graphite electrodes uric acid is oxidized in a $2e^-$ reaction to a diimine species (II, equation 1, Chapter 1) which is very short lived (e.g., it has a half-life at pH 8.0 of about 21 ms). This diimine primary product is attacked by water in a (pseudo) first-order reaction to give the u.v.-absorbing intermediate described in this chapter which has been proposed[59] to be an imine-alcohol species (III, equation 1, Chapter 1). Clearly, since the imine-alcohol is formed under both electrochemical and enzymatic (peroxidase) conditions it seems quite justifiable to conclude that this species is derived from the same precursor under both oxidative conditions, i.e., from the diimine. There is no simple way to observe the diimine precursor formed upon enzymatic oxidation of uric acid because it is too unstable. The imine-alcohol formed either electrochemically or enzymatically is hydrated to the uric acid-4,5-diol (IV, equation 1, Chapter 1) which then breaks down to the various observed products.

This study establishes clearly, perhaps for the first time, that investigations of the electrochemical behavior of naturally occurring biological molecules can provide unique insights into the

possible biological redox reactions of such molecules. Indeed in the case of the electrochemical and enzymatic (peroxidase) oxidation of uric acid there is every evidence that the reactions are identical.

EXPERIMENTAL

Chemicals

Uric acid was obtained from Eastman and was used without further purification. Peroxidase, obtained from horseradish (crude, RZ≈0.3; type VI, RZ≈3.0; type VII, RZ≈3.0; type VIII, RZ≈3.0; and type IX, RZ≈3.2) was obtained from Sigma. The crude enzyme and the various isoperoxidases were stored at -5°C when not in use. Catalase was obtained from Sigma and had an activity of 2000 units mg^{-1} at 25°C. Buffer solutions were prepared from reagent grade chemicals. All buffers were prepared from potassium phosphates and had an ionic strength of 1.0 M with the exception of certain phosphate buffers at pH 4.0 which had an ionic strength of 0.1 M.

Apparatus

The apparatus used was described in Chapter 2.

Procedure for enzymatic oxidation of uric acid

Preliminary studies of the enzymatic oxidation of uric acid revealed that crude horseradish peroxidase had insufficient activity (i.e., caused only a slow reaction of uric acid) for our purposes. Accordingly, a number of partially purified isoperoxidases isolated from horseradish peroxidase were studied. Type VI peroxidase contains

two basic isoenzymes (the term basic indicates that the enzyme migrates towards the cathode in electrophoresis experiments of the type described by Davis[60]) but exhibited very little activity for uric acid. Type VII peroxidase, an acidic isoenzyme exhibited only slight uric acid activity. Type IX peroxidase, a basic isoenzyme, exhibited no uric acid activity. However, type VIII peroxidase, another acidic isoenzyme, exhibited quite high activity for uric acid and this isoenzyme was therefore used in our investigations.

The most convenient method for enzymatic oxidation of uric acid was to prepare suitable solutions of uric acid, type VIII peroxidase, and H_2O_2 in a pH 4.0 phosphate buffer having an ionic strength of 0.1 M. Then, 0.5 ml of the peroxidase and 0.5 ml of the uric acid solutions were transferred to a 1.0 cm quartz spectrophotometer cell and the cell placed into the spectrophotometer. The oxidation of uric acid was initiated by adding 0.5 ml of the H_2O_2 solution. Mixing was achieved by rapidly drawing the resulting solution in and out of a disposable pipet using a small pipetting bulb. The oxidation of uric acid was followed by monitoring its absorbance at 290 nm. When 95% or more of the uric acid had been oxidized, 1.5 ml of a phosphate buffer of the desired pH having an ionic strength of 1.0 M was added to the solution and the wavelength being monitored was switched to 302 nm. The latter wavelength corresponds to the λ_{max} of the absorbing intermediate species between pH 7.0-9.3. Mixing was achieved in the same manner described previously.

For experiments where the oxidation of uric acid with peroxidase and H_2O_2 was terminated with the enzyme catalase the following

procedures were employed. A solution was prepared from 0.5 ml each of suitable solutions of uric acid and type VIII peroxidase in phosphate buffer pH 4.0, ionic strength 0.1 M. The reaction was initiated with a mixture of 0.5 ml of 1200 μM H_2O_2 in pH 4.0 phosphate buffer, ionic strength 0.1 M, and 1 ml of pH 7.0 phosphate buffer, ionic strength 1.0 M. The latter volume of pH 7.0 buffer was sufficient to give the entire solution a pH of 7.0. When the oxidation of uric acid was ca. 95% complete 0.5 ml of pH 7.0 phosphate buffer ionic strength 1.0 M, containing 0.5 mg catalase was added and the solution mixed thoroughly. The absorbance of the u.v.-absorbing intermediate at 302 nm was then monitored as a function of time. For the pH-step method, the oxidation of uric acid in the presence of peroxidase and H_2O_2 was carried out at pH 4.0 in a phosphate buffer of ionic strength 0.1 M, and when oxidation of the uric acid was ca. 95% complete the pH was adjusted with 1.5 ml of a phosphate buffer pH 7.0 with an ionic strength of 1.0 M which contained 0.5 mg of catalase. The solution was mixed thoroughly and again the reaction of the u.v.-absorbing intermediate was followed spectrophotometrically at 302 nm.

Test solutions utilized for thin-layer spectroelectrochemical studies were 5 mM in uric acid. The buffer systems consisted of 50% of a pH 4.0 phosphate buffer having an ionic strength of 0.1 M and 50% of a phosphate buffer of the desired pH value having an ionic strength of 1.0 M. The procedures used in thin-layer spectroelectrochemical studies of uric acid were essentially the same as those in Chapter 2 except that in studies involving repetitive spectral

sweeps a rather larger spectral range (225-375 nm) was scanned. R.s.s. studies of the enzymatic oxidation of uric acid scanned the same spectral region.

SUMMARY

The oxidation of uric acid was studied by thin-layer spectroelectrochemistry using an optically transparent gold minigrid electrode and enzymatically using peroxidase. Under both enzymatic and electrochemical conditions a u.v.-absorbing intermediate (λ_{max} = 302-304 nm between pH 7-9.3) is observed. This intermediate is proposed to be an imine-alcohol species formed by rapid hydration of the primary reaction product, which is a diimine. Under the conditions employed in both the enzymatic and electrochemical studies the imine-alcohol intermediate is hydrated in a first-order reaction with an observed rate constant of 3.5×10^{-3} sec^{-1} between pH 7-9.3. This study establishes the similarity between the electrochemical and enzymatic oxidation, and indicates that electrochemical investigations of the redox behavior of purines can provide unique insights into their biological redox properties.

ENZYMATIC AND ELECTROCHEMICAL OXIDATION OF GUANOSINE

CHAPTER 4

INTRODUCTION

Guanosine is an important constituent of biological systems. In the past, however, the oxidation of guanosine had not been thoroughly studied. It was decided, therefore, to undertake a detailed study of the electrochemical and enzymic oxidations of guanosine. It was felt that the techniques utilized in the studies of uric acid and xanthine, such as rapid scan spectroscopy and thin-layer spectroelectrochemistry, would be particularly useful in elucidating mechanistic details. Obviously, however, other techniques would be needed as well, such as the more traditional electrochemical methods, a wide variety of separation methods, and mass spectroscopy.

RESULTS

Voltammetry

Guanosine is oxidized at the PGE *via* three peaks (see figure 15). A 0.5 mM guanosine solution at a 5 mV sec^{-1} sweep rate shows the following pH dependence:

$$E_{P_{III_a}} = (1.16-0.050\ pH)V,\ pH\ 4-11$$

$E_{p_{IV_a}}$ = (1.18-0.035 pH)V, pH 2-11

$E_{p_{V_a}}$ = (1.33-0.031 pH)V, pH 2-8

$E_{p_{V_a}}$ = 1.08 V, pH 8-11

If the sweep is reversed after scanning through peak V_a two reduction peaks are observed (see figure 15). At pH 7 peak I_c occurs at 0.35 V and peak II_c at -0.75 V. Peak II_c occurs in the midst of a general plateau. This plateau almost completely disappears if the potential sweep is reversed between peaks IV_a and V_a (pH 7-9.3), while peaks I_c and II_c are still readily observed. Upon reversing the sweep after scanning through peak II_c to begin a second positive going sweep two new oxidation peaks appear. At pH 7 and 200 mV sec^{-1} sweep rate peak I_a occurs at E_p = 0.36 V and peak II_a at E_p = 0.43 V (see figure 15).

A concentration study was performed for guanosine at pH 7 using a sweep rate of 5 mV sec^{-1}. Figure 16 shows the plots of peak current (i_p) *versus* the bulk concentration of guanosine (C_o). For a process in which no adsorption is occurring this plot should be a straight line passing through the origin. The curvature of the plots indicates some adsorption is occurring in all three peaks. The rise in i_p for peak III_a at low concentrations and the attainment of a limiting current at about 0.3 mM could indicate an adsorption peak.[61] The view that peak III_a is an adsorption peak is further supported by its disappearance above 0.75 mM. Adsorption peaks are often not observed at high concentrations because the adsorption current becomes a very small component of the total current.[61]

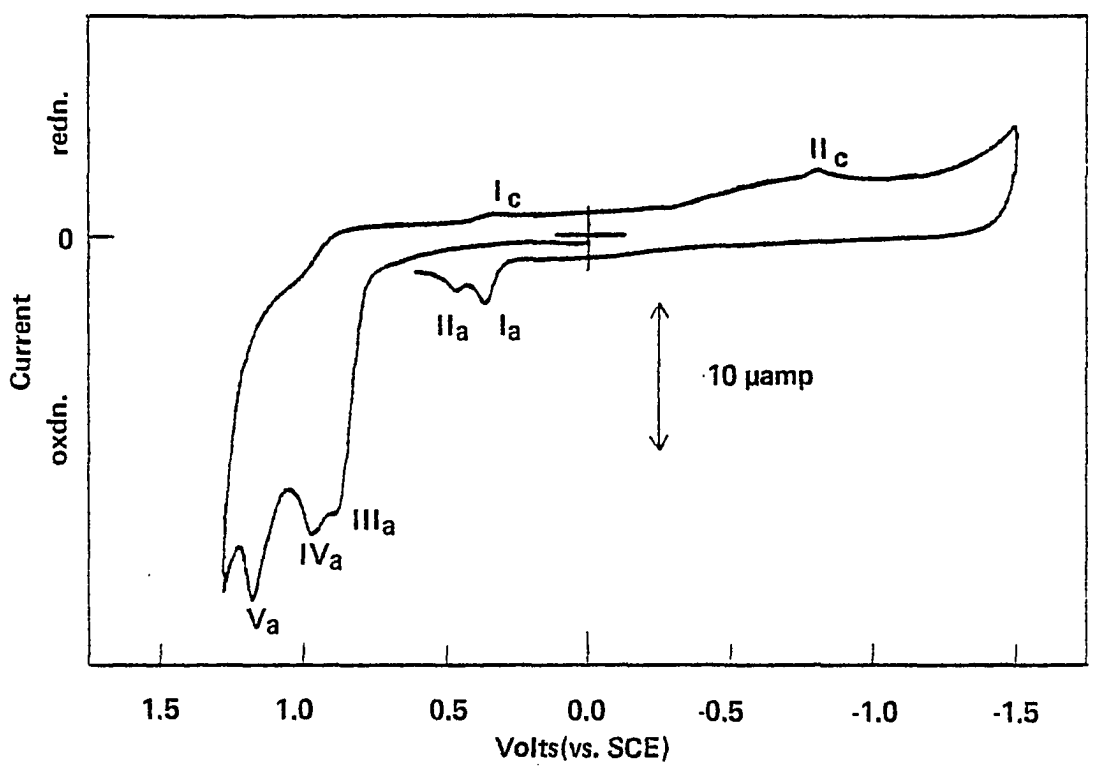

Figure 15. Cyclic voltammogram of 0.5 mM guanosine in pH 7 phosphate buffer at a PGE with an area of 0.016 cm^2. Sweep rate = 200 mV sec^{-1}.

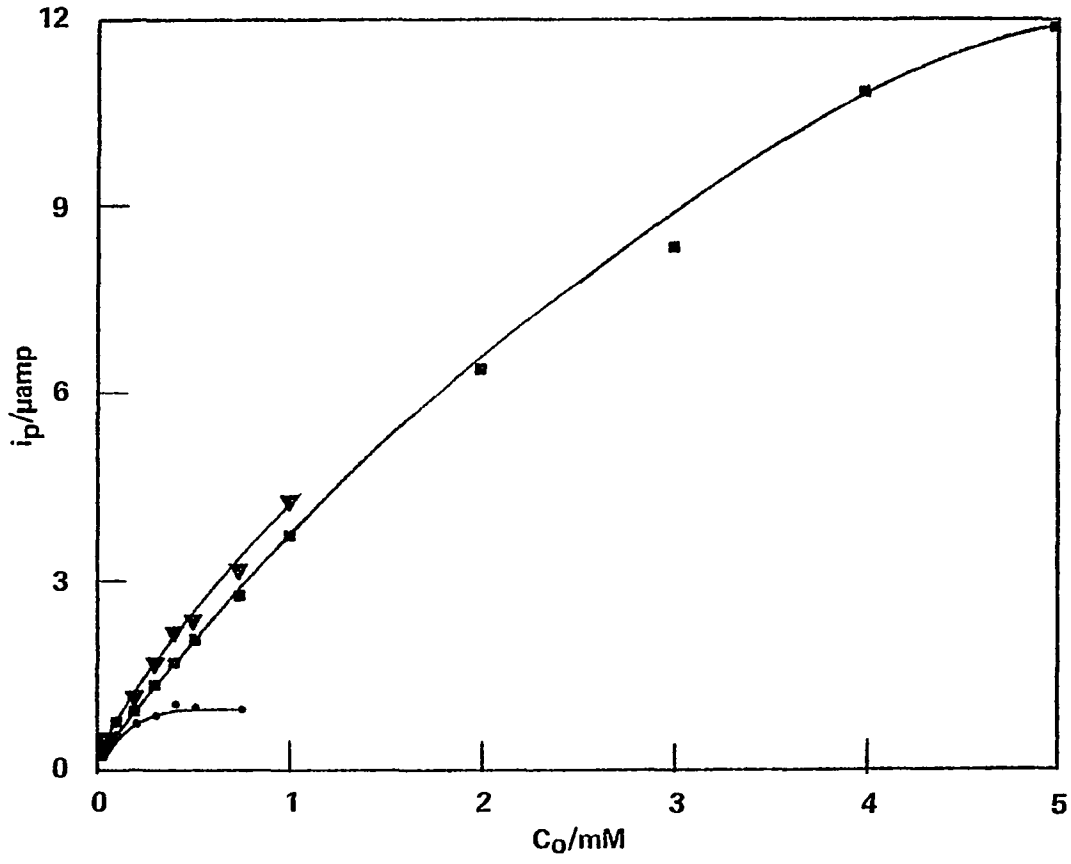

Figure 16. Plot of peak current (i_p) versus concentration (Co) for peaks III_a (•), IV_a (■), and V_a (▼) of guanosine at pH 7 and 5 mV sec^{-1} sweep rate.

Careful examination of the voltammograms shows that peak V_a is present, but too small to measure accurately at 2, 3, and 4 mM (see figure 17). At guanosine concentrations above 4.0 mM peak V_a was not observable at all. It seems that at concentrations above 1 mM peak IV_a broadens until above 4 mM peak V_a can not be observed.

A scan rate study was performed using a 0.5 mM solution of guanosine in pH 7 phosphate buffer. Figure 18 shows plots of $i_p/C\ V^{1/2}$ versus $V^{1/2}$ (where V = scan rate in Volts sec^{-1}). For an uncomplicated diffusion controlled process a plot of $i_p/C_o\ V^{1/2}$ versus $V^{1/2}$ should be a horizontal line.[61] The increase in the peak current function with increasing scan rate indicates that at least some adsorption is occurring in all three of the oxidation peaks of guanosine. The downturn at very high sweep rates of the peak current function for peaks III_a and IV_a is probably due to changes in the peak shape. Figure 19 shows a voltammogram of guanosine run at 5 V sec^{-1} sweep rate. Compared to the voltammogram in figure 15 peaks III_a and IV_a in figure 19 are more severely overlapped which causes inaccuracies in the measurement of i_p.

Peak III_a also shows some indications of being strictly an adsorption peak. For example, the ratios $i_{p_{III_a}}/I_{p_{IV_a}}$ and $i_{p_{III_a}}/i_{p_{V_a}}$ (see Table 6) increase with increasing scan rate up to 0.5 V sec^{-1}. The inconsistencies above 0.5 V sec^{-1} can be explained by the changes in the peak shape discussed earlier in this section. The increase in peak current ratios seen in Table 6 is consistent with the idea that peak III_a is an adsorption peak.

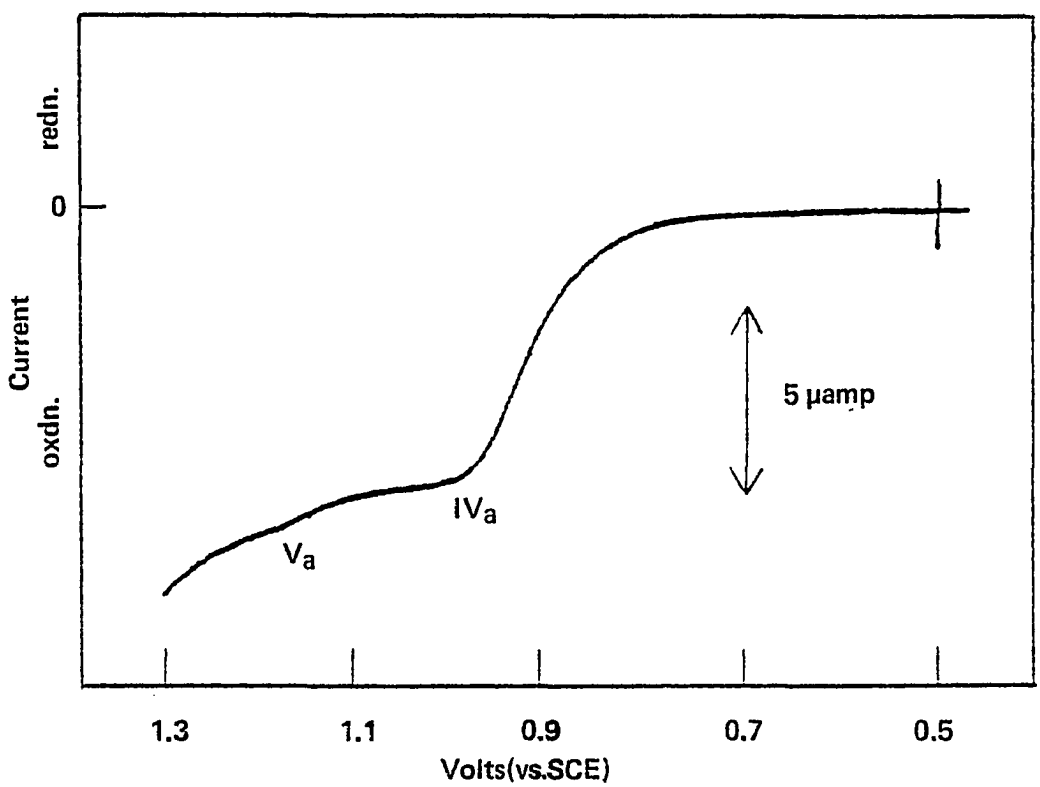

Figure 17. Linear sweep voltammogram of 3 mM guanosine in pH 7 phosphate buffer at a sweep rate of 5 mV sec^{-1}.

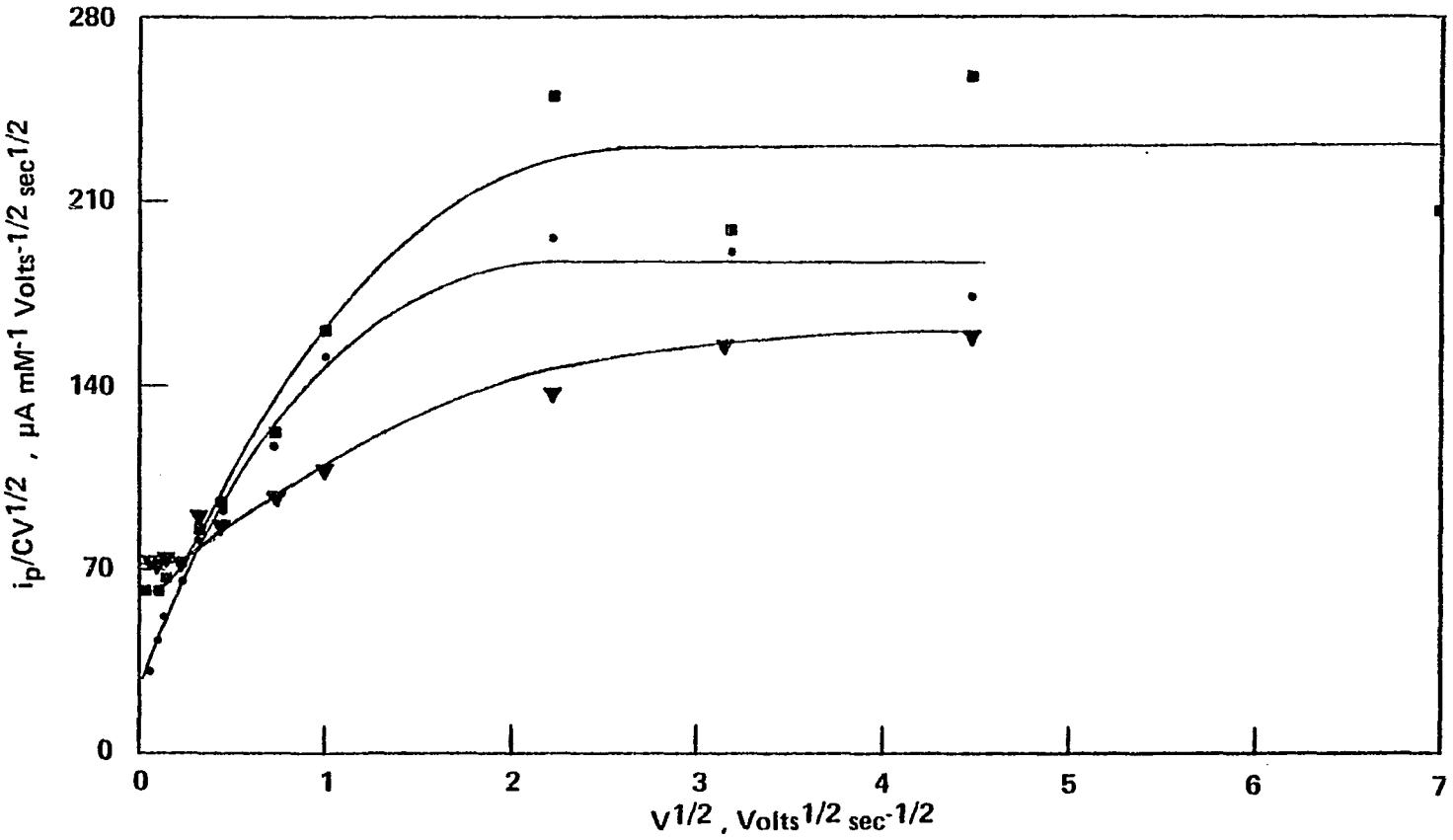

Figure 18. Plot of peak current function ($i_p/CV^{1/2}$) versus the square root of scan rate ($V^{1/2}$) for voltammetric peaks III_a (•), IV_a (■), and V_a (▼) of a 0.5 mM guanosine solution in pH 7 phosphate buffer.

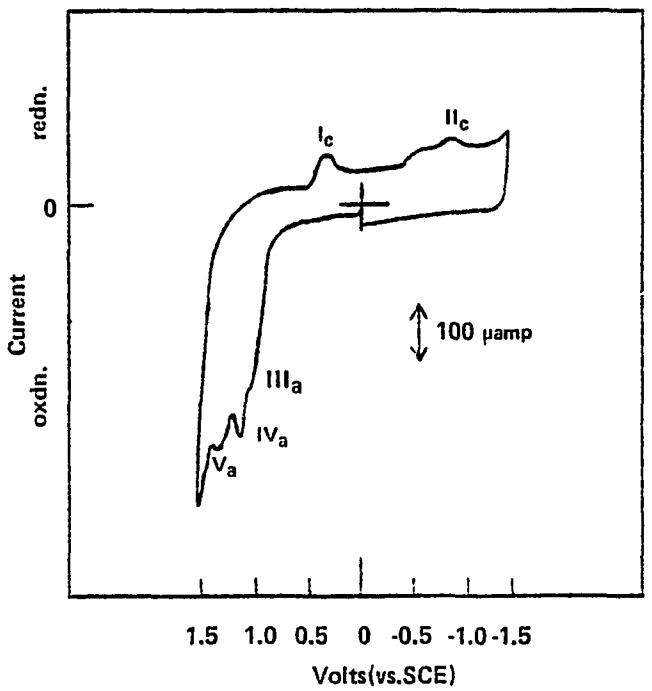

Figure 19. Cyclic voltammogram of 0.5 mM guanosine in pH 7 phosphate buffer at a sweep rate of 5 V sec^{-1}.

Table 6

Peak current ratios for electrooxidation peaks III_a, IV_a, and V_a of 0.5 mM guanosine at pH 7

Scan rate (V sec^{-1})	$i_{p_{III_a}}/i_{p_{IV_a}}$	$i_{p_{III_a}}/i_{p_{V_a}}$
0.005	0.52	0.44
0.010	0.68	0.61
0.020	0.79	0.70
0.050	0.90	0.87
0.10	0.96	0.90
0.20	0.97	1.06
0.50	0.99	1.23
1.0	0.95	1.44
5.0	0.79	1.42
10.0	0.98	1.24
20.0	0.67	1.09
50.0	-	-

Peak V_a is not observed at sweep rates above ca. 20 V sec^{-1} because it shifts to such positive potentials that it is obscured by background oxidation.

It was considered likely that guanosine would be initially oxidized to 8-hydroxyguanosine. For that reason voltammetric studies were carried out on 8-hydroxyguanosine.

8-Hydroxyguanosine is oxidized at the PGE via three voltammetric

oxidation peaks (see figure 20). The three peaks show the following pH dependence:

$$E_{p_{I_a}} = (0.732-0.056\ pH)V,\ pH\ 2-11$$

$$E_{p_{II_a}} = (0.758-0.052\ pH)V,\ pH\ 2-11$$

$$E_{p_{III_a}} = (1.172-0.038\ pH)V,\ pH\ 2-7$$

$$E_{p_{III_a}} = 0.87\ V,\ pH\ 8-10$$

On the reverse sweep towards negative potentials reduction peaks I_c and II_c are observed at $E_p = 0.35$ V and $E_p = -0.75$ V respectively at pH 7 (see figure 20). Both peaks can be enhanced by reversing the sweep at potentials between 0.6 and 0.4 volts (see figure 21). In addition it is necessary to sweep only into oxidation peak I_a in order to observe reduction peaks I_c and II_c.

The variation of the peak current with concentration for 8-hydroxyguanosine was studied in pH 7 phosphate buffer at a sweep rate of 5 mV sec^{-1} over the concentration range 0.05-5.0 m$\underline{M}$. The results are shown in figure 22. At 0.005 V sec^{-1} peak III_a was observable only at concentrations below 1 m$\underline{M}$. Even at concentrations where peak III_a is observable it is too small to measure accurately (see figure 23). The nonlinearity of the i_p/C_o plots indicates adsorption is occurring in both oxidation peaks.[61] The behavior of peak II_a is typical of an adsorption peak. That is at low concentrations (below 0.1 m$\underline{M}$) it is larger than peak I_a. For 8-hydroxyguanosine concentrations above 0.1 m$\underline{M}$ peak II_a diminishes with respect to oxidation peak I_a until above

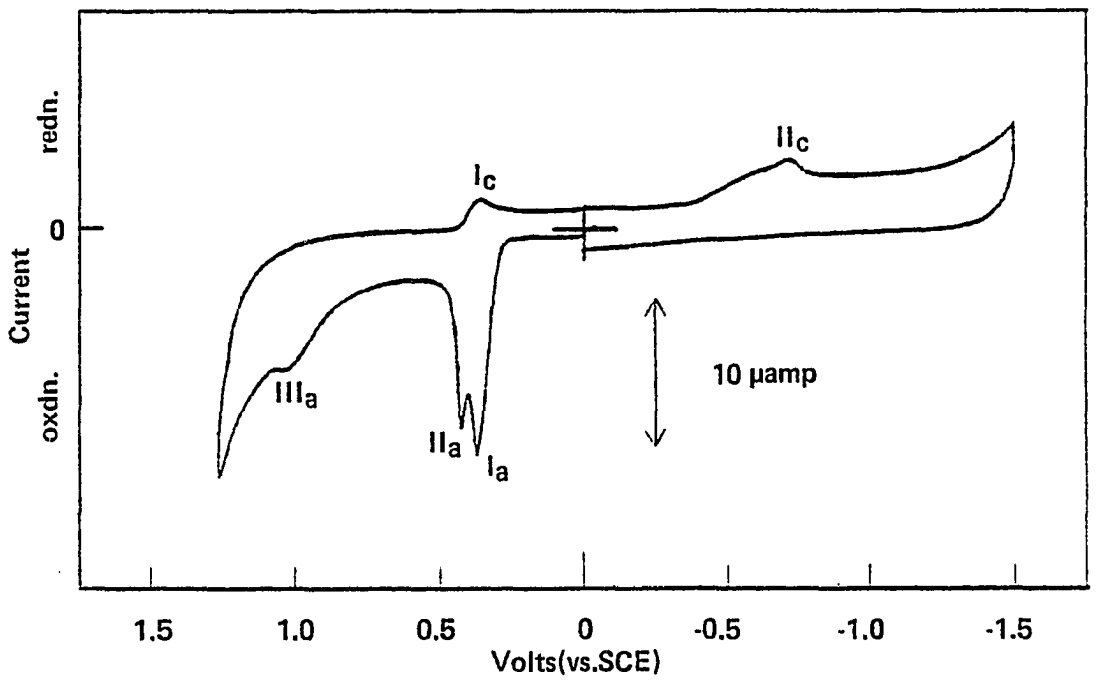

Figure 20. Cyclic voltammogram of 0.5 mM 8-hydroxyguanosine in pH 7 phosphate buffer at a PGE with an area of 0.016 cm^2. Sweep rate = 200 mV sec^{-1}.

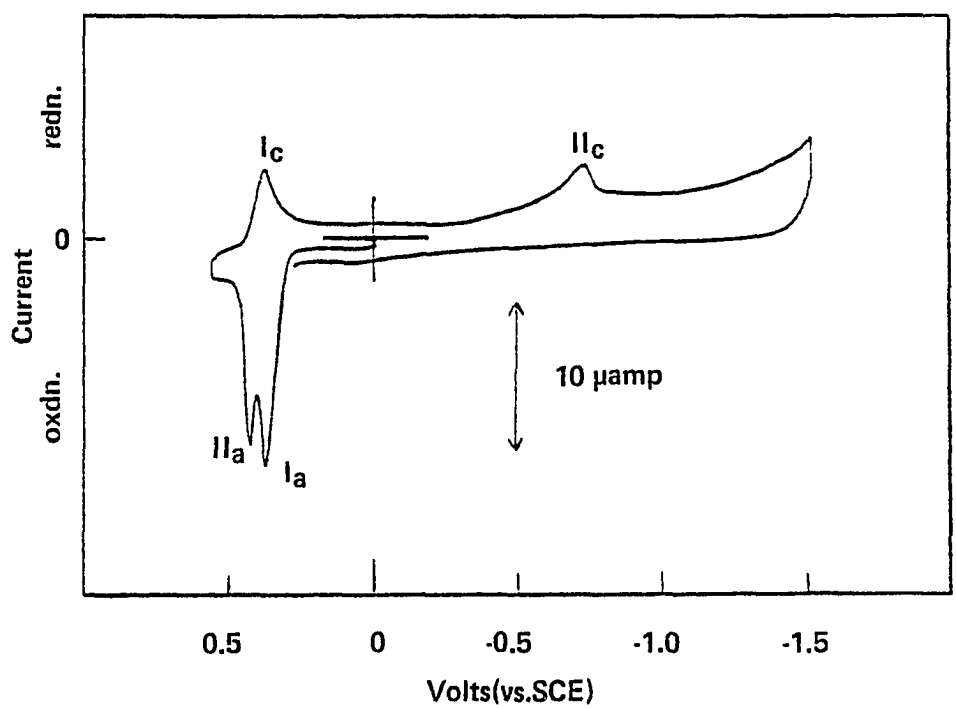

Figure 21. Cyclic voltammogram of a 0.5 mM 8-hydroxyguanosine solution at pH 7 and 200 mV sec^{-1} sweep rate.

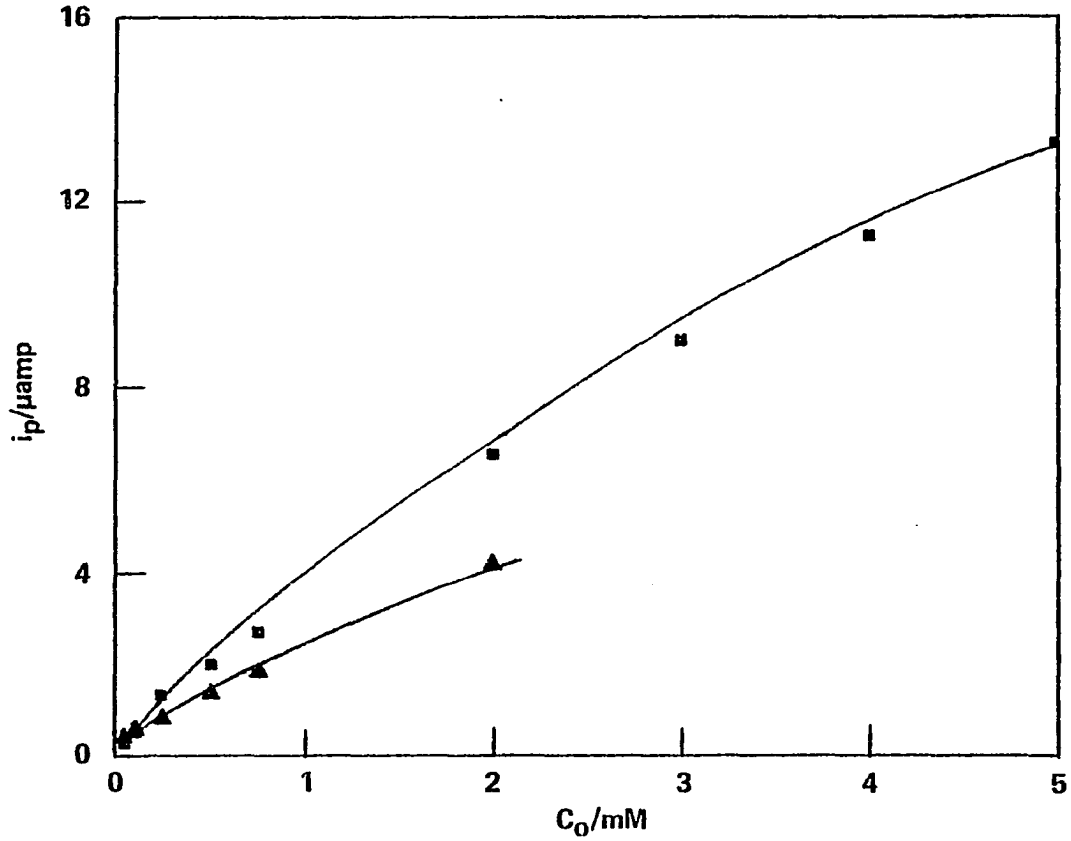

Figure 22. Plot of peak current (i_p) versus concentration (Co) for oxidation peaks I_a (■) and II_a (▲) of 8-hydroxyguanosine in pH 7 phosphate buffer at a sweep rate of 5 mV sec^{-1}.

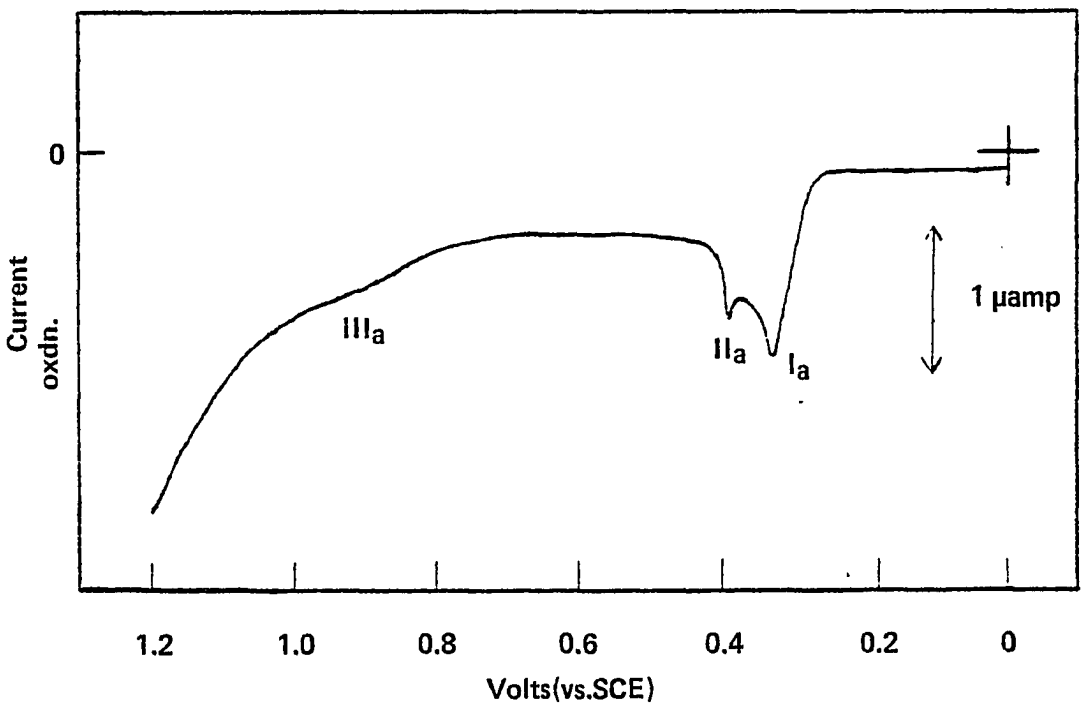

Figure 23. Linear sweep voltammogram of 0.25 mM 8-hydroxyguanosine solution at pH 7 and a sweep rate of 5 mV sec^{-1}.

2.0 m$\underline{M}$ peak II_a is not observed.

A scan rate study was also performed at pH 7 utilizing a 0.5 m$\underline{M}$ 8-hydroxyguanosine solution. Oxidation peaks I_a and II_a both show an increase in peak current function with increasing scan rate (see figure 24). In both cases the increase in peak current function indicates adsorption is occurring. The downturn in the peak current function at sweep rates higher than 1 V sec^{-1} for peak I_a and 20 V sec^{-1} for peak II_a (see figure 24) is probably due to the obvious changes in peak shape which can be seen in figure 25. As can be seen in Table 7 the ratio of peak current functions (II_a/I_a) increases with increasing scan rate which indicates oxidation peak II_a is an adsorption peak.

Thus it would appear from the occurrence of oxidation peaks I_a and II_a on the second positive going sweep of guanosine, and the

Table 7

Peak current ratios for electrooxidation peaks I_a and II_a of 0.5 m$\underline{M}$ 8-hydroxyguanosine at pH 7

Scan rate (v sec^{-1})	$I_{p_{II_a}}/I_{p_{I_a}}$
0.005	0.68
0.020	0.69
0.10	0.79
0.20	0.82
0.50	0.97
1.0	1.04

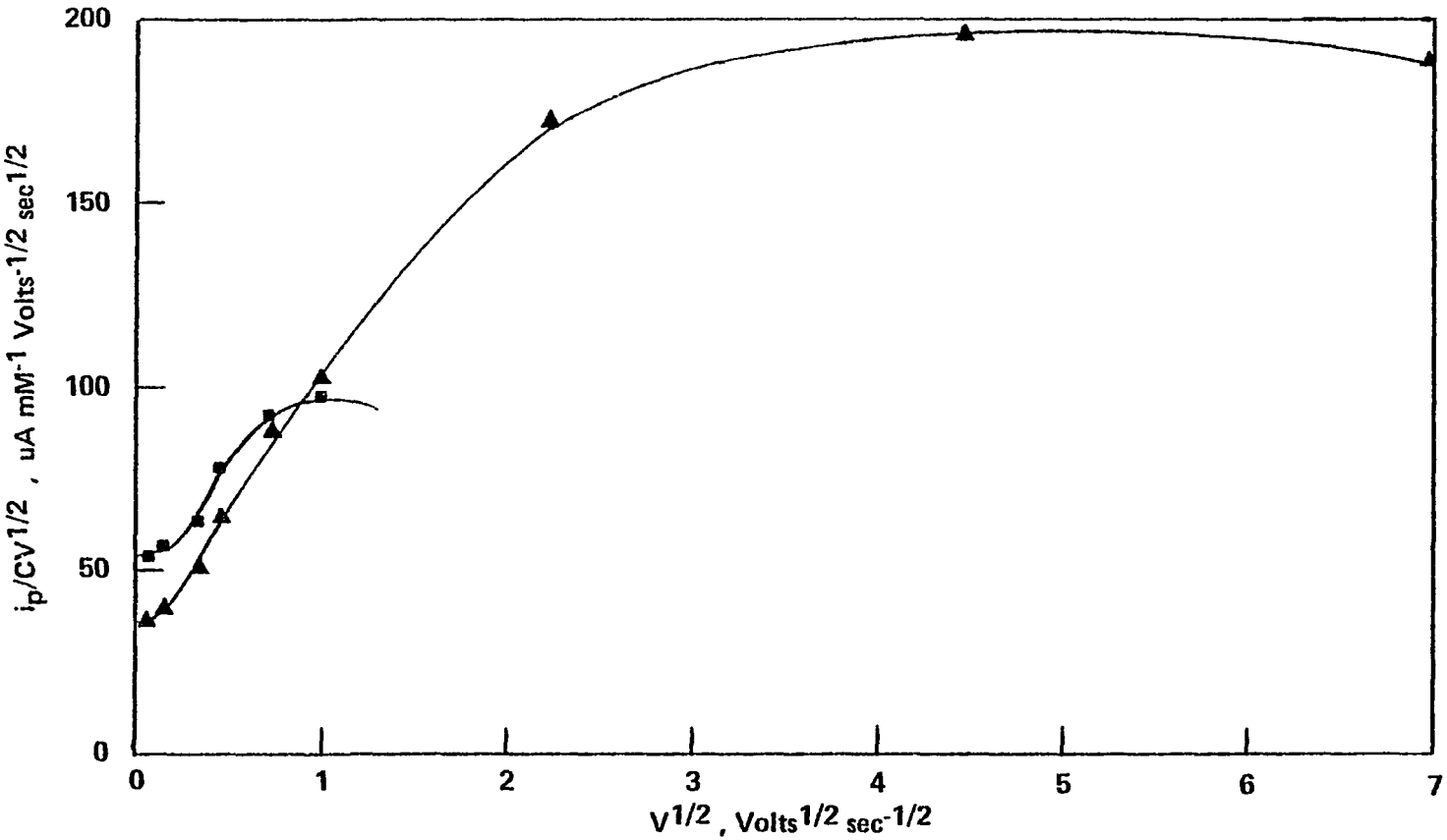

Figure 24. Plot of peak current function ($i_p/CV^{1/2}$) versus the square root of sweep rate ($V^{1/2}$) for peaks I_a (■) and II_a (▲) of 0.5 mM 8-hydroxyguanosine in pH 7 phosphate buffer.

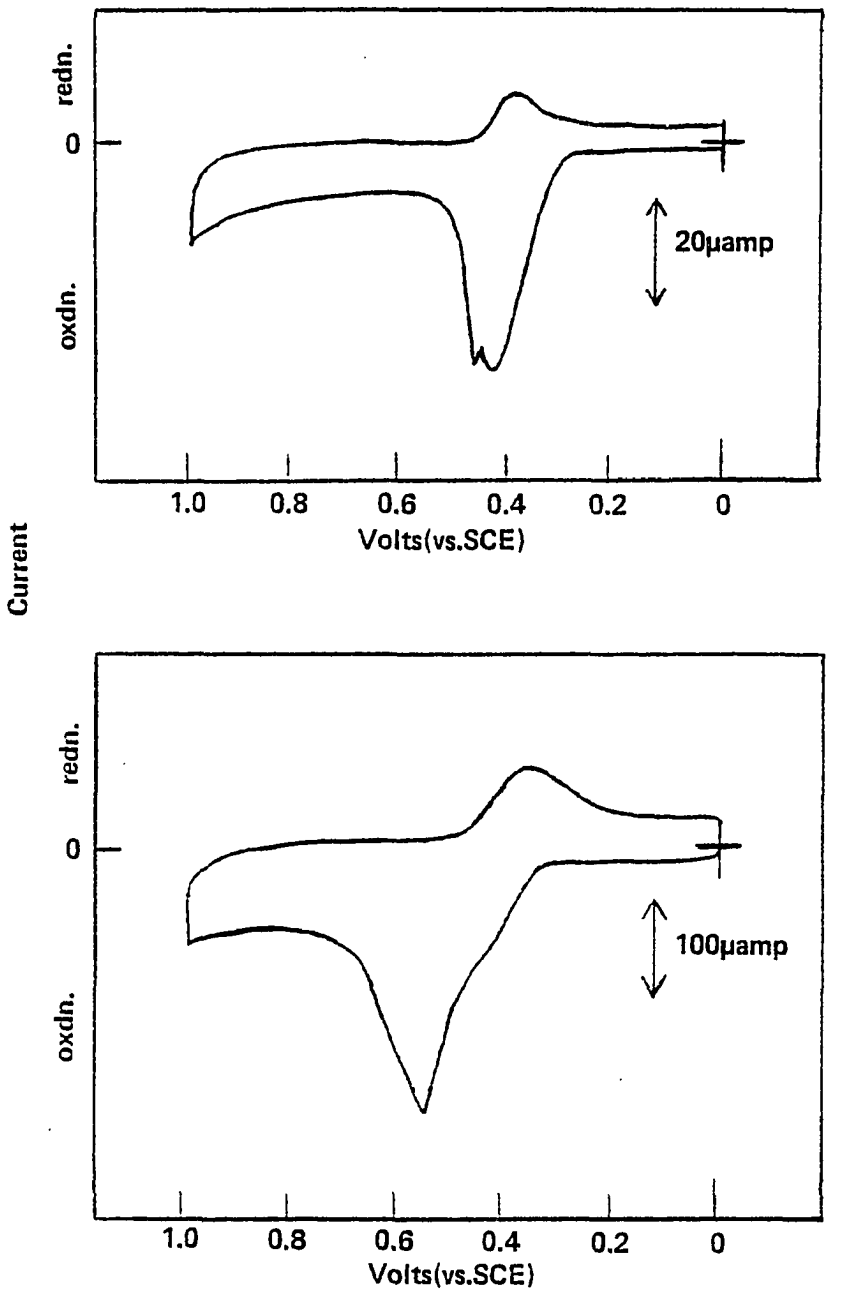

Figure 25. Cyclic voltammograms of 0.5 mM 8-hydroxyguanosine in pH 7 phosphate buffer at sweep rates of 0.5 V sec^{-1} (upper trace) and 5.0 V sec^{-1} (lower trace).

fact that at pH 7 oxidation peaks I_a and II_a of 8-hydroxyguanosine occur at the same potentials as peaks I_a and II_a of guanosine (0.36 V and 0.43 V, respectively) that one of the steps in the oxidation of guanosine is the formation of 8-hydroxyguanosine.

The occurrence and behavior of reduction peaks I_c and II_c in guanosine and 8-hydroxyguanosine is very similar to the behavior of the reduction peaks in the voltammetry of guanine[62] and uric acid.[39] This would suggest a mechanism analogous to guanine (see equation 2, Chapter 1). That is guanosine is oxidized to 8-hydroxyguanosine (as indicated by oxidation peaks I_a and II_a), 8-hydroxyguanosine is oxidized to a diimine species (III, equation 1) (indicated by reduction peak I_c), the diimine hydrolyses to an imine-alcohol (IV, equation 1) (believed to be represented by reduction peak II_c). The imine-alcohol would then further hydrolyze to form a 4,5-diol (V, equation 1) and this diol would then break up to final products.

While the voltammetric data does indicate that the reaction proposed above occurs the voltammetric data does not indicate that these are the only reactions occurring or even necessarily the major reactions occurring. Obviously oxidation peak V_a of guanosine and oxidation peak III_a of 8-hydroxyguanosine are not explained by the scheme proposed above since it is not necessary to scan into either of these peaks in order to see reduction peaks I_c and II_c. Presumably peak V_a of guanosine and III_a of 8-hydroxyguanosine are due to the oxidation of some product or intermediate formed during the oxidations at more negative potentials. This is not to suggest that peak V_a of guanosine and peak III_a of 8-hydroxyguanosine represent the same

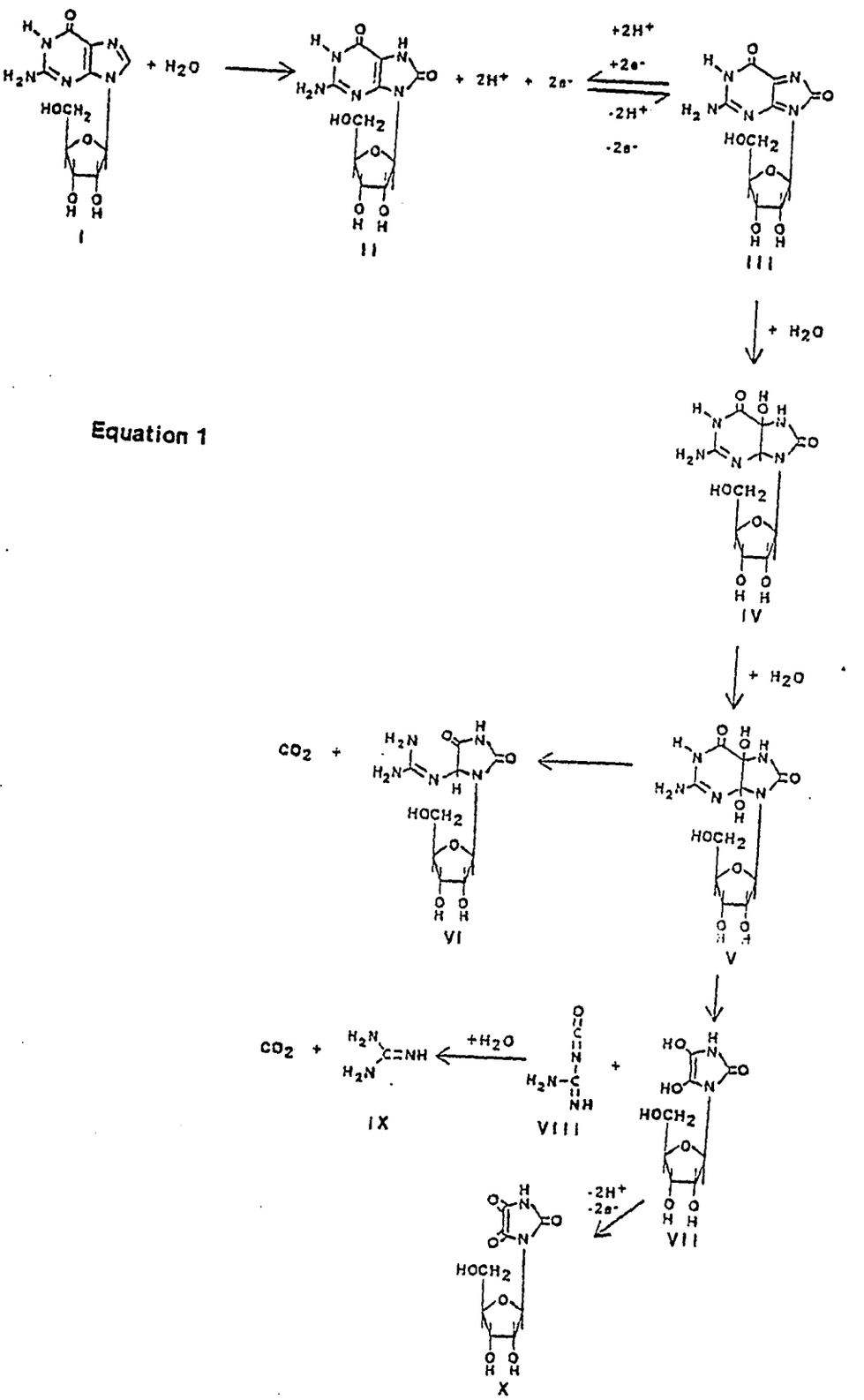

Equation 1

process. The peak potentials (see figures 15 & 20) are too different for them to both be the oxidation of the same molecule, but both do appear to be the oxidation of a product or intermediate.

The scan rate study and concentration study of 8-hydroxyguanosine clearly show that peak II_a is an adsorption peak.

The various voltammetric studies of guanosine appear to indicate that peak III_a in the voltammetry of guanosine is also an adsorption peak.

Coulometry

Coulometry was performed on guanosine at potentials corresponding to peak IV_a or V_a (see Table 8 for n values). Since peak III_a is an adsorption peak and will not contribute to the n-value no electrolyses were performed at peak III_a potentials. Initial coulometric experiments at pH 7 utilizing 0.3 mM and 0.8 mM guanosine were performed at peak IV_a potentials (≈0.95 V) until voltammetric peak IV_a was eliminated. At this point peak V_a was smaller, but still present and the n-value was 3.5±0.08. If coulometry was carried out at a potential corresponding to oxidation peak V_a the n-value increased to 5.0±0.11 and all oxidation peaks disappeared. The n-values obtained at peak V_a potentials remains approximately 5.0 over the concentration range 0.3-1.6 mM (see Table 8). When a wider concentration range was investigated at peak IV_a potentials (≈0.95 V at pH 7) it was found that the n-value changed at low (0.1 mM) and high (≥2 mM) concentrations. At low concentrations the n-value is approximately 5.0 (see Table 8) and at high concentrations it is 1.7±0.1 (see Table 8). This type of

Table 8

Coulometric n-values of guanosine at pH 7

Concentration (mM)	Oxidation peak	n
0.05	IV_a	5.3
0.05		6.0
0.05		5.2
0.30		3.6
0.30		3.6
0.30		3.4
0.65		3.5
0.80		3.5
2.50		1.6
3.20		1.7
2.50		1.8
0.30	V_a	4.8
0.30		4.9
0.30		5.0
0.80		5.0
0.80		5.1
0.80		5.0
0.80		4.9
0.80		5.1
0.80		5.1
0.80		5.0
1.30		5.0
1.30		5.1
1.60		4.9
1.60		5.2
1.60		5.2
1.60		5.1

behavior could indicate a competing 1e process or a second-order process. A dimerization step is a distinct possibility.

Initial coulometric studies of 8-hydroxyguanosine were performed utilizing 0.84 mM and 0.67 mM concentrations of 8-hydroxyguanosine at pH 7. When peak I_a or II_a potentials (0.38-0.5 V) were used on n-value of 1.92±0.006 was obtained. After an electrooxidation at

these potentials peaks I_a and II_a were gone, but peak III_a was unchanged. Oxidation at potentials corresponding to peak III_a gave n-values of 2.5±0.10 (see Table 9) and no oxidation peaks could be observed at the end of the electrolysis. However, when much higher and lower concentrations were investigated quite different results were obtained. At low concentrations (0.1 mM, see Table 9) an n-value of 1.95 0.05 was obtained at peak II_a potentials (≈0.5 V) and 3.05±0.25 at peak III_a potentials (≈1.0 V). For concentrations of 2.0 mM and higher the n-value was approximately 1.2 at peak II_a and peak III_a potentials.

It is obvious, from the coulometric data that neither guanosine nor 8-hydroxyguanosine is being oxidized in a manner strictly following equation 1 despite the indications from voltammetry that such processes are occurring. It would seem then that for both compounds there is some competing process taking place. The coulometric data would not be inconsistent with the formation of a dimer. Xanthosine, a molecule similar to guanosine, has been shown to form a dimeric species in which the number eight carbon in two xanthosine molecules are linked.[63] A dimer such as this is possible for guanosine, but not possible for 8-hydroxyguanosine. Since the liquid chromatographic separation of products formed upon oxidation of guanosine and 8-hydroxyguanosine suggest that the products formed are essentially the same (see figures 26-30) it would seem necessary that a different type of dimer be formed. It is likely that if a dimer is formed it is via an N-N bond.

Table 9

Coulometric n-values of 8-hydroxyguanosine at pH 7

Concentration (mM)	Oxidation peak	n
0.84	I_a	1.92
0.03	II_a	1.90
0.05		2.00
0.67		1.91
0.67		1.92
0.84		1.92
2.00		1.10
3.00		1.15
0.05	III_a	3.3
0.05		2.8
0.67		2.3
0.67		2.5
0.84		2.4
0.84		2.6
0.84		2.5
0.84		2.4
2.00		1.2
2.50		1.1

Product separation on G-10 Sephadex

In order to compare the products obtained from the oxidations performed in the coulometry in the previous section identical chromatographic separations were carried out on electrolysis product mixtures obtained by oxidizing guanosine (pH 7) at peak IV_a and V_a potentials and from oxidizing 8-hydroxyguanosine (pH 7) at peak II_a and III_a potentials, and at 1.15 V. Chromatography was performed using a single column of Sephadex G-10 with 0.025 M pH 7 phosphate buffer as the eluant (see Experimental for details). Figure 26 shows a typical chromatogram of the product mixture obtained from guanosine oxidized

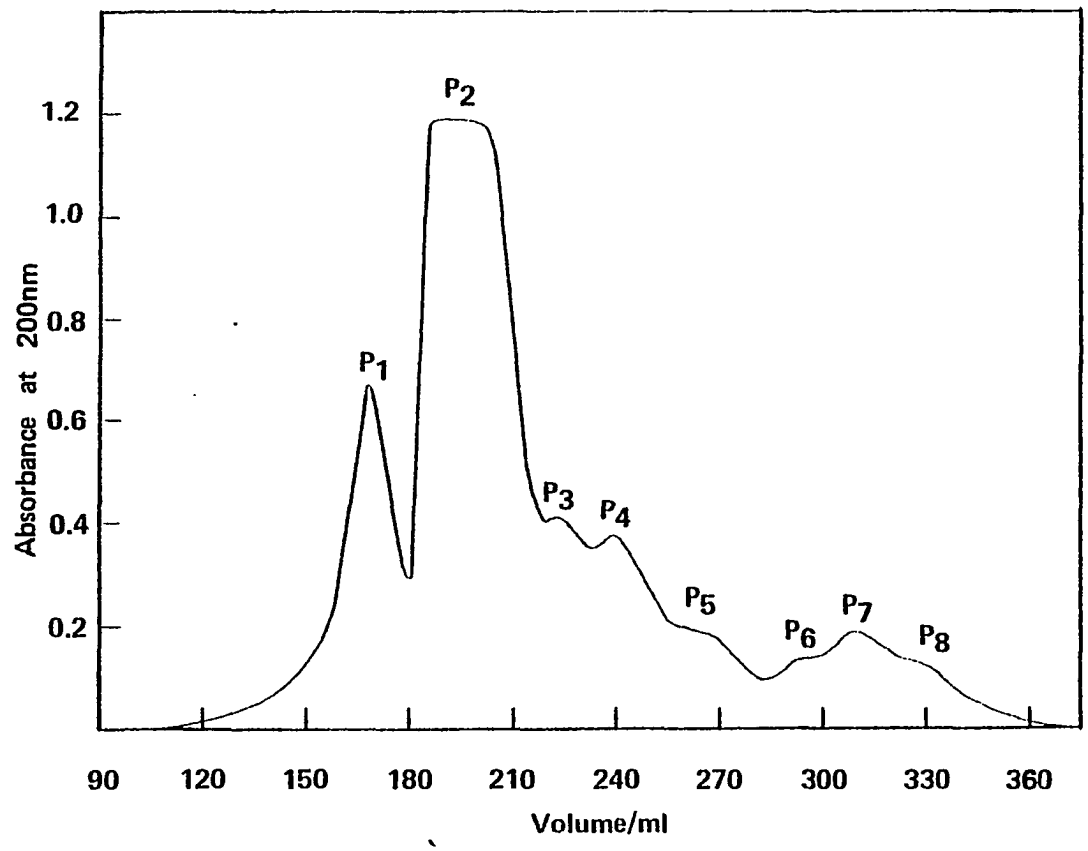

Figure 26. Liquid chromatogram of the products from the oxidation of a pH 7, 0.8 mM guanosine solution at 1.15 V (peak V_a) utilizing a single 90 cm x 2.5 cm column of G-10 resin with 0.025 M pH 7 phosphate buffer as the eluant.

at peak V_a potential (ca. 1.15 V). Peak 1 is inorganic phosphate (used in the electrolysis buffer). Peaks 2-8 are oxidation products with peak 2 being the major product (although you cannot necessarily assume that peak 2 represents only one product). Figure 27 is a chromatogram of the products obtained upon electrooxidation of guanosine at peak IV_a (ca. 0.96 V). Apart from some minor peak height changes peaks 1-7 in figure 27 appear to be the same as those in figure 26. However, in figure 27 peak 8 is totally absent. Figure 28 shows the separation of the products of electrooxidation of 8-hydroxyguanosine electrolyzed at peak II_a potentials (ca. 0.5 V). Peaks 1 and 2 appear to be the same as peaks 1 and 2 in figures 26 and 27. Peak 3 which appears in figures 26 and 27 either does not occur in figure 28 or it is so severely overlapped with peak 2 that it cannot be seen. Peaks 4 and 5 occur at the same retention volumes in figures 26, 27, and 28. Peak 6', however, is a peak which was not observed in the chromatograms obtained for the products obtained upon electrooxidation of guanosine. Figure 29 is a chromatogram of the oxidation products of 8-hydroxyguanosine oxidized at 1.0 V (peak III_a) in pH 7 buffer. This chromatogram bears a striking resemblance to that obtained for the products obtained upon electrooxidation of guanosine at 0.96 V (figure 27). All seven peaks appear to correlate with respect to retention volume. Also peak 6' observed on chromatography of the oxidation products of 8-hydroxyguanosine at 0.5 V (see figure 28) is not present after the oxidation of 8-hydroxyguanosine at 1.0 V. Figure 30 shows the chromatogram of 8-hydroxyguanosine oxidized at 1.15 V. This was done to see if peak 8 in figure 27 would appear in

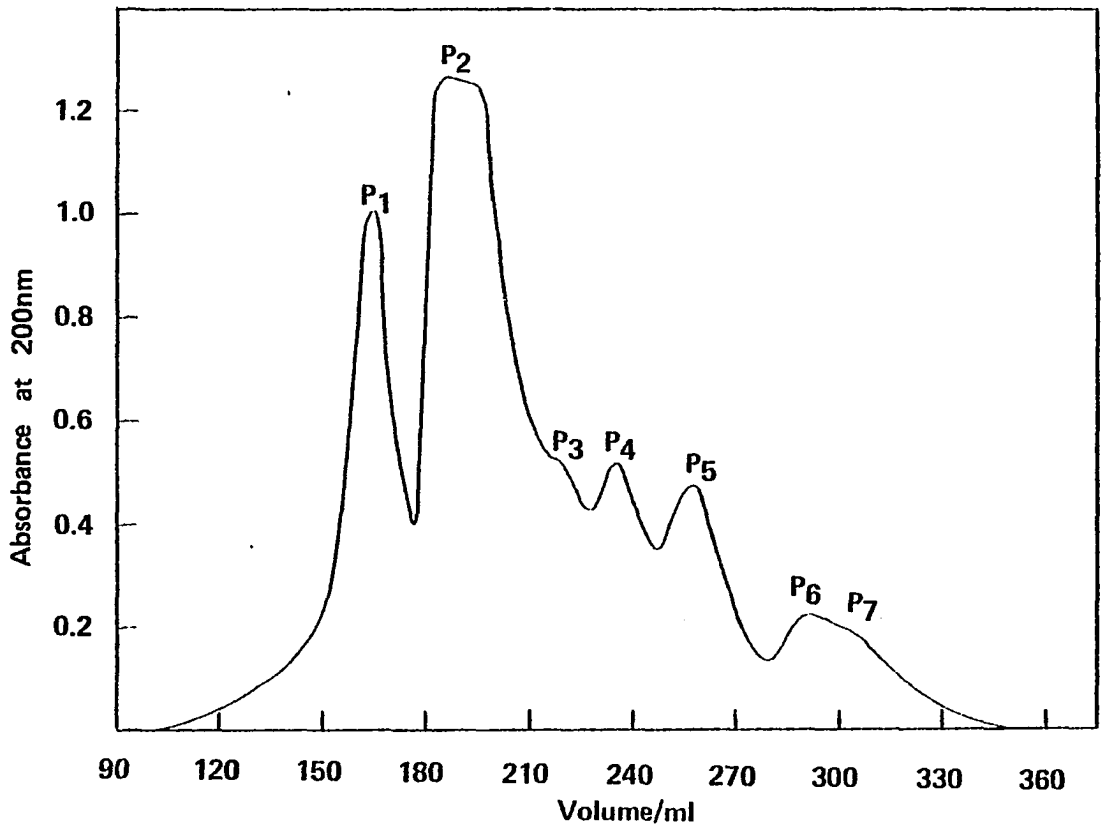

Figure 27. Liquid chromatogram of the products from the oxidation of a pH 7, 0.8 mM guanosine solution at 0.96 V (peak IV_a) utilizing a single 90 cm x 2.5 cm column of G-10 resin with 0.025 M pH 7 phosphate buffer as the eluant.

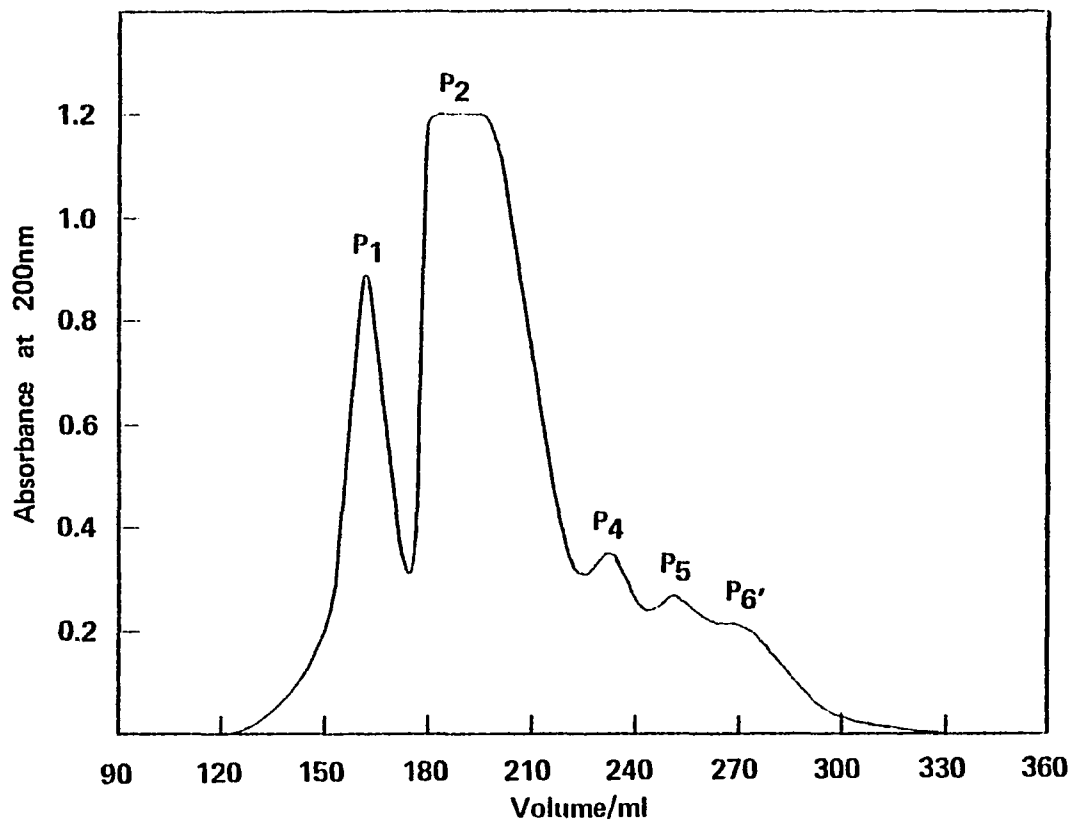

Figure 28. Liquid chromatogram of the products from the oxidation of a pH 7, 0.84 mM 8-hydroxyguanosine solution at 0.5 V (peak II_a) utilizing a single 90 cm x 2.5 cm column of G-10 resin with 0.025 M pH 7 phosphate buffer as the eluant.

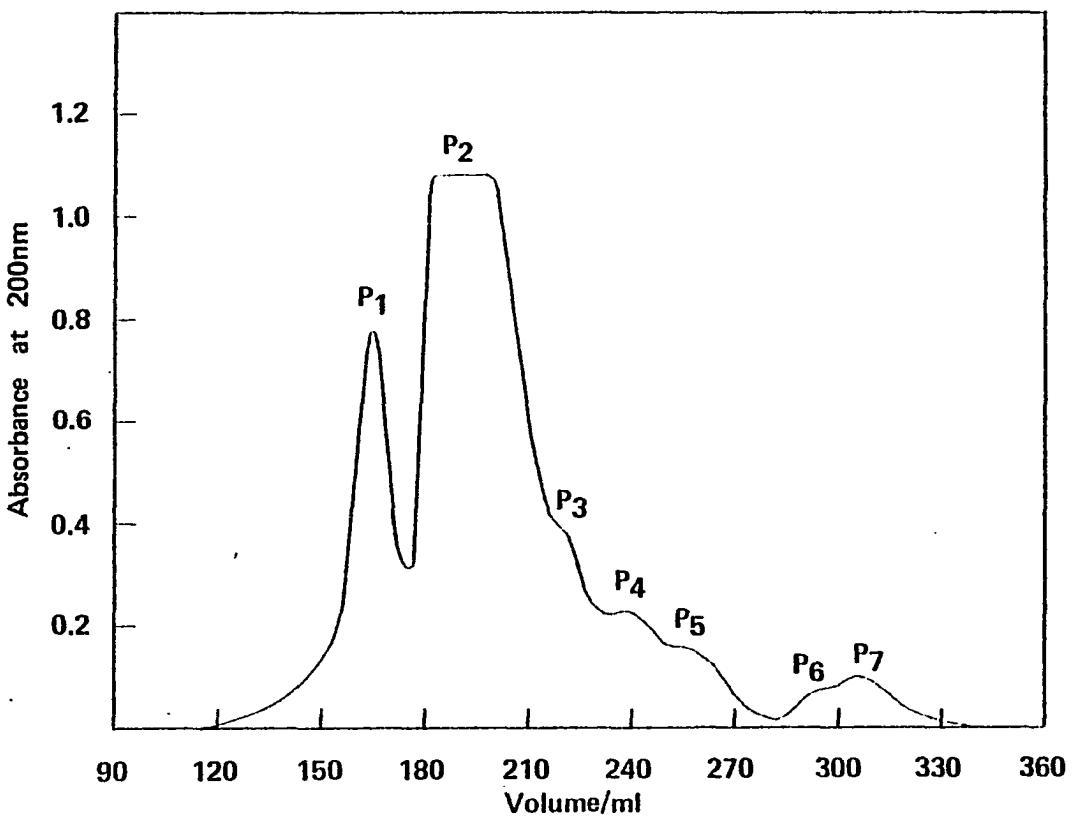

Figure 29. Liquid chromatogram of the products from the oxidation of a pH 7, 0.84 mM 8-hydroxyguanosine solution at 1.0 V (peak III_a) utilizing a single 90 cm x 2.5 cm column of G-10 resin with 0.025 M pH 7 phosphate buffer as the eluant.

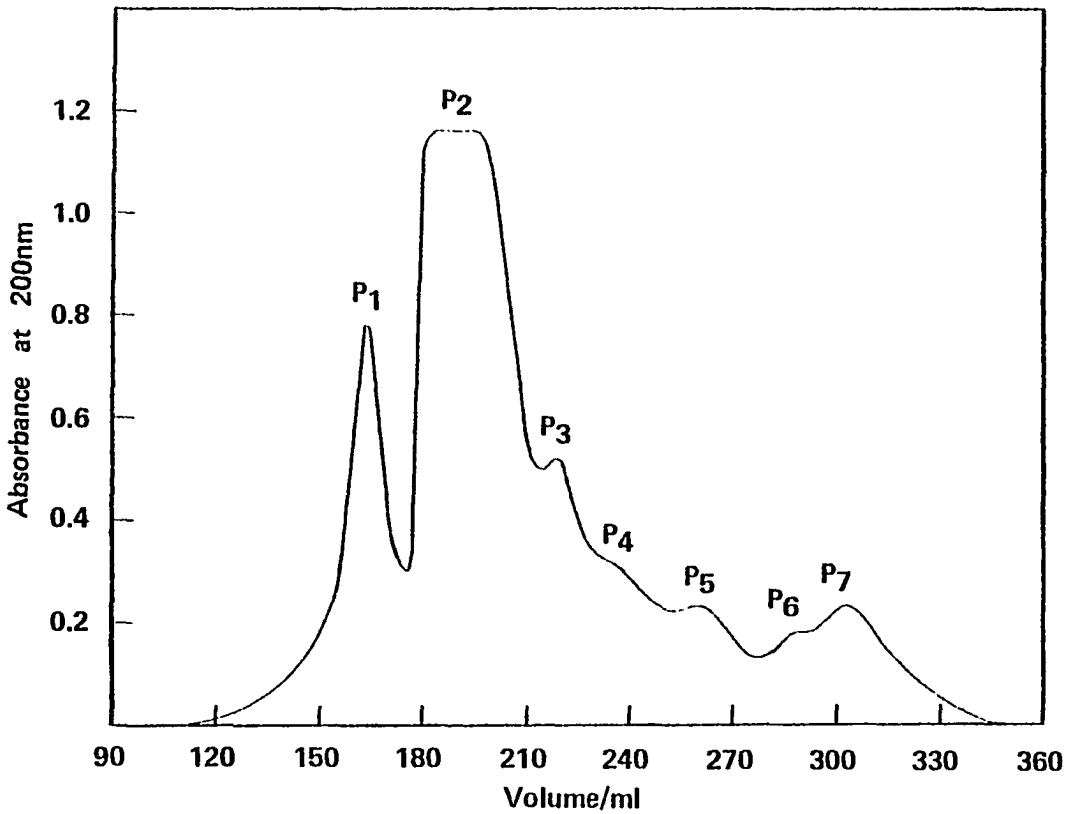

Figure 30. Liquid chromatogram of the products from the oxidation of a pH 7, 0.84 mM 8-hydroxyguanosine solution at 1.15 V (peak V_a of guanosine) utilizing a single 90 cm x 2.5 cm column of G-10 resin with 0.025 M pH 7 phosphate buffer as the eluant.

the chromatogram of 8-hydroxyguanosine oxidized at the same potential (1.15 V, peak V_a of guanosine). Peak 8 did not appear and figure 30 is virtually identical to figure 29.

Thus, peak 6' appears to be due to a product formed only during the oxidation of 8-hydroxyguanosine. Since peak 6' disappears when the oxidation is carried out at 1.0 V (peak III_a) it would seem that peak 6' is the product responsible for oxidation peak III_a in the voltammetry of 8-hydroxyguanosine. A voltammogram run on peak 6' confirmed the presence of a voltammetric peak at 1.0 V, the same potential as oxidation peak III_a. Peak 8 appears only in the chromatograms of guanosine oxidized at 1.15 V (peak V_a, see figure 26). It is possible then that peak 8 is the product of the oxidation process represented by voltammetric peak V_a of guanosine.

Thin-layer spectroelectrochemical studies

Thin-layer spectroelectrochemical studies of guanosine and 8-hydroxyguanosine using a rapid scan spectrometer (RSS) employed a thin-layer cell utilizing reticulated vitreous carbon (RVC) as the working electrode material (see Experimental for details of cell construction). This cell is similar to that used by Norvell and Mamantov,[64] and offers several advantages over a gold minigrid. The primary advantage of the RVC electrode is that it has a much wider potential range. With gold electrodes gold oxides are formed[57] at about 1.0 V over the pH 6-9 range. These oxides cause a severe slowdown in the rate of electrooxidation reactions. In addition, it then becomes necessary to precathodize the electrode prior to every run. The RVC

electrode, however, may be used at 1.3 V without difficulty. Beyond 1.3 V some surface changes appear to occur. If spectra are recorded after potentials $\geq$1.3 V have been applied there is a tendency for the entire spectrum to shift to higher absorbance values with no potential applied. During kinetic measurements the problem manifests itself as odd bumps and sudden changes in the curvature of absorbance versus time plots. Also the RVC electrode is more similar to the PGE used for voltammetric studies than is gold. Finally an advantage in this particular work is that the RVC electrode is about 10 times thicker than a gold minigrid allowing one to work at lower concentrations of the electroactive species. This is a distinct advantage with purines because of their low solubility and very high molar absorptivities.

A typical u.v. spectrum obtained prior to electrolysis of guanosine at pH 7.0 at the RVC electrode in a thin-layer cell is shown in curve 1 of figure 31 where it may be observed that guanosine exhibits an absorption peak with λ_{max} of 255 nm and a shoulder at 277 nm. Upon application of a potential of 1.2 V (peak V_a) the u.v. peak of guanosine decreases with time and simultaneously the absorbance grows in the 288-360 nm and 210-230 nm regions. If the potential is turned off when the increase in absorbance in the 288-360 nm region reaches a maximum (curve 2, figure 31) one then observes a decrease in absorbance over the 220-360 nm region and an accompanying increase in the 220-200 nm region. Curve 3 in figure 31 shows the spectrum after all absorbance changes have ceased. While the spectrum still shows evidence of guanosine being present the spectrum is undeniably altered. The peak originally at 255 nm has shifted to 243 nm and a peak has grown in at

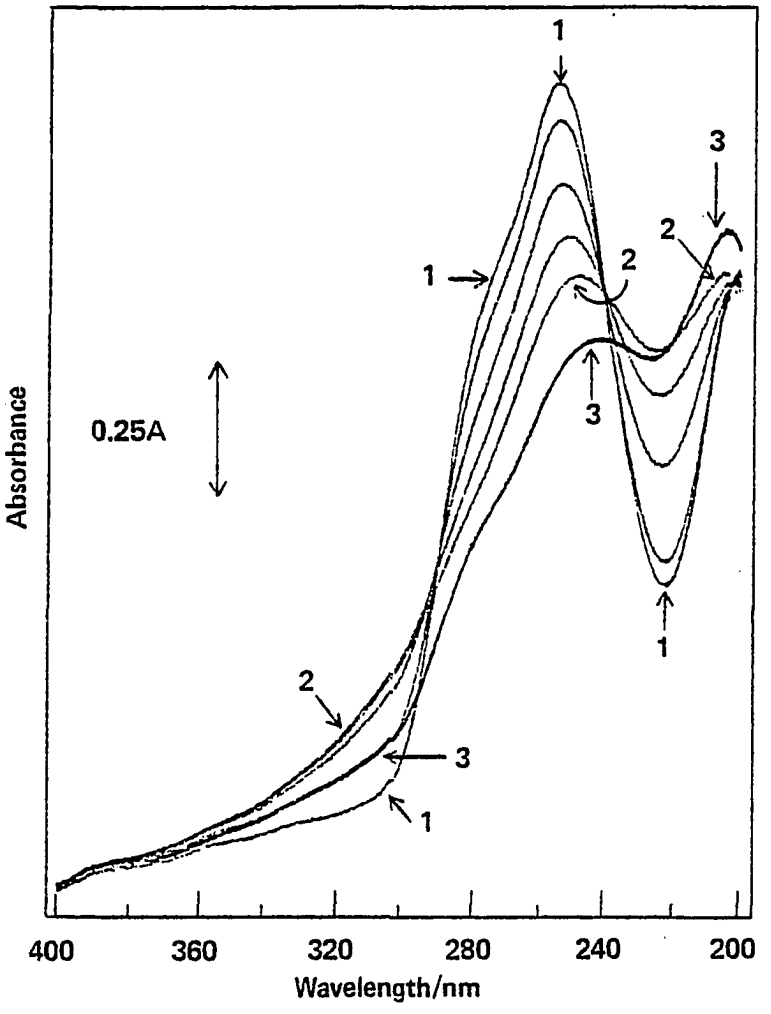

Figure 31. Spectrum of 1.0 mM guanosine solution electrolyzing at 1.2 V in pH 7 phosphate buffer in a thin-layer cell with a RVC working electrode. Curve 1 is the guanosine spectrum before electrolysis. Repetetive scans (200 nm to 400 nm) of 40 sec are shown. Curve 2 is the spectrum when the absorbance increase around 310 nm has reached a maximum. The potential was turned off immediately prior to curve 2. Curve 3 was obtained 20 min after curve 2 and is the spectrum after all absorbance changes had ceased.

205 nm. The change in absorbance after the potential is turned off indicates that an unstable intermediate is formed upon electrooxidation of guanosine.

The result of leaving the potential on may be seen in figure 32. From the time at which the absorbance at 300 nm reaches a maximum the absorbance over the 240-330 nm region decreases and the absorbance in the 200-240 nm region increases. The trace after all absorbance change has stopped may be seen in curve 1 of figure 32. The absorbance peak of guanosine is completely gone and peaks at 230 and 211 nm have appeared. Thin-layer spectroelectrochemical studies of guanosine over a range of concentrations (0.2-2 mM) at pH 7 gave results similar to those shown in figures 31 and 32. The spectra look essentially the same over the pH range of 4-9.3. The change in absorbance after the potential was turned off becomes somewhat smaller below pH 6, but the general appearance of the spectra remains the same.

A typical u.v. spectrum of 8-hydroxyguanosine prior to electrolysis in a thin-layer cell is shown in figure 33, curve 1. Adsorption maxima occur at 212, 251, and 296 nm. When a potential of 0.7 V (peak II_a) is applied there is a general decrease in absorbance in the 245-300 nm region. Although, initially the decrease is very slight in the area around 250 nm. This may imply that the species being generated has a λ_{max} at approximately 250 nm. From 245-216 nm there is an increase in absorbance when the potential is applied. From 215-200 nm there is a slight decrease in absorbance. If the potential is turned off when the 251 peak is noticeably shifted toward shorter wavelengths (as shown in figure 33, curve 2) there is a broad decrease in absorbance

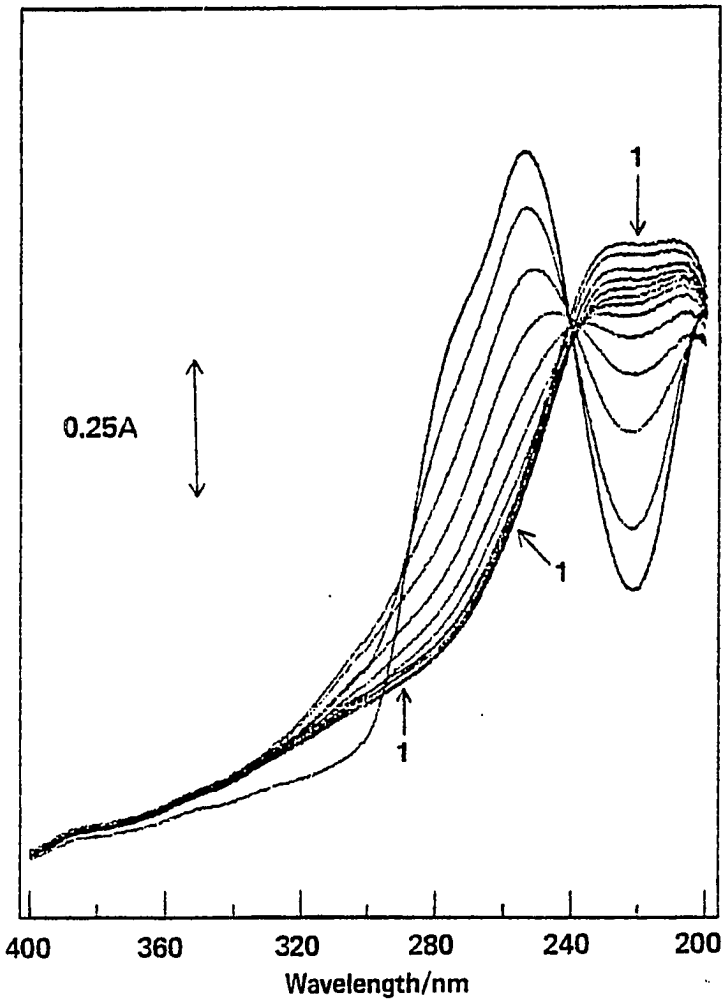

Figure 32. Spectrum of 1.0 mM guanosine solution electrolyzing at 1.2 V in pH 7 phosphate buffer in a thin-layer cell with an RVC working electrode. The potential was left on until all absorbance changes had ceased. Curve 1 is the spectrum obtained after all absorbance change had ceased. The total time of electrolysis was approximately 45 minutes. The time between sweeps varied from 40 sec during initial sweeps to 10 minutes between the final two sweeps. This was done to clearly display the absorbance changes occurring.

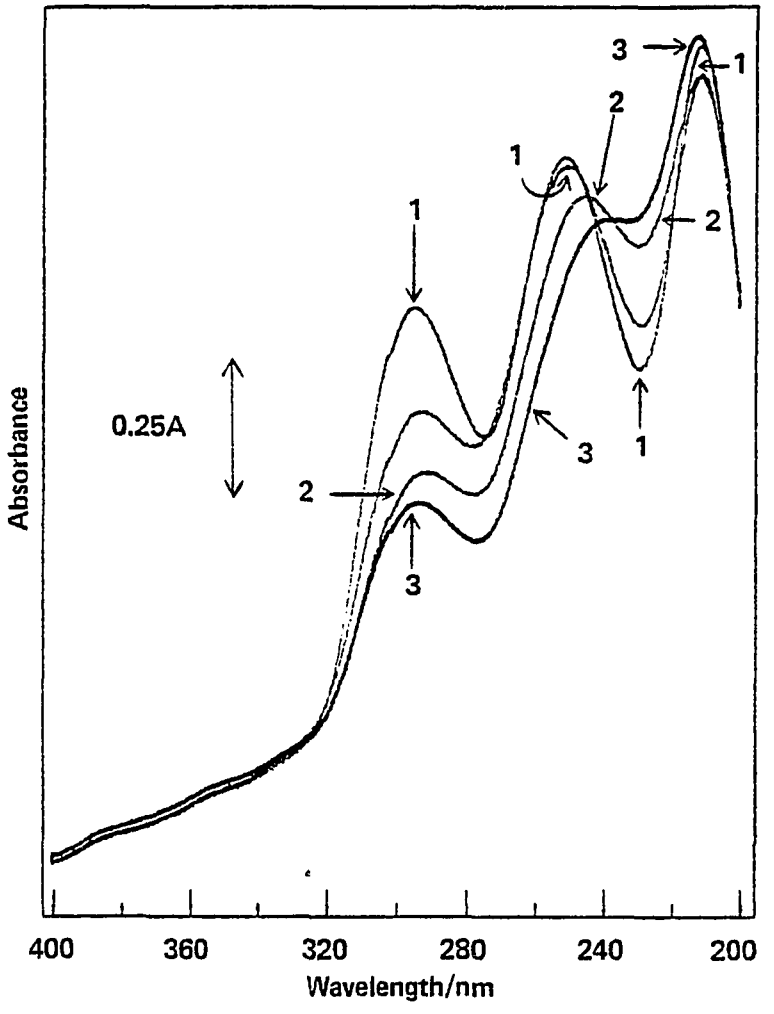

Figure 33. Spectrum of 1.0 mM 8-hydroxyguanosine solution electrolyzing at 0.7 V in pH 7 phosphate buffer in a thin-layer cell with an RVC working electrode. Curve 1 is the spectrum of 8-hydroxyguanosine before electrolysis. Repetetive scans (200 nm to 400 nm) of 40 sec are shown. Curve 2 is the first spectrum in which the peak originally at 251 nm has shifted significantly toward shorter wavelengths. If the potential was removed immediately prior to curve 2 (so that no absorbance changes occurring later could be attributed to an applied potential). Curve 3 was obtained approximately 30 min later when all absorbance changes had ceased.

over the 240-320 nm region (see figures 33, curve 3). Over the 200-240 nm region the absorbance increases. These changes are clearly shown in curve 3 of figure 33 which is the spectrum approximately 30 minutes after the potential was turned off. The continued changes in the spectrum after the applied potential was turned off indicates that the electrooxidation of 8-hydroxyguanosine generates an unstable intermediate.

Figure 34 shows the effect of leaving the potential on during electrooxidation of 8-hydroxyguanosine. In this case there is a continued decrease in absorbance over the 240-320 nm region and a continued increase in the 200-240 nm region. Curve 1 of figure 34 is the spectrum after all absorbance changes have ceased. All indications of 8-hydroxyguanosine have disappeared and peaks at 214 and 231 nm have grown in. Essentially the same spectral behavior was noted over the 0.2-2.0 mM concentration region. It was noticed (particularly in later kinetic studies) that at low concentrations the absorbance change after the potential was removed was larger in proportion to the substrate peaks than at high concentration. The spectra over the pH range of 4-9.3 were similar in appearance. The change in absorbance after the potential was removed was smaller below pH 6, but the general appearance of the spectra remained the same.

Thus, while the initial spectra of guanosine and 8-hydroxyguanosine are quite different the behavior of the two while a potential is applied, the behavior after the potential is removed, and the appearance of the spectra after exhaustive electrolysis is essentially the same.

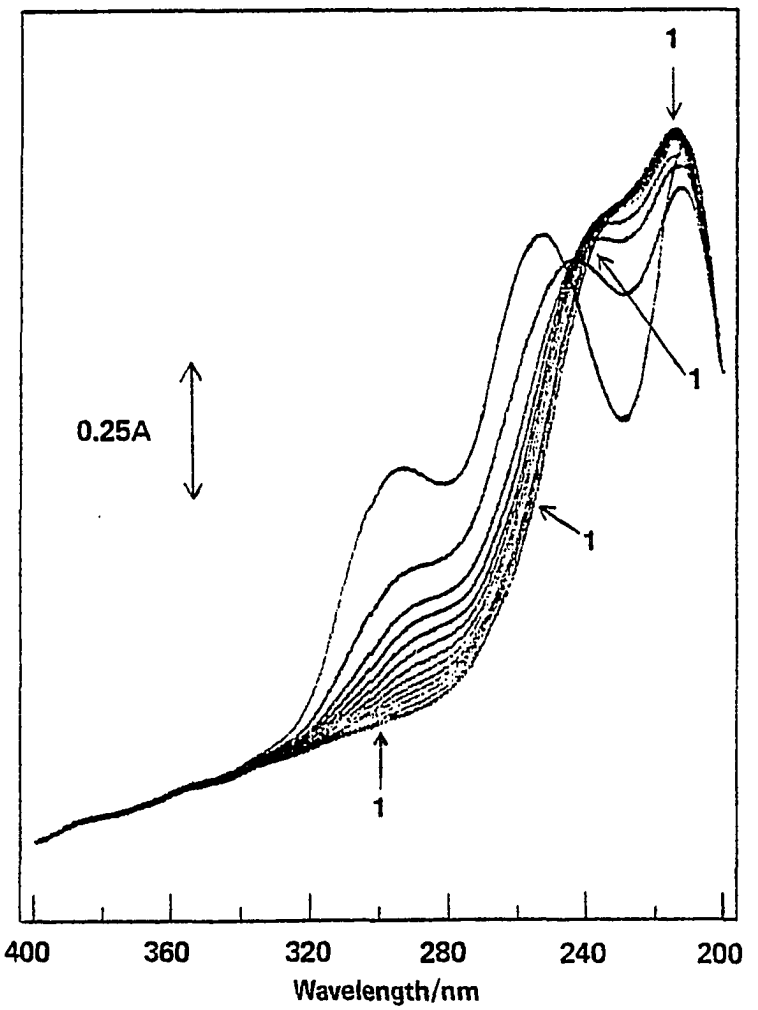

Figure 34. Spectrum of 1.0 mM 8-hydroxyguanosine solution electrolyzing at 0.7 V in pH 7 phosphate buffer in a thin-layer cell. Curve 1 is the spectrum obtained after all absorbance change had ceased (the potential was applied during the entire experiment). The total time of electrolysis was approximately 45 minutes.

Kinetic measurements

The kinetics of disappearance of the unstable intermediate formed upon electrooxidation of guanosine was studied by thin-layer spectroelectrochemistry. Absorbance as a function of time was monitored at two wavelengths, 250 and 300 nm. Owing to the overlap in the spectra of guanosine and the unstable intermediate it was not possible to determine the λ_{max} for the intermediate and monitor at that wavelength. Accordingly, it was decided to monitor the intermediate species at 300 nm where the absorbance grows while the potential is on, and at 250 nm where the largest change in absorbance occurred after the potential was turned off. The absorbance at these wavelengths was measured as a function of time after the solution had been oxidized for 50 seconds and the potential turned off. A typical plot of absorbance versus time for the intermediate generated by the electrooxidation of guanosine is shown in figure 35A. Analysis of the $\log|A-A_{\infty}|$ versus time plot in figure 35B shows a distinct break at about 200 seconds. From figure 35B it appears that there are two kinetically distinguishable intermediates present. One intermediate decays relatively rapidly, and one decays much more slowly. The rate constant for the slow step may be determined in the usual way, but before the rate constant can be determined for the fast step the absorbance due to the more slowly decaying intermediate must be subtracted from the absorbance values at the times where the fast step is observed (see Experimental). A typical rate plot for the fast step is shown in figure 35C. The same two step decay is observed at both 250 nm and 300 nm. The only significant difference in the observations made at the two wavelengths is that at 300 nm the signal

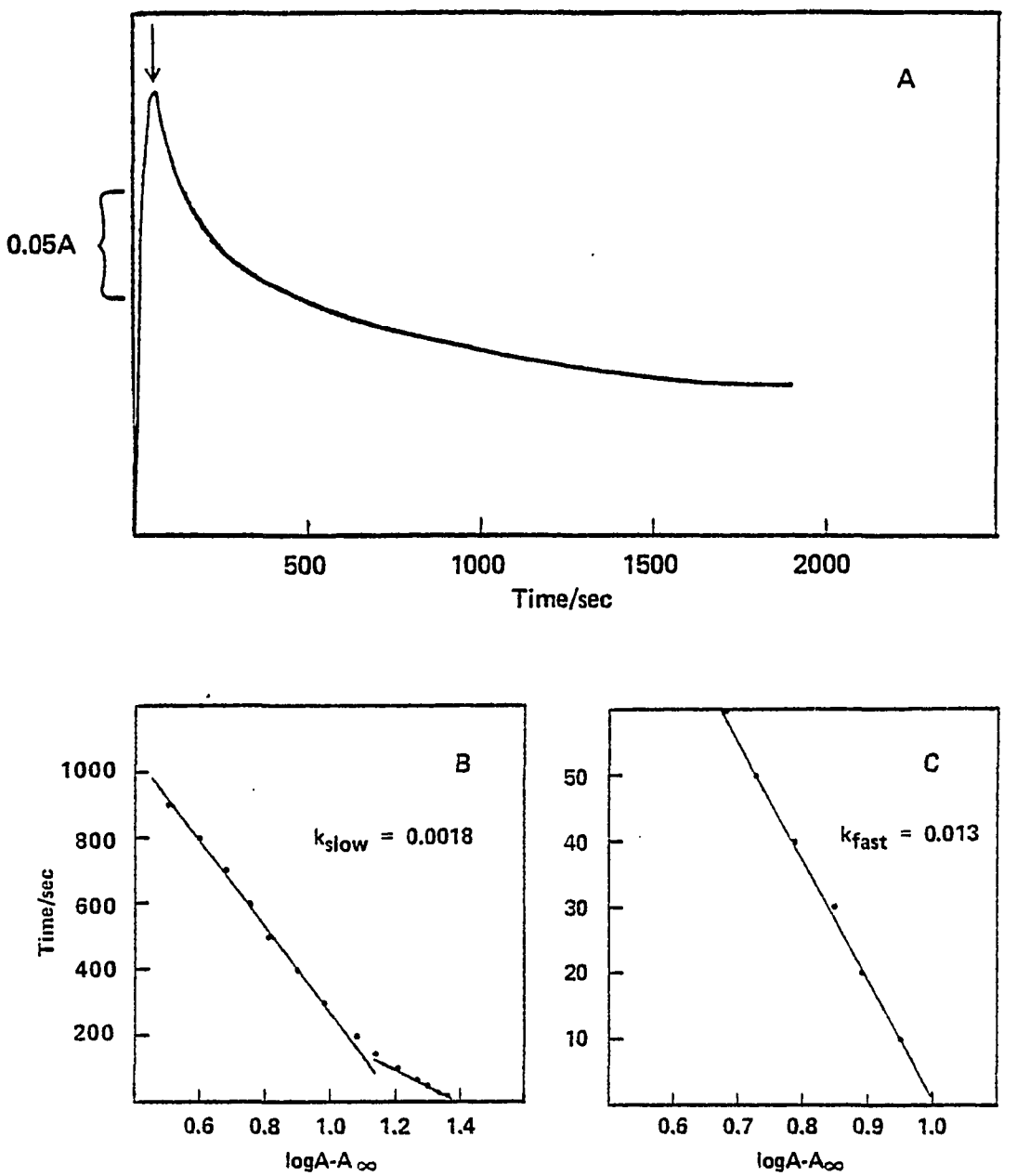

Figure 35. A is the plot of absorbance versus time for a 1.0 mM guanosine solution in pH 7 phosphate buffer electrolyzed at 1.2 V for 50 seconds (potential was removed at time indicated by the arrow). B is the plot of time versus log $A-A_\infty$ for the slow step and the fast step. C is the time versus log $A-A_\infty$ plot for the fast step after the contribution from the slow step has been subtracted out.

is smaller and somewhat noisier.

The kinetic behavior of the intermediates formed upon electrooxidation of 8-hydroxyguanosine was essentially identical to that of guanosine. In figure 36A a typical absorbance versus time plot for 1 mM 8-hydroxyguanosine at pH 7 electrolyzed in a thin-layer cell at 0.7 V is shown. In figure 36B and 36C typical rate plots are presented. Studies also showed that the same rate constants are observed for the intermediates formed upon the electrooxidation of 8-hydroxyguanosine whether the applied potential was 0.7 V or 1.2 V.

Table 10 shows the fast and slow observed first-order rate constants for the intermediates generated upon electrooxidation of guanosine and 8-hydroxyguanosine. The agreement is reasonable especially when one considers that at pH 7 and 250 nm the relative standard deviation is approximately 8%, and at 300 nm or higher and lower pH the relative standard deviation is somewhat larger (≈12%). The deviation is also larger for the fast process rate constants (≈15%). Nevertheless, the rate constants for the more slowly decaying intermediate formed upon electrooxidation of guanosine and 8-hydroxyguanosine are generally the same within experimental error. The rate constants for the fast step all show the same trend with a minimum around pH 5.6.

Thus electrooxidation of guanosine and 8-hydroxyguanosine yields u.v. absorbing intermediates which are spectrally and kinetically the same.

Enzymic studies

It was decided to attempt enzymic oxidation of guanosine and

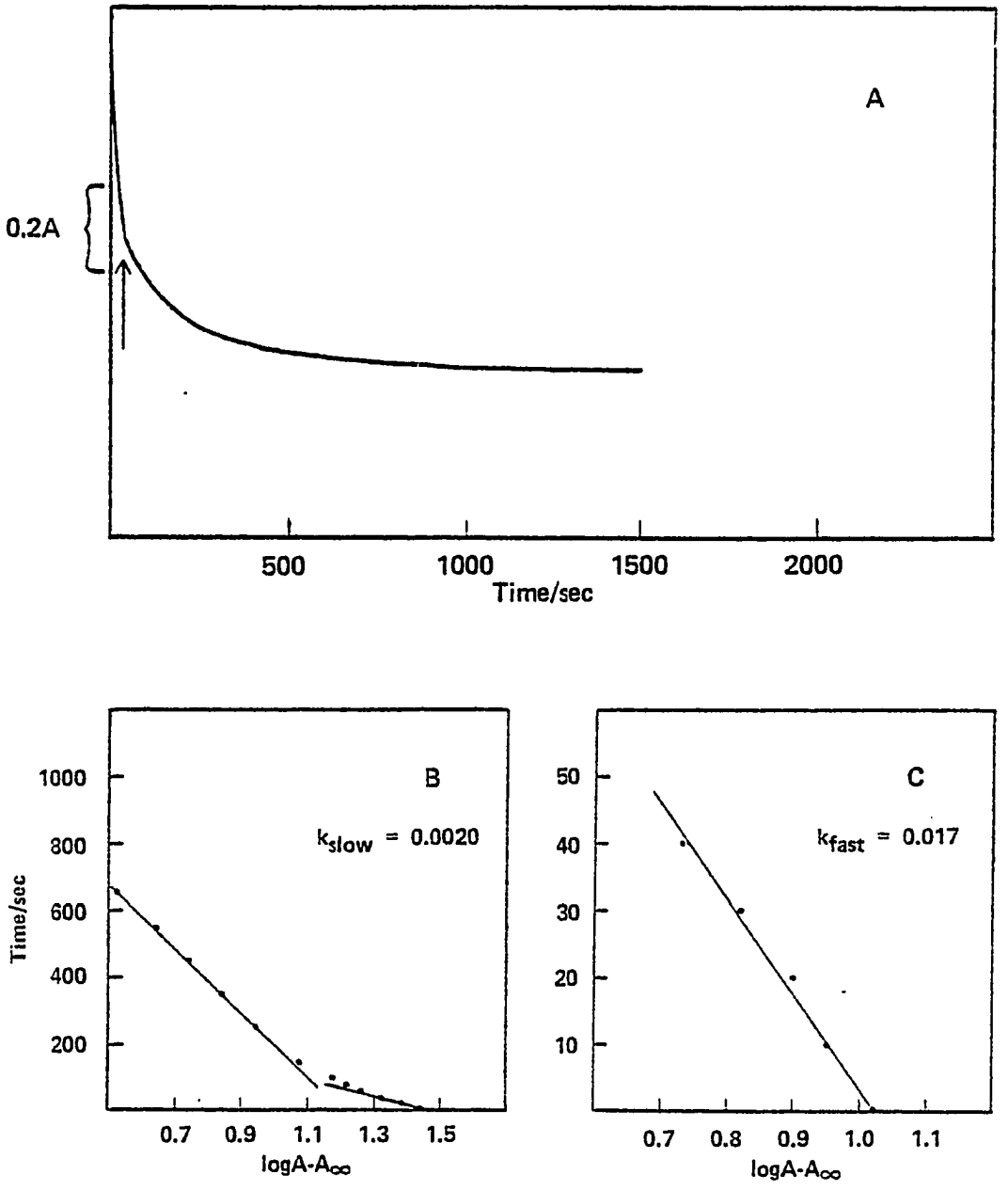

Figure 36. A is the plot of absorbance versus time for a 1.0 mM 8-hydroxyguanosine in pH 7 phosphate buffer electrolyzed at 0.7 V for 50 seconds (potential was removed at time indicated by the arrow). B is the plot of time versus log $A-A_\infty$ for the slow step and the fast step. C is the time versus log $A-A_\infty$ plot for the fast step after the contribution from the slow step has been subtracted out.

Table 10

Observed first-order rate constants for the electrochemical oxidation of guanosine and 8-hydroxyguanosine

Slow Process

$k(sec^{-1})$*

pH	250 nm		300 nm	
	Guanosine	8-Hydroxyguanosine	Guanosine	8-Hydroxyguanosine
4.0	0.0016	0.0015	0.0025	-
4.6	0.0021	0.0018	0.0023	-
5.6	0.0022	0.0017	-	0.0033
7.0	0.0021	0.0016	0.0017	0.0030
8.0	0.0023	0.0013	0.0015	0.0019
9.3	0.0015	0.0013	0.0015	0.0022

Fast Process

$k(sec^{-1})$*

pH	250 nm		300 nm	
	Guanosine	8-Hydroxyguanosine	Guanosine	8-Hydroxyguanosine
4.0	0.024	0.038	0.026	-
4.6	0.022	0.020	0.012	-
5.6	0.007	0.008	-	0.008
7.0	0.013	0.016	0.015	0.018
8.0	0.042	0.036	0.027	0.041
9.3	0.036	0.047	0.027	0.046

*All values are averages of replicate runs at 0.2, 1.0, and 2.0 mM.

-Where no k-value is reported the change in absorbance was too small to allow calculation of a rate constant.

8-hydroxyguanosine and compare the results to the electrooxidation of these compounds. The oxidizing system chosen was the same as that used for oxidizing uric acid in Chapter 3, that is type VIII peroxidase isolated from horseradish (HRP) and hydrogen peroxide. Initial studies showed that guanosine was not oxidized by the HRP and hydrogen peroxide system. 8-Hydroxyguanosine was oxidized, but required much higher enzyme concentrations than did uric acid (≈5X more HRP).

Figure 37 shows the spectrum of 50 μM, pH 7 8-hydroxyguanosine solution being oxidized in the presentce of 1.0 μM HRP and 200 μM hydrogen peroxide (Note: all concentrations given in this section will be the concentration after all components of the solution are mixed together unless otherwise noted). The general appearance of the spectrum is basically the same as that observed for the electrochemical oxidation of 8-hydroxyguanosine (see figure 34). The final trace for the enzymic oxidation shows λ_{max} at 212 nm and 226 nm as compared to 214 nm and 231 nm for the electrooxidation. It was not feasible to obtain good spectra after the reaction had been stopped with catalase. This was so primarily due to the large amounts of HRP and catalyase present simultaneously. Thus, in order for the oxidation to proceed rapidly enough for a significant amount of intermediate to be present when the reaction is stopped HRP concentrations of at least 5.0 μM must be used. This is five times the HRP concentration used in figure 37. The five-fold increase in HRP concentration alone is enough to cause noticeable distortion of the spectra at wavelengths shorter than approximately 275 nm. When 0.3 mg of catalase in 1.5 ml of buffer is added the total absorbance due to the enzymes is so

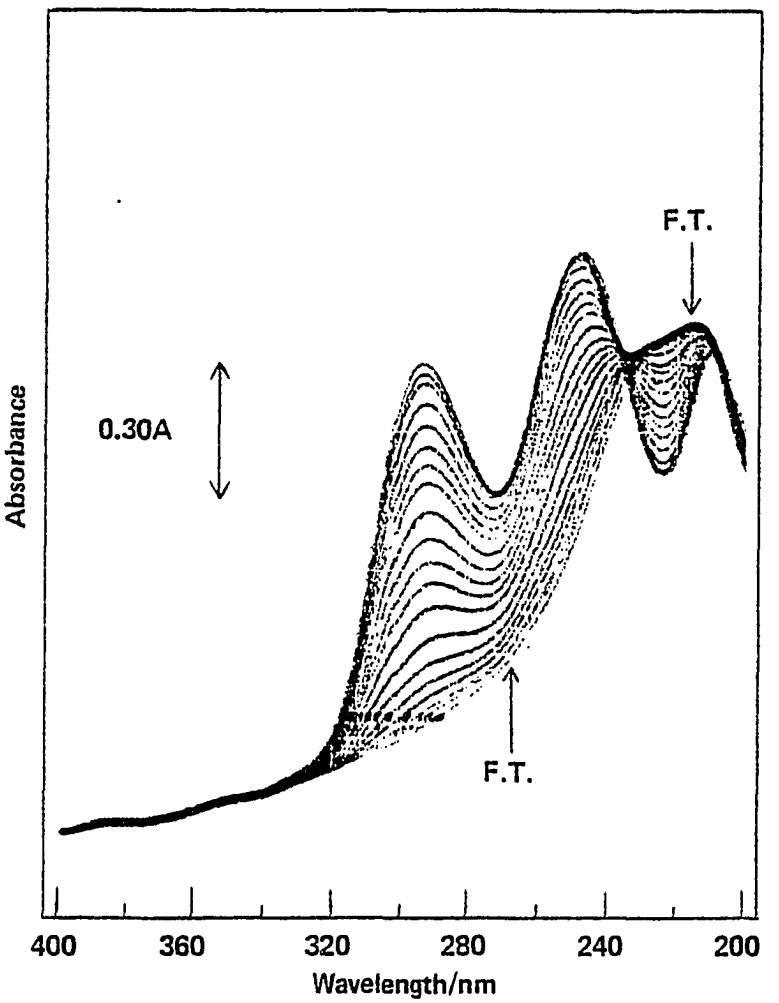

Figure 37. Spectrum of 50 μM 8-hydroxyguanosine at pH 7 being oxidized by the presence of 200 μM hydrogen peroxide and 1.0 μM horseradish peroxidase. The final trace (F.T.) when all absorbance change had ceased was observed approximately 1.5 hours after the oxidation was initiated. The time between sweep was varied from 40 sec-15 min to show clearly the absorbance changes taking place.

large that the spectra are unrecognizable, although in absorbance versus time studies the decay was readily observable. Attempts to obtain better spectra by increasing the 8-hydroxyguanosine concentration simply resulted in absorbances too large for the spectrophotometer to measure.

Kinetic measurements

In order to compare the kinetic data obtained from the enzymic oxidation of 8-hydroxyguanosine with that obtained by electrochemical oxidation, the absorbance versus time curves for the enzymic oxidation were recorded at 250 nm and 300 nm. Kinetic data was obtained over the pH range of 4-9.3 utilizing a HRP concentration of 2.5 μM, a hydrogen peroxide concentration of 200 μM, and 8-hydroxyguanosine concentrations of 5, 25, and 50 μM at each pH value.

A typical absorbance versus time curve is shown in figure 38A. The log $|A-A_\infty|$ plot in figure 38B shows the same break around 200 seconds observed in figure 36B for the thin-layer spectroelectrochemical oxidation of 8-hydroxyguanosine. Figure 38C is the log $|A-A_\infty|$ versus time plot for the more rapidly decaying intermediate formed upon enzymatic oxidation of 8-hydroxyguanosine. Table 11 presents the observed first-order rate constants for decomposition of the intermediates generated from the enzymic oxidation of 8-hydroxyguanosine. The values presented in Table 11 compare well with those presented in Table 10 for the intermediates generated upon electrooxidation of guanosine and 8-hydroxyguanosine. Thus, the kinetic data supports the view that the enzymic oxidation of 8-hydroxyguanosine goes through the same steps and inter-

Table 11

Observed first-order rate constants for the enzymic oxidation of 8-hydroxyguanosine

	Slow Process $k(sec^{-1})^*$	
pH	250 nm	300 nm
4.0	-	-
4.6	0.0016	-
5.6	0.0017	0.0024
7.0	0.0016	0.0013
8.0	0.0012	0.0018
9.3	0.0024	0.0021

	Fast Process $k(sec^{-1})^*$	
pH	250 nm	300 nm
4.0	-	-
4.6	0.014	-
5.6	0.008	0.009
7.0	0.014	0.015
8.0	0.030	0.039
9.3	0.022	0.040

*All values are averages of replicate runs at 5, 25, and 50 μM.

-Where no k-value is reported the change in absorbance was too small to allow calculation of a rate constant.

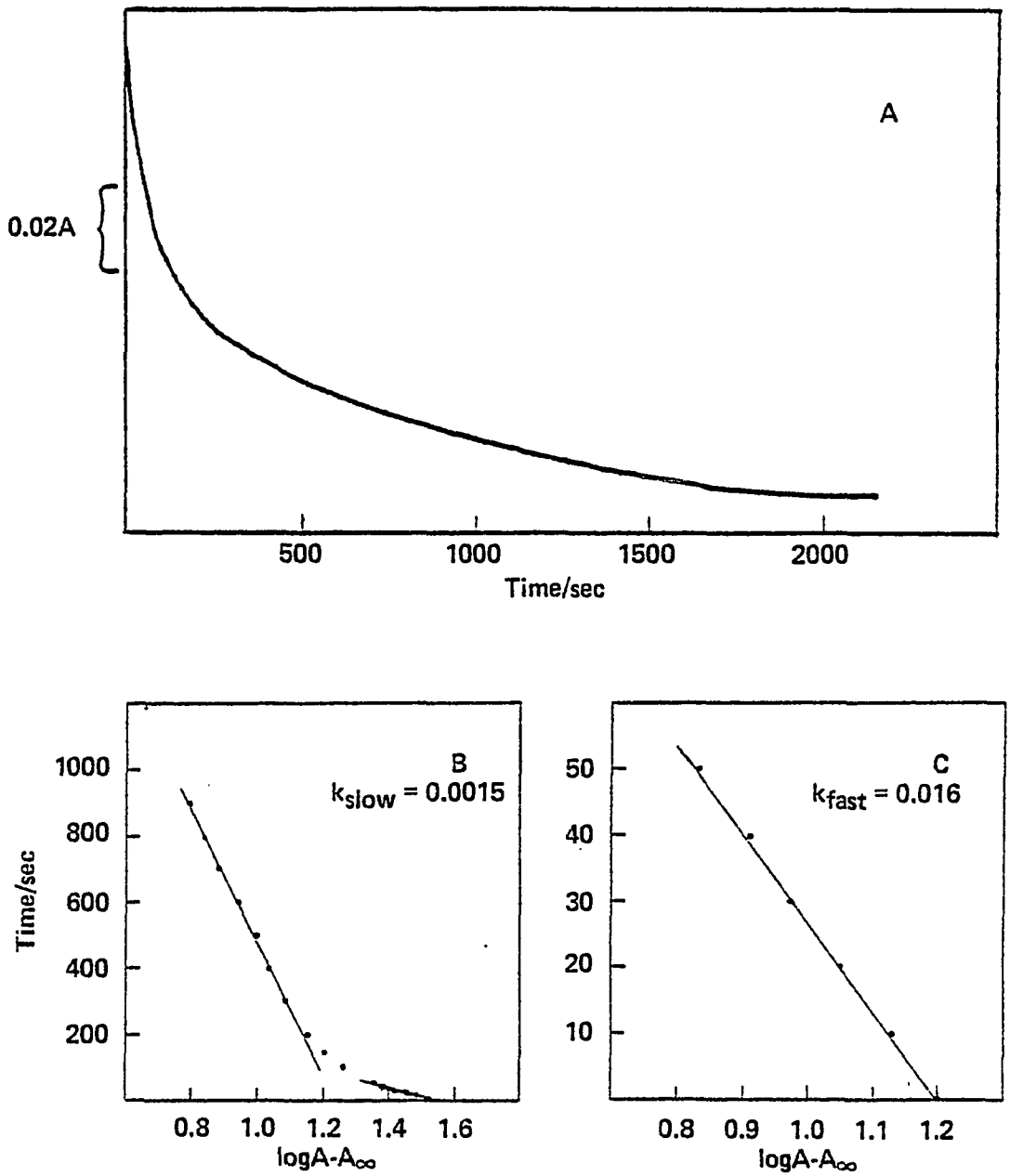

Figure 38. A is the plot of absorbance versus time for a 50 μM pH 7 solution of 8-hydroxyguanosine oxidized for 50 sec by 200 μM hydrogen peroxide and 2.5 μM HRP. The oxidation was stopped after 50 sec by the addition of 0.3 mg of catalase in 1.5 ml of pH 7 phosphate buffer. Only the absorbance changes after the oxidation was stopped are shown. B is the time versus log $A-A_\infty$ plot for the slow step and fast step. C is the time versus log A-A plot for the fast step after the contribution from the slow step has been subtracted.

mediates as the electrooxidation of guanosine and 8-hydroxyguanosine.

Further support for the similarity between the enzymic and electrochemical oxidation of 8-hydroxyguanosine is shown in figure 39. Figure 39 is a voltammogram run during the enzymic oxidation of 8-hydroxyguanosine at pH 7. The scan starts from 0.0 V and proceeds toward negative potentials. In a normal voltammogram no reduction peaks would be observed. However, in figure 39 a peak is observed at -0.75 V which corresponds to reduction peak II_c seen in the normal voltammetry of 8-hydroxyguanosine only after oxidation at peak I_a has been performed. This indicates that the enzymic oxidation is generating the same species (as evidenced by the presence of peak II_c) as the electrooxidation.

Product separation and identification

A basic prerequisite in the identification of products is the ability to separate the products from each other and any substances present which might interfere with the techniques used for identification. Towards this end a number of different separation techniques were applied. The primary identification techniques utilized was mass spectrometry coupled with gas chromatography.

Initial separations employed the system reported by Cleary and Dryhurst.[65] This utilizes a 90 cm x 2.5 cm column of Sephadex G-10 coupled to a 35 cm x 2.5 cm column of Sephadex QAE A-25, and using 0.025 M pH 7.0 phosphate buffer as the eluant. A typical chromatogram is shown in figure 40. Peaks 1 and 2 are due to the phosphate buffer used in the electrolysis. Peaks 3-9 are apparently

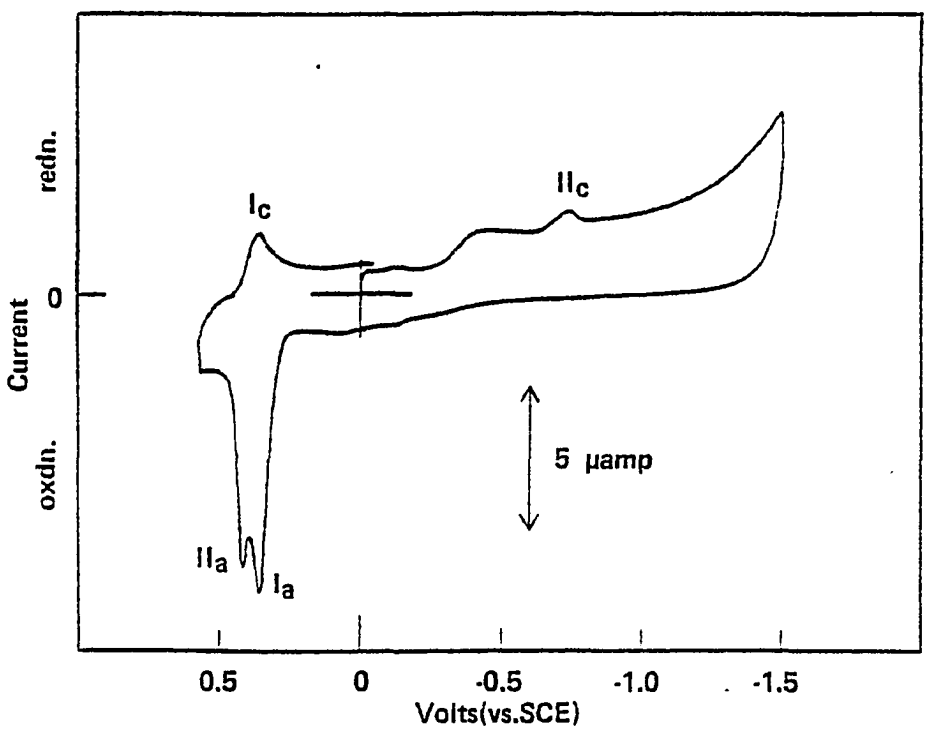

Figure 39. Cyclic voltammogram of 100 µM 8-hydroxyguanosine during oxidation by 5 µM HRP and 400 µM hydrogen peroxide at pH 7 with a sweep rate of 200 mV sec^{-1}.

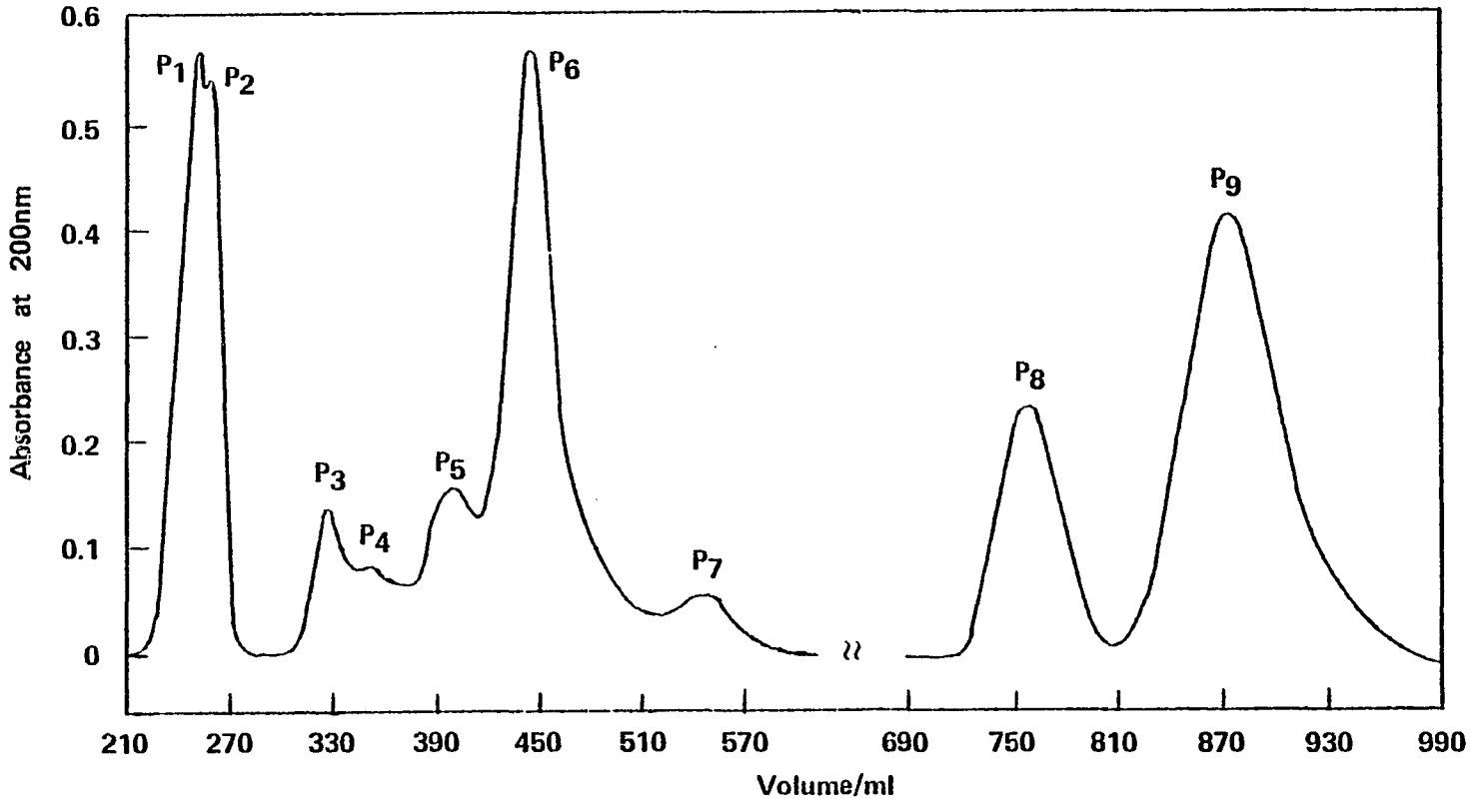

Figure 40. Liquid chromatogram of the products from the oxidation at 1.15 V (peak V_a) of a pH 7 0.8 mM guanosine solution utilizing a 90 cm x 2.5 cm column of G-10 resin coupled to a 35 cm x 2.5 cm column of QAE A-25 resin with 0.025 M pH 7 phosphate buffer as the eluant.

product peaks. Each peak was collected into a separate flask, frozen, and lyophylized. The material eluted under the peak would then be dissolved in 1 ml of doubly distilled water and passed through a chromatographic system consisting of two 90 cm x 2.5 cm columns packed with Sephadex G-10, utilizing doubly distilled water as the eluant. This separates the product from phosphate. Usually two passes through this system were necessary to obtain baseline separation between phosphate and the product peak. Once the peak appeared to be desalted tests could be run to try and identify the products eluted under it. In order to run mass spectroscopy of the product it was first necessary to convert it to a fully silylated derivative (see Experimental for details of the silylation procedure). Many purine nucleosides and some of the possible products do not give good mass spectra with direct insertion mass spectroscopy due to their low volatility even under vacuum. Silylation increases the volatility so that the molecule can be more readily observed in the mass spectrometer. The increase in volatility is sufficient that the molecule can pass through a gas chromatogram, this gives a second separation step where small impurities due to peak overlap in the liquid chromatographic system can be isolated from the peak of interest. When GC/MS was attempted on the silylated peaks from separations like that in figure 40 no peaks appeared in the gas chromatogram which were due to organic molecules. In most cases the gas chromatogram was identical to that obtained for silylating reagents alone. When peaks were observed in the gas chromatogram the mass spectrum of these generally corresponded to some form of silylated phosphate. These experiments were repeated several times utilizing

several different silylation techniques, but the results were the same. Infrared spectra were also run on the products eluted under the larger peaks after they had been desalted. The spectra were basically the same and were almost featureless. Only a few low, very broad bands were observed.

At this point it was felt that a better desalting technique was needed. It was decided to try high performance liquid chromatography (HPLC) utilizing a preparative scale Waters μ Bondpack C_{18} reverse phase column. Initial investigations were carried out with a 7.5% methanol + 92.5% water mixture as the eluant. This system gave baseline separation between allantoin and phosphate, guanosine and phosphate, and allantoin and guanosine. An injection from an electrolysis mixture showed several peaks and good separation from phosphate. However, after several days of use the column was flushed with methanol in preparation for storing the column for several days. It was found that a very large amount of material had remained on the column until the methanol wash. This was unacceptable since only small quantities of product would be available any losses would be unwelcome, and some molecules might be retained entirely and thereby lost. Eluants consisting of 50% methanol + 50% water and 70% methanol + 30% water were tried but resulted in very poor separation of phosphate from other materials. It was then decided to try using pure water as the eluant in the hope that organic compounds would retain completely on the column. The phosphate would then be flushed from the column by the water and when the phosphate had completely eluted the organic molecules could be removed from the column by a 2 ml injection of methanol. This seemed to work quite

well for guanosine, allantoin, and urea. However, the oxidation products of guanosine did not completely retain on the column. Further, it was discovered that the phosphate peak, while it appeared relatively narrow from the detector readout (using a u.v. detector set to 254 nm the peak appeared to be ≈5 ml wide) in actuality it was found to be spread out over several hundred milliliters. Then 0.001 M HCl was tried as the eluant. It was hoped that the additional ionic strength would decrease the tailing of the phosphate peak without decreasing the retention of organic molecules. In fact the 0.001 M HCl separation looked virtually identical to the one obtained with pure water. Various acetonitrile-water mixtures were tried as eluants, but they gave mixtures very similar to the methanol-water mixtures.

It was then decided to return to the gravity flow Sephadex G-10 columns, but to try water, methanol mixtures as the eluant. Eluants containing 10%, 30%, and 100% methanol were utilized with no success. Phosphate and the organic materials eluted as a single peak.

Next it was attempted to desalt the electrolysis product directly with no prior separation. It was felt that the separation of components could be achieved later by gas chromatography after silylation. Two 90 cm x 2.5 cm Sephadex G-10 columns coupled together with water as the eluant was the system chosen. Figure 41 shows a typical chromatogram from 5 mg of guanosine oxidized at 1.15 V (peak V_a) in 20 ml of pH 7 phosphate buffer. Peaks 1 and 2 are due to phosphate used in the electrolysis. Peak 3 is the only other peak observed. Some phosphate was still present after one pass through the columns, so peak 3 was collected, lyophylized, and passed through the

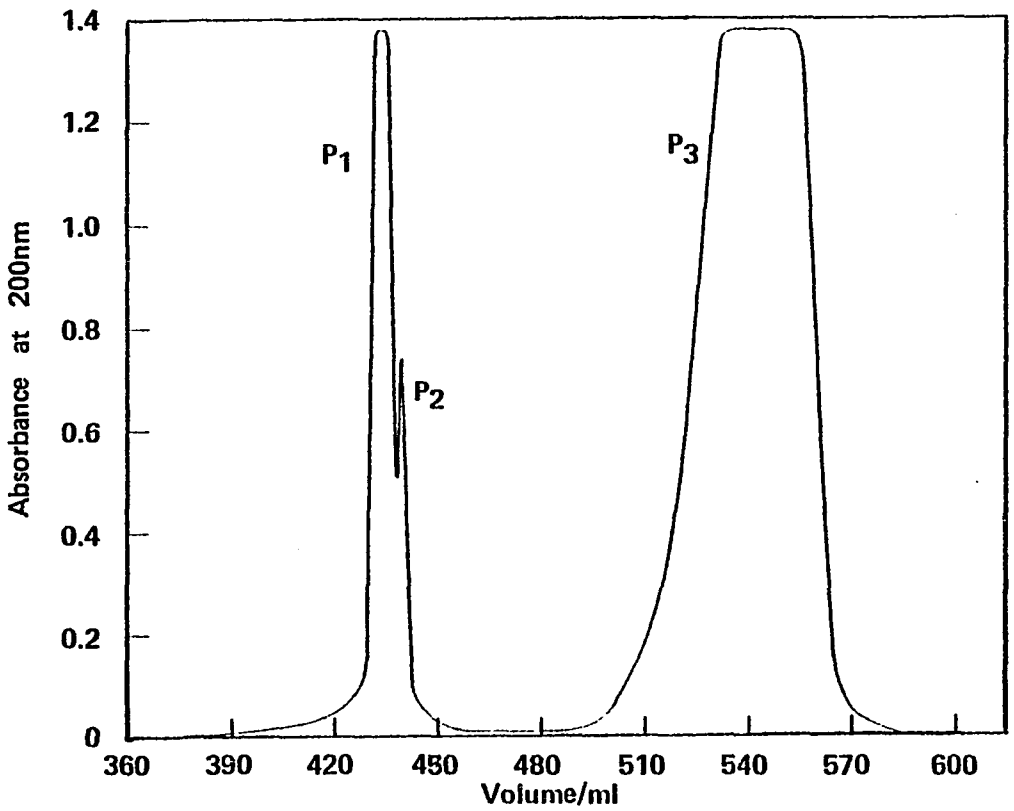

Figure 41. Liquid chromatogram of the products from the electrooxidation of a pH 7, 0.80 mM guanosine solution at 1.15 V (peak V_a) utilizing two 90 cm x 2.5 cm columns of G-10 resin coupled together with water as the eluant.

columns again. There was no typical chromatogram for the second time through. In all cases both the phosphate peaks and the product peak eluted at smaller volumes. Peaks 1 and 2 were always much smaller and peak 2 was often absent. Peak 3 sometimes appeared much as it does in figure 41. At times it was much shorter and broader, but still relatively symmetrical. Sometimes it appeared as it does in figure 42. The shape of peak 3 in figure 42 suggests that some of the products were decomposing. The view that the broadening is due to decomposition was supported by the behavior a particular desalting of peak 3. In this case peak 3 was passed through the double G-10 system four times (the peak broadened, but remained relatively symmetrical). Upon silylation two very large peaks were observed in the gas chromatogram (see figure 43). The mass spectral data for the GC peak with a retention time of 30.25 minutes is given in figure 44. The molecular ion is 518. This mass would correspond with allantoin which has been fully silylated (5 trimethyl silyl groups). Also the fragmentation

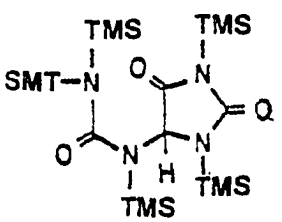

pattern matches very well the fragmentation pattern of authentic silylated allantoin. The mass spectral data for the GC peak with a retention time of 23.15 minutes is presented in figure 45. The

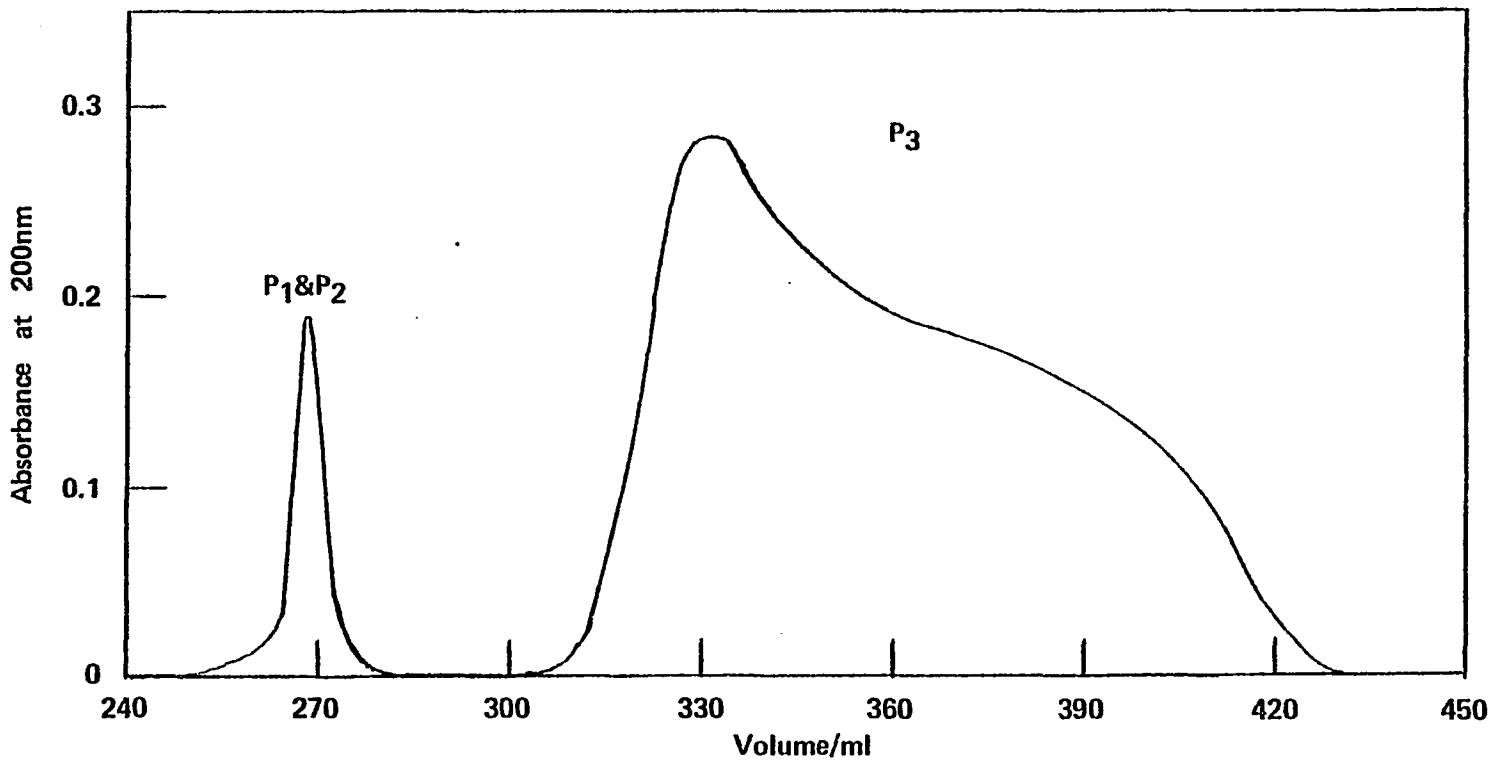

Figure 42. Liquid chromatogram of the material eluted under peak 3 of figure 41 utilizing two 90 cm x 2.5 cm columns of G-10 resin coupled together with water as the eluant.

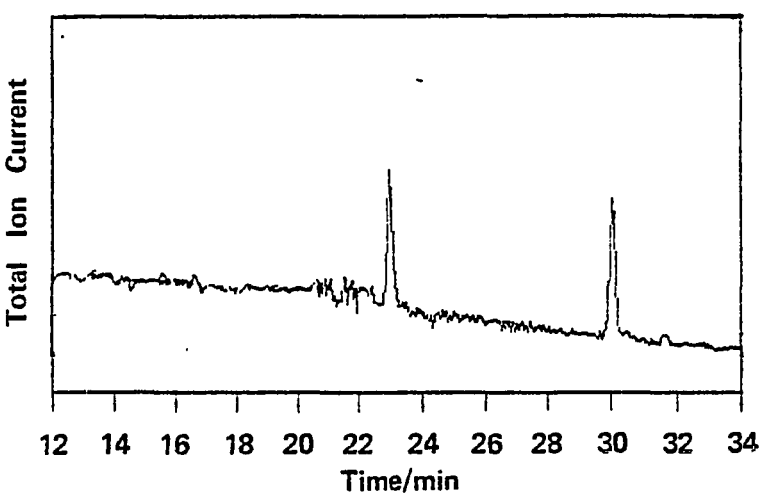

Figure 43. Gas chromatogram of the silylated material eluted under peak 3 of figure 41 after four passes through the coupled G-10 columns.

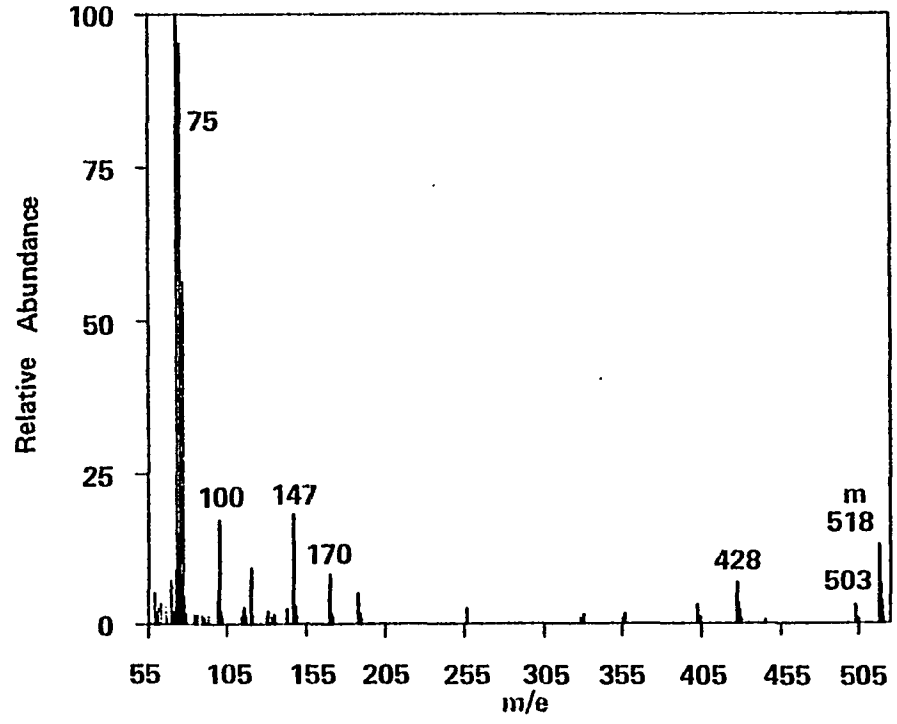

Figure 44. Mass spectrum of the material appearing at 30.25 min in figure 43.

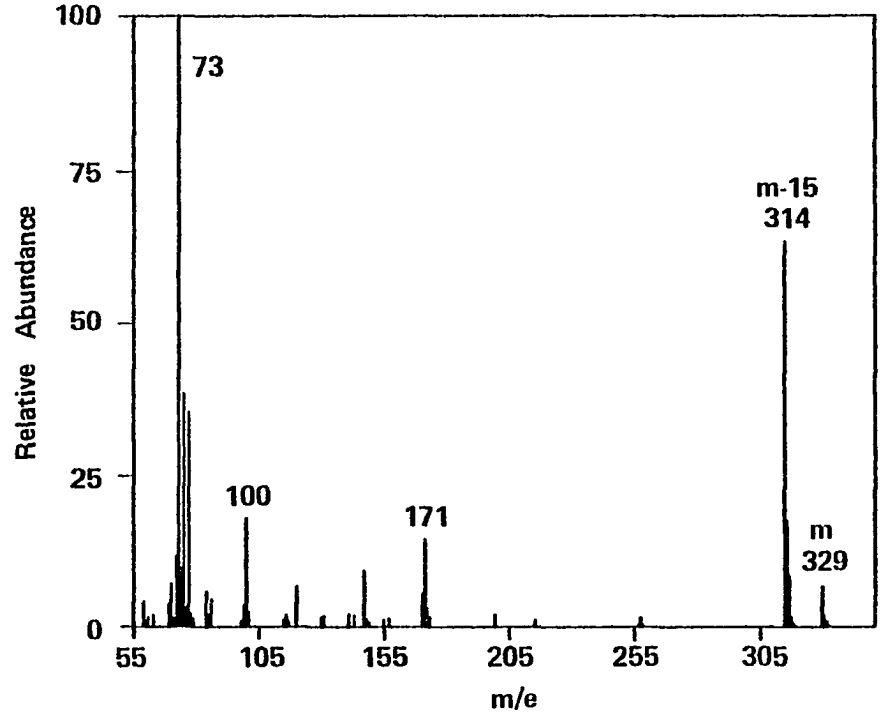

Figure 45. Mass spectrum of material appearing at 23.15 min in figure 43.

molecular ion (M) has a mass of 329. The M-15 peak (314) is quite prominent and M-72 (loss of one trimethylsilyl group) is present. This could correspond to 5-imino-2,4-imidazodione which has been silylated in three positions. Both allantoin and 5-imino-2,4-imidazo-

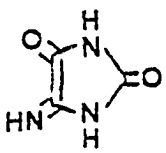

dione would seem to be reasonble decomposition products from the kinds of oxidation products one might expect for guanosine. It is a bit surprising to find allantoin rather than oxalylguanidine but apparently

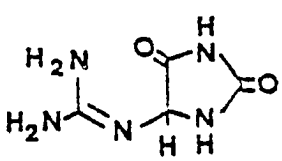

the imino group on the number 7 carbon is relatively easy to hydrolyze.[66] Attempts to find products which had not decomposed were unsuccessful with this system.

Since the use of low ionic strength phosphate eluant produced

a superior separation to that obtained with pure water (compare figures 26 and 27), but created a problem in removing the phosphate from products it was decided to try using 0.001 M HCl as the eluant. The HCl would provide some ionic strength and it was hoped improve the separation. Unlike phosphate, however, HCl is relatively volatile and could (it was felt) be removed by lyophylization. This would result in a product which was separated from other products and relatively phosphate and HCl free. Figure 46 shows a typical chromatogram of the electrolysis products of 5 mg guanosine oxidized at 1.15 V (peak V_a) in 20 ml of pH 7 phosphate buffer. Peak 1 in this chromatogram is phosphate from the electrolysis buffer. Peaks 2-9 are product peaks. Each peak was collected into a separate flask, frozen, and lyophylized. The resulting substance in each case was rather sticky as if still moist. Attempts to silylate these samples gave only peaks due to background in the GC chromatogram. It was believed that not all the HCl had been removed. In an attempt to remove the HCl more completely the lyophylized products were washed with acetone. Hydrogen chloride is somewhat soluble in acetone but most purines and their known products are not. This resulted in substances which no longer appeared sticky, but brought no improvement in the gas chromatograms.

An attempt was made to perform the initial separation utilizing a single 90 cm x 2.5 cm column of Sephadex G-10 with 0.025 M phosphate buffer as the eluant, and then desalting the product peaks on a dual G-10 water system. The system used for the initial separation has been discussed earlier and typical chromatograms are shown in figures 26-30. This yielded no better results than those obtained previously

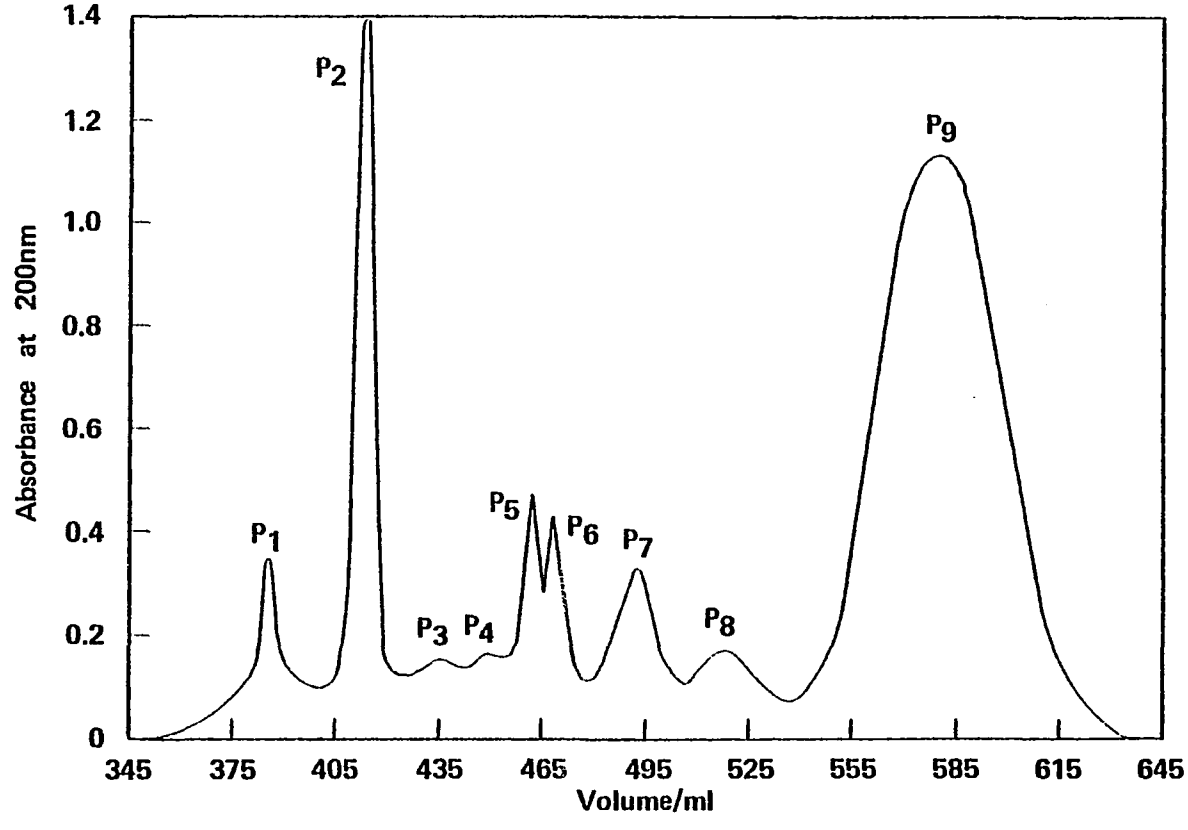

Figure 46. Liquid chromatogram of the products from the electrooxidation at 1.15 V (peak V_a) of a pH 7, 0.8 mM guanosine solution utilizing two 90 cm x 2.5 cm columns of G-10 resin coupled together with 0.001 M HCl as the eluant.

using Sephadex G-10 coupled to Sephadex QAE for the initial separation.

It was known that the silylation process could tolerate small amounts of phosphate. Therefore a chromatogram was run which utilized a single 90 cm x 2.5 cm G-10 column and 0.005 M pH 7 phosphate buffer as the eluant. It was hoped that the low phosphate eluant would not interfere with the silylation, but would provide a better separation between electrolysis phosphate and the products. A chromatogram of 5 mg 8-hydroxyguanosine oxidized at 1.0 V (peak III_a) is presented in figure 47. Peak 1 is the phosphate from the electrolysis buffer and peaks 2-8 are product peaks. Peaks 2, 3, and 4 were collected together, frozen, and lyophylized. Peak 5 was collected, frozen, and lyophylized, and peaks 6, 7, and 8 were collected, frozen, and lyophylized. The lyophylized samples were then silylated. The gas chromatogram for the silylated sample containing the components eluted under peaks 2, 3, and 4 is shown in figure 48. Figures 49-52 show the mass spectral data for GC peaks eluting at 24.73, 25.45, 25.98, and 26.25 minutes, respectively. All four peaks appear to be due to free ribose. The peak at 26.25 minutes matches very well with authentic ribose (see figure 53). The peaks at shorter times show the base peak with a mass of 217, and a fragmentation pattern essentially the same as authentic ribose except that some of the higher masses are not present. The mass spectra for GC peaks eluting at 36.62 minutes, 37.22 minutes and 38.07 minutes (figure 54) are virtually identical. The peak at 38.07 shows some higher masses at 503, 504, and 505. Other than these masses the mass spectra of the three GC peaks are the same. All show the presence of ribose. Since none show a M-15

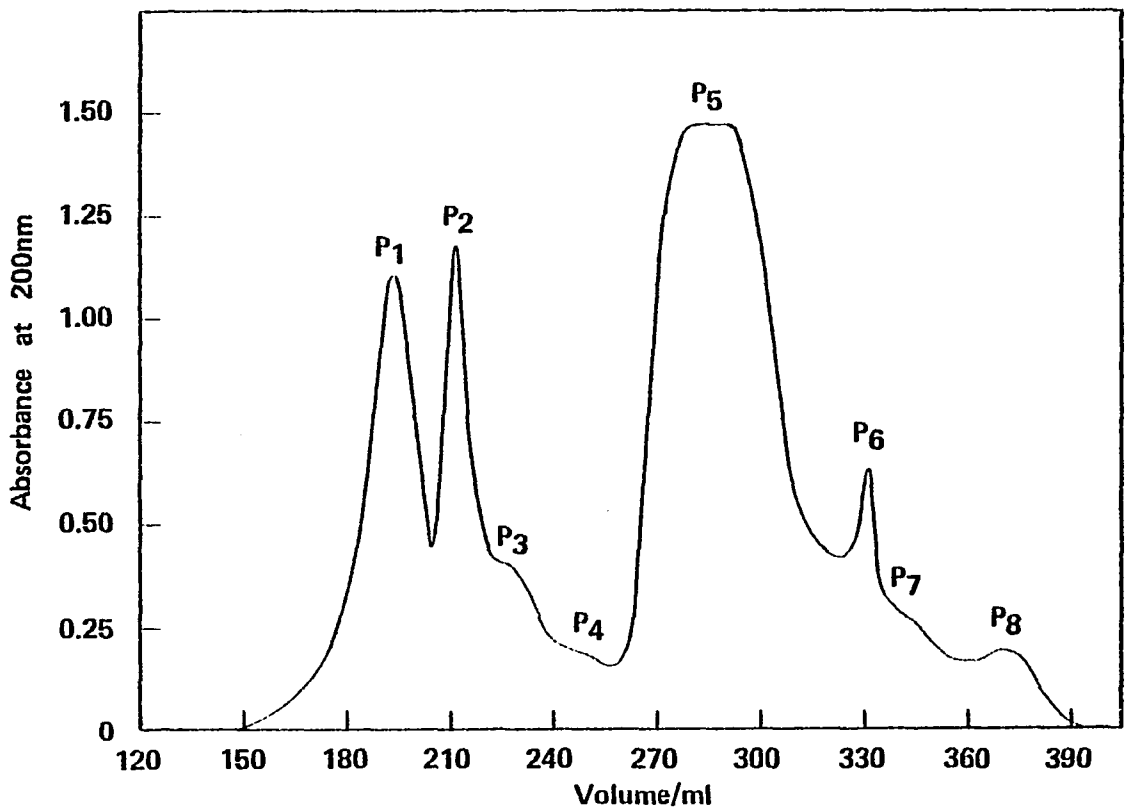

Figure 47. Liquid chromatogram of the products from the electrooxidation at 1.0 V (peak III_a) of a pH 7, 0.84 mM 8-hydroxyguanosine solution utilizing a single 90 cm x 2.5 cm column of G-10 resin with 0.005 M pH 7 phosphate buffer as the eluant.

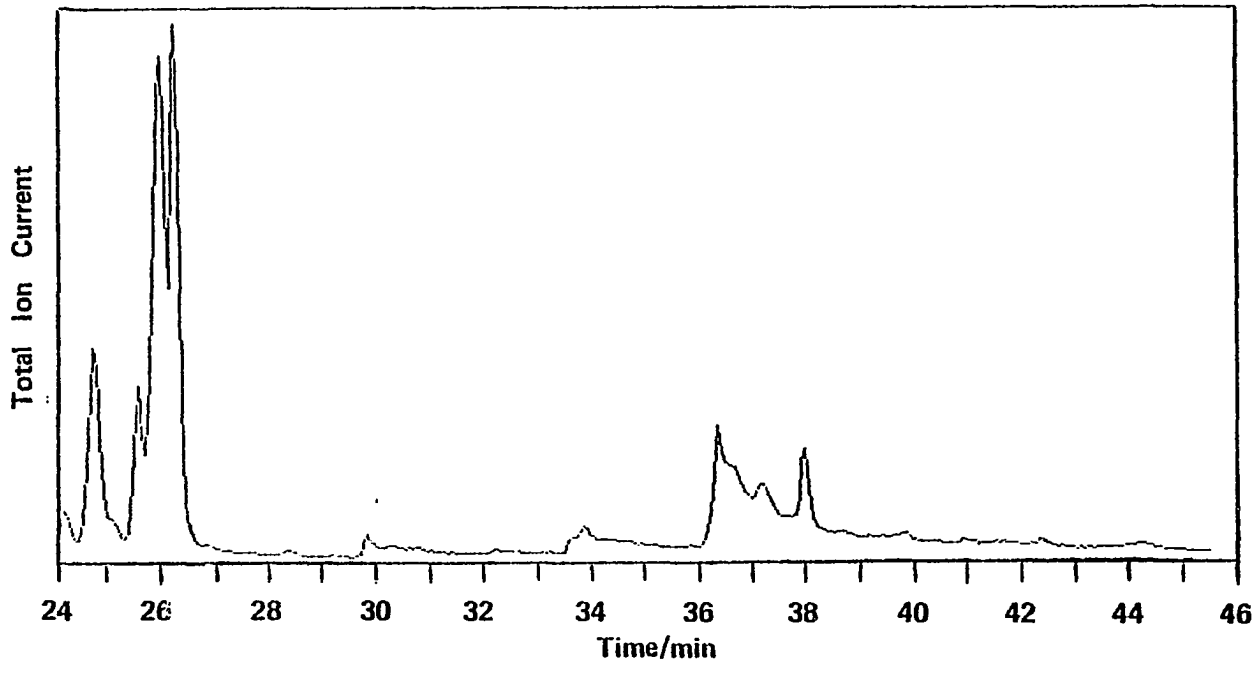

Figure 48. Gas chromatogram of the material eluted under L.C. peaks 2, 3, and 4 of figure 43, after silylation.

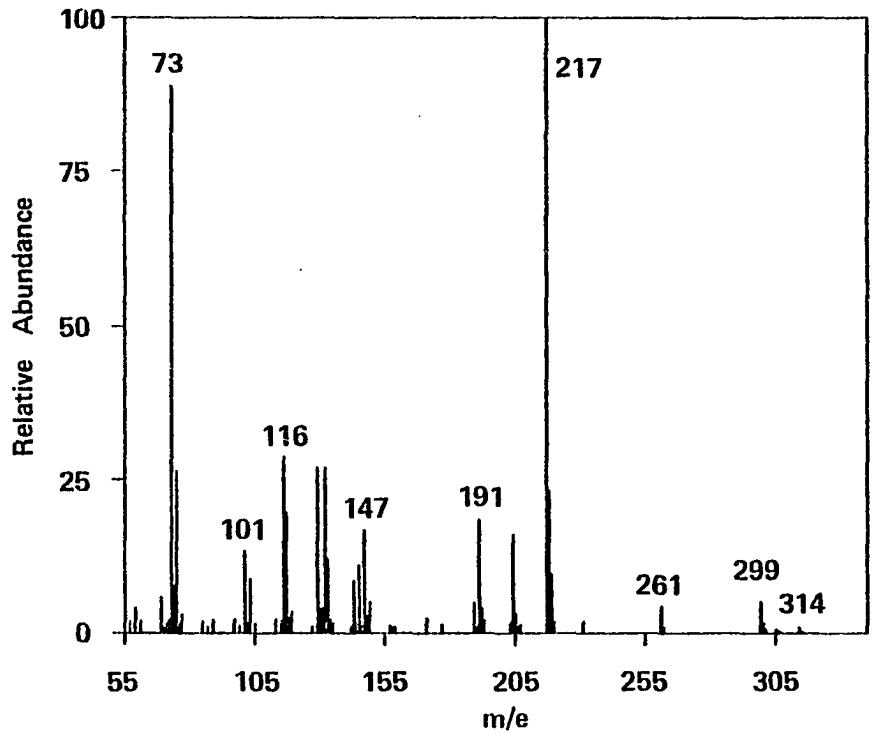

Figure 49. Mass spectrum of material occurring at 24.73 min in figure 48.

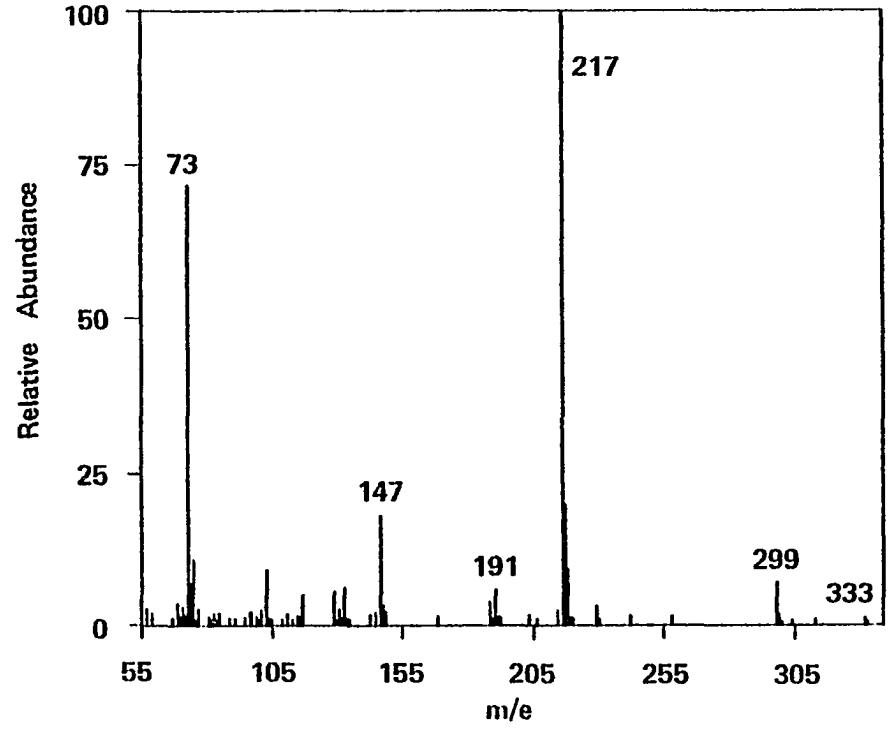

Figure 50. Mass spectrum of material eluting at 25.45 min in figure 48.

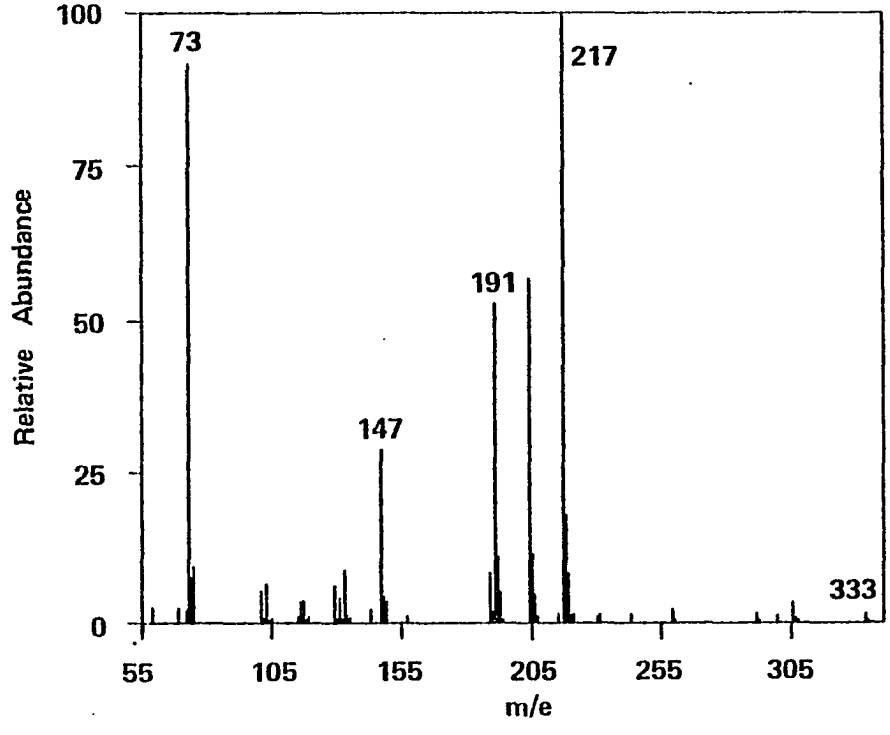

Figure 51. Mass spectrum of material eluting at 25.90 min in figure 48.

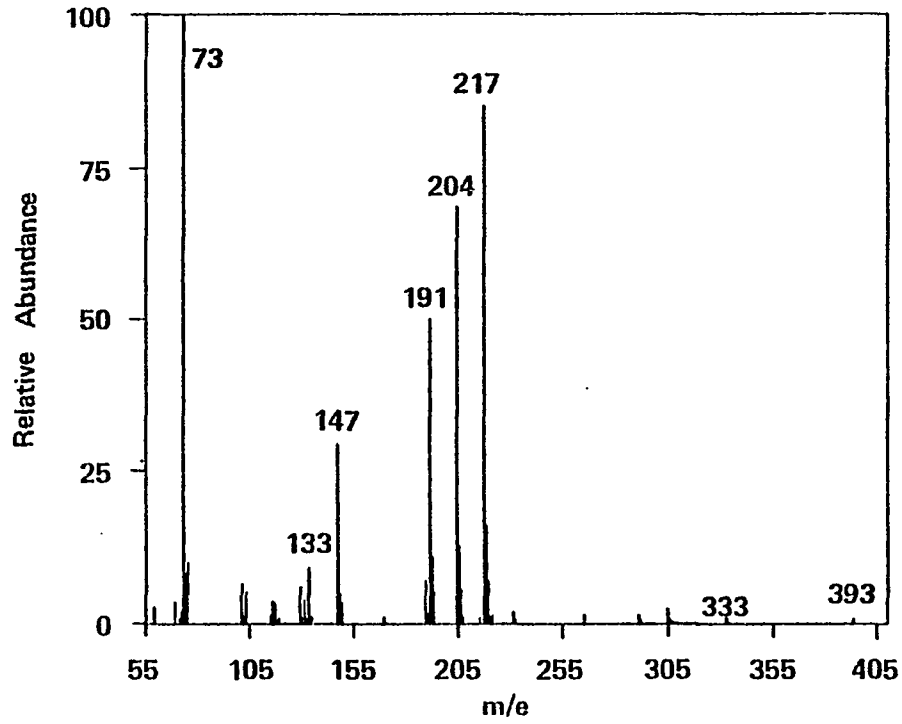

Figure 52. Mass spectrum of material eluting at 26.25 min in figure 48.

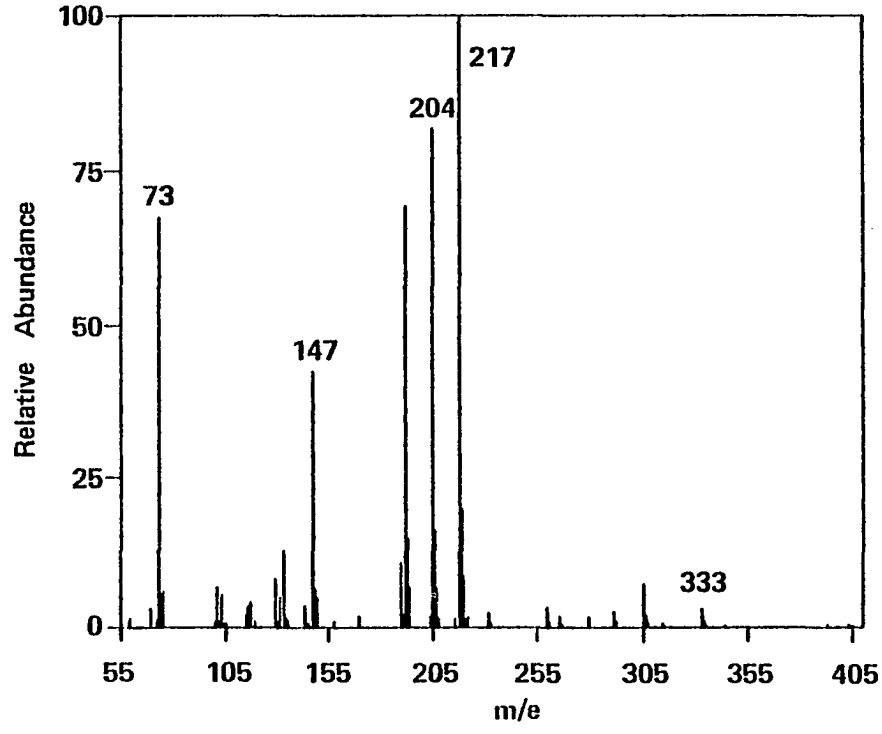

Figure 53. Mass spectrum of authentic silylated d-ribose.

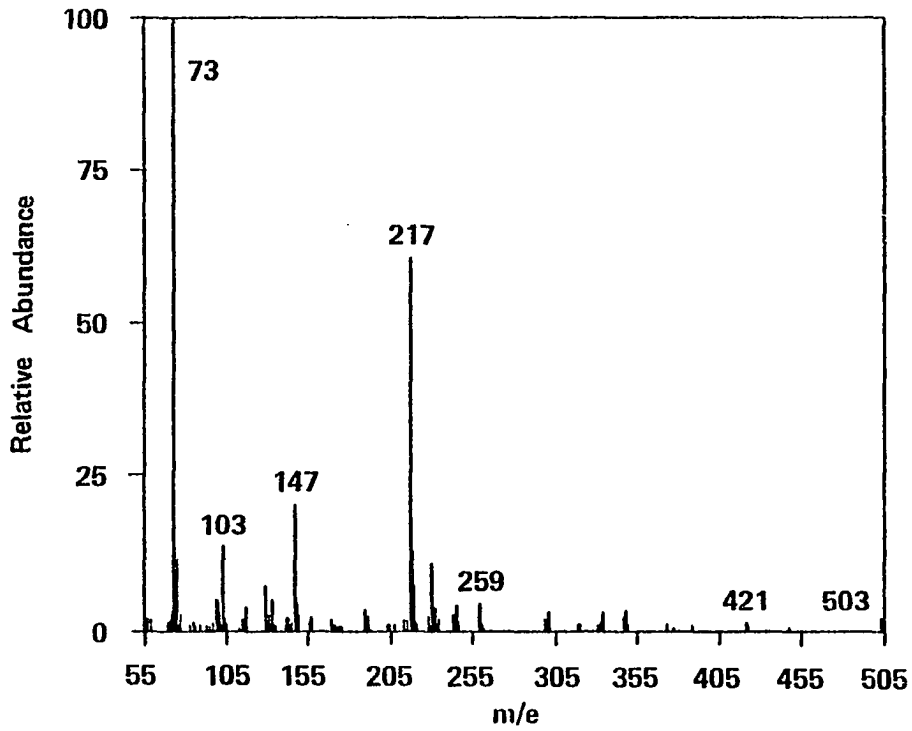

Figure 54. Mass spectrum of material eluting at 38.07 min in figure 48.

peak in the mass spectral data it is unlikely that the molecular ion appears. They all seem to be fragments of some larger species. The largest mass observed in the mass spectral data (m/e = 580) occurred at 39.85 minutes in the gas chromatogram. The mass spectrum is presented in figure 55. This seems to be simply a larger fragment which also has ribose present. The gas chromatogram for the silylated peak 5 of figure 47 is shown in figure 56. The significant peaks occur at 40.55, 41.28, and 42.27 minutes. The mass spectral data is not terribly informative. All indicate the presence of a ribose fragment, all seem to be fragments of some larger species. The largest mass present was 514 in the 41.28 min peak. The gas chromatogram for the silylated combination of LC peaks 6, 7, and 8 was almost totally devoid of peaks. The largest was at 26 minutes and appeared to correspond to free ribose.

In an effort to avoid giving the products a long period of time to decompose during the separation and desalting process it was decided to try using a 35 cm x 2.5 cm column of Sephadex G-10 with water as the eluant. Taking the lyophylized sample obtained from oxidizing 5 mg of guanosine at 1.0 V and placing it on the short G-10, water column resulted in the liquid chromatogram presented in figure 57. There is more detail present than one would expect based upon the chromatogram in figure 41 which utilized two 90 cm x 2.5 cm columns of Sephadex G-10, but the separation from phosphate is much poorer. Peak 3 was collected (although the first nine milliliters were discarded in order to reduce the amount of phosphate present), lyophylized, and silylated. Peak 4 was collected, lyophylized, and silylated.

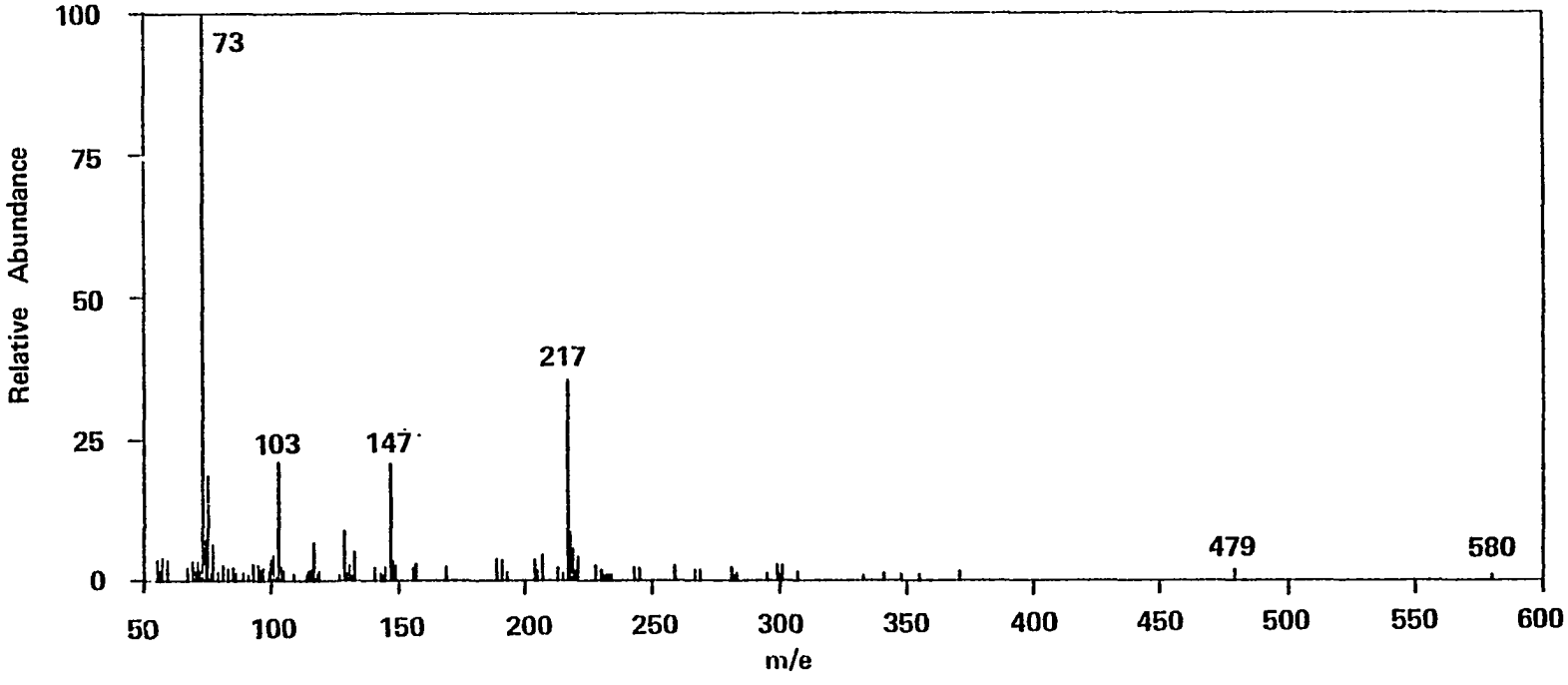

Figure 55. Mass spectrum of material eluting at 39.85 min in figure 48.

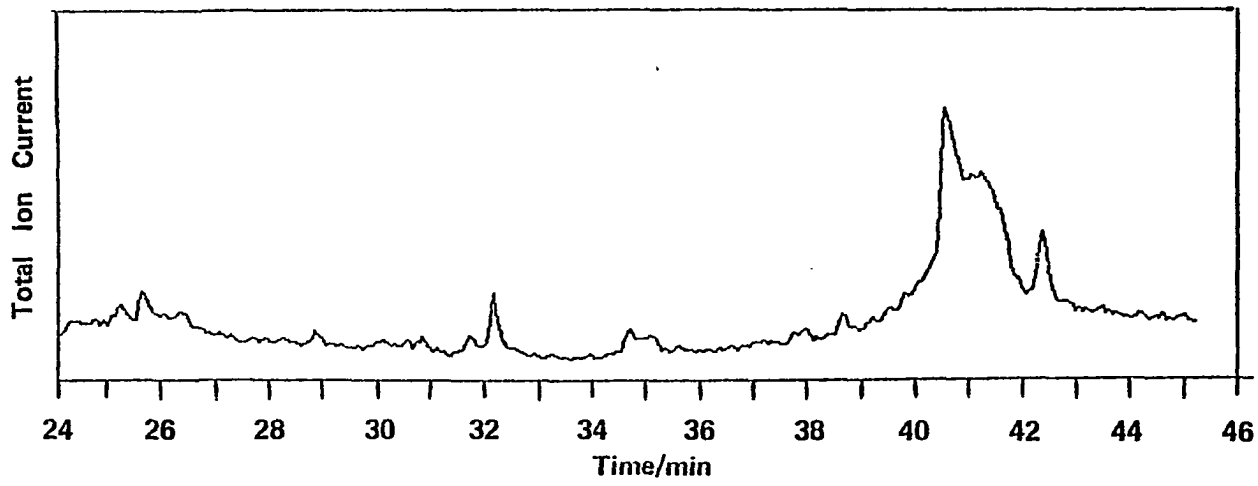

Figure 56. Gas chromatogram of the material eluting under L.C. peak 5 of figure 47, after silylation.

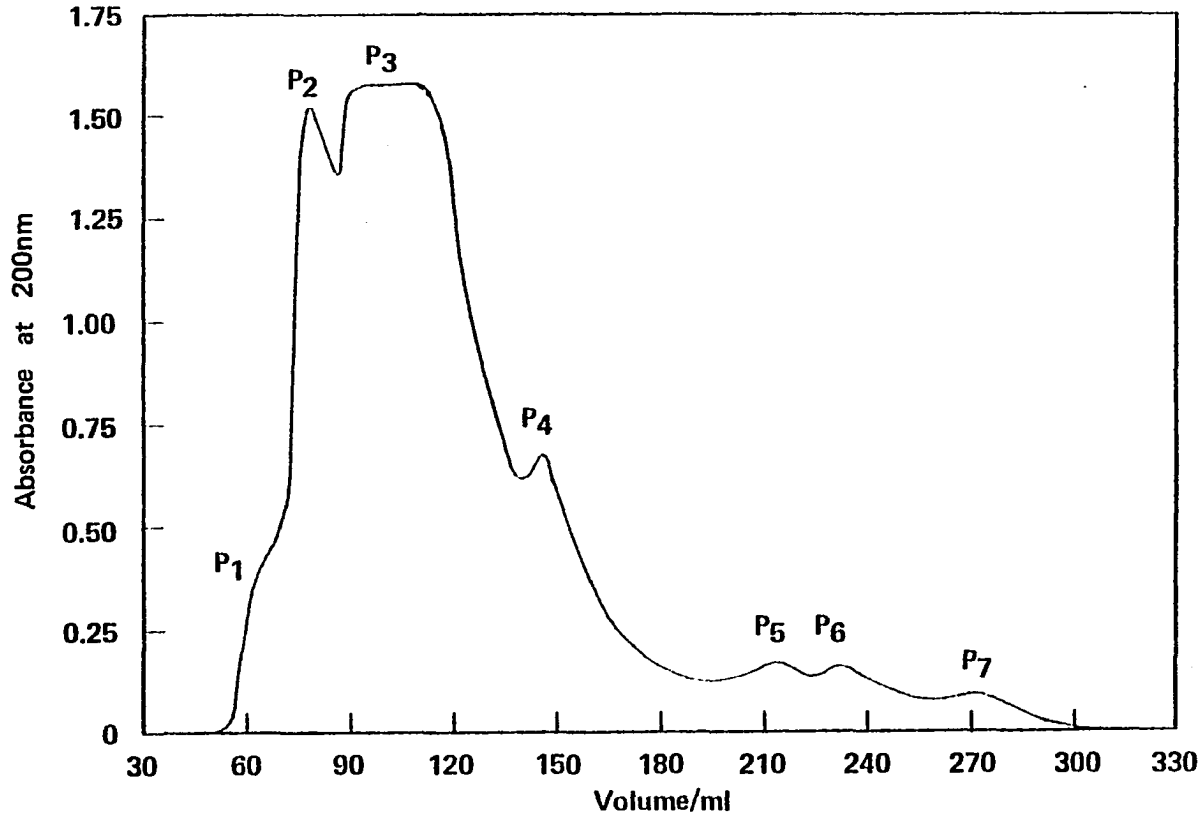

Figure 57. Liquid chromatogram of the products obtained from the oxidation of a pH 7, 0.84 mM 8-hydroxyguanosine solution at 1.0 V (peak III_a) utilizing a 35 cm x 2.5 cm column of G-10 resin with water as the eluant.

Peaks 5, 6, and 7 were collected together, lyophylized, and silylated. The mass spectral data for LC peak 3 in figure 57 showed a great deal of free ribose and no other significant information. The gas chromatogram for the silylated LC peak 4 showed no significant peaks. The gas chromatogram for the silylated LC peaks 5, 6, 7 is shown in figure 58. The mass spectral data for the gas peak at 28 minutes is shown in figure 59. It seems clear the molecular ion is 343 and M-15 (328) is even more prominent. A likely guess for the number of trimethylsilyl groups is three. This would give a molecular weight of 127 (343-(72)3). A molecular weight of 127 gives a possible molecular formuls of $C_4H_5N_3O_2$. Two plausible structures would be:

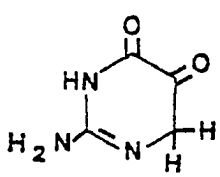

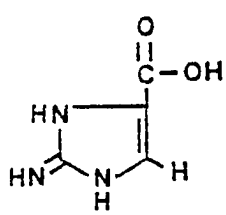

During much of the time that various separation techniques were being tried on large scale electrolysis mixtures another approach was also being investigated. Since the silylation procedure can tolerate small amounts of phosphate it was decided to carry out electrolyses in the RVC thin-layer cells using a buffer consisting of 0.5 M NaCl and pH 7 phosphate buffer 2.5 times greater than the electroactive species concentration (0.5-5.0 mM). The electrolyzed sample was then blown from the thin-layer cell, transferred as quickly as possible to a silylation reaction vessel, frozen, and lyophylized. This sample was then

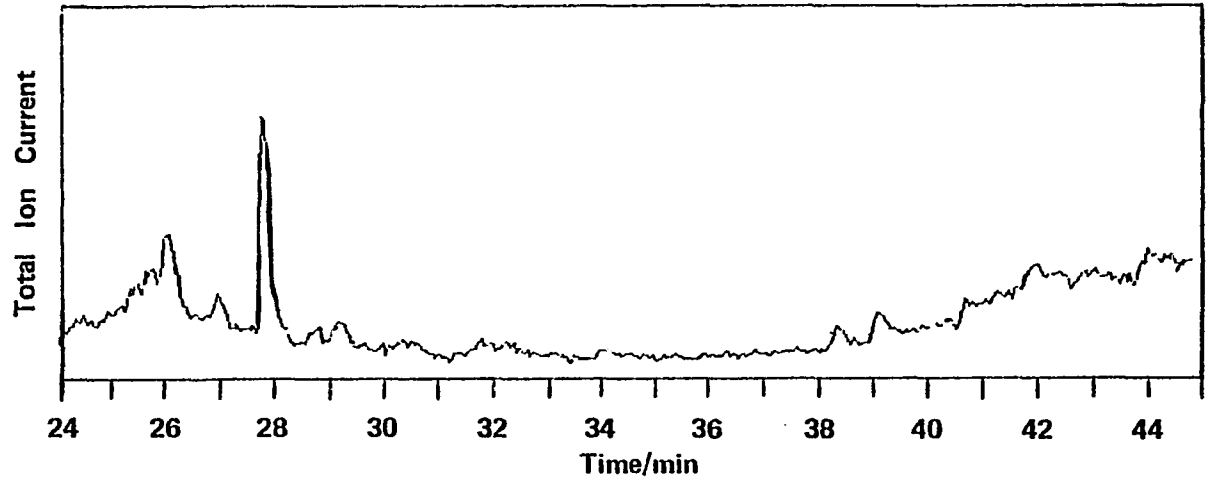

Figure 58. Gas chromatogram of the material eluting under L.C. peaks 5, 6, and 7 in figure 57, after silylation.

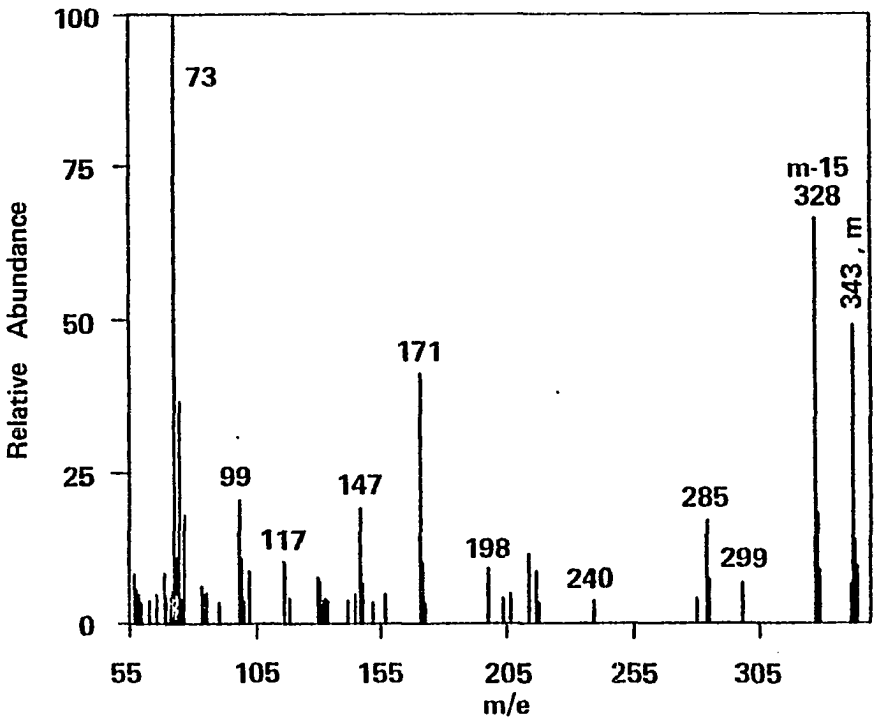

Figure 59. Mass spectrum of material eluting at 28.03 min in figure 58.

silylated and GC/MS data collected. Forty different samples were prepared by oxidation in the thin-layer cells. Among these forty samples the silylating reagents were varied, the duration and temperature of the silylation was varied, the number of oxidations collected, the potential the oxidation was performed at, the electroactive species, and the concentration of phosphate were all varied. From these forty samples six provided information of interest. The rest showed only starting material or various background peaks.

In figure 60 the gas chromatogram for thin-layer sample number three (TL #3) is presented. The mass spectral data for the G.C. peak with a retention time of 42.2 minutes is presented in figure 61. This data matches quite well with authentic 8-hydroxyguanosine (see figure 62). Between 38.9 and 39.9 minutes in the gas chromatogram are a series of four peaks whose mass spectral data are relatively similar. The data for the peaks at 38.9 and 39.43 minutes (figure 63) are essentially identical. The peaks at 39.9 and 41.57 look somewhat similar to each other and to the peaks at 38.9 and 39.43 minutes. However, from the higher masses appearing they may be somewhat contaminated with starting material. Nevertheless, all four peaks show marked similarities below masses of 400, none show a clear molecular ion, and if one chooses a mass as appearing to be a molecular ion none show an M-15 peak which is normally quite prominent in the mass spectra of silylated compounds. All four show large amounts of a ribose residue as indicated by the large 217 peak in the mass spectra. All of these peaks would appear to be decomposition peaks from some larger molecule. This would explain the lack of any molecular ion peak, if the species

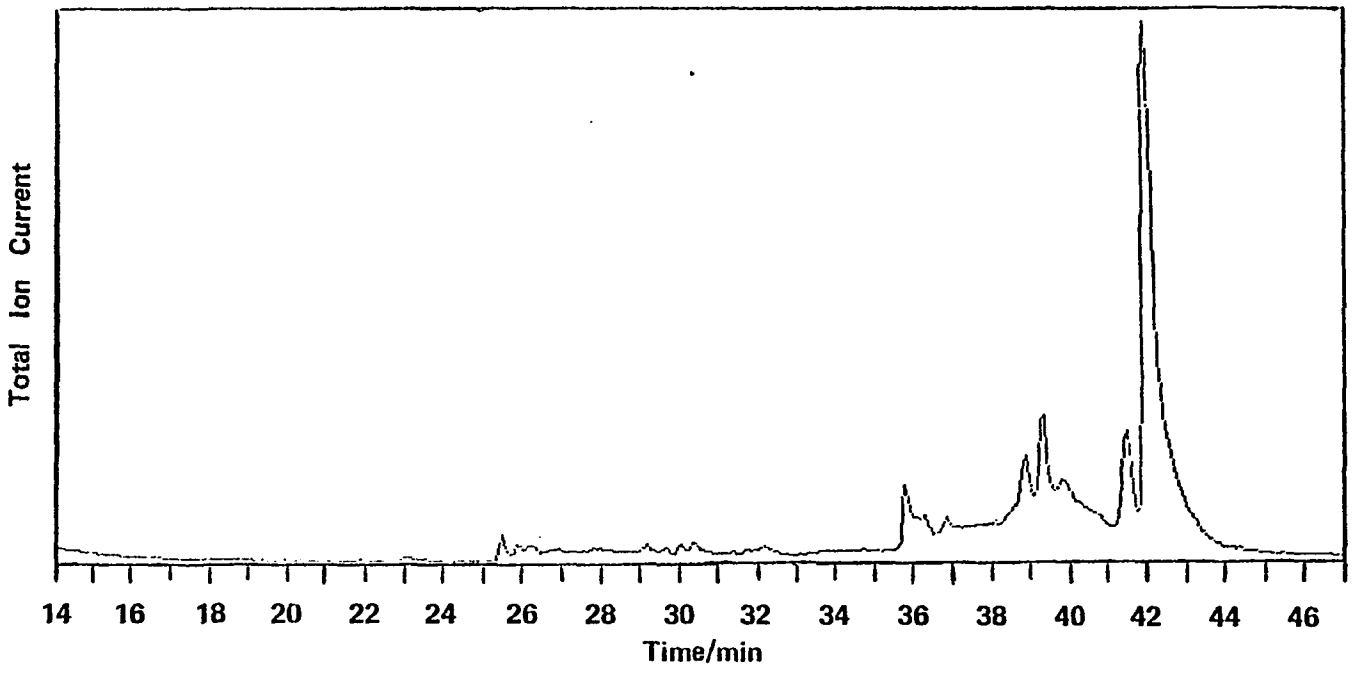

Figure 60. Gas chromatogram of the silylated material of thin-layer sample number three (TL #3).

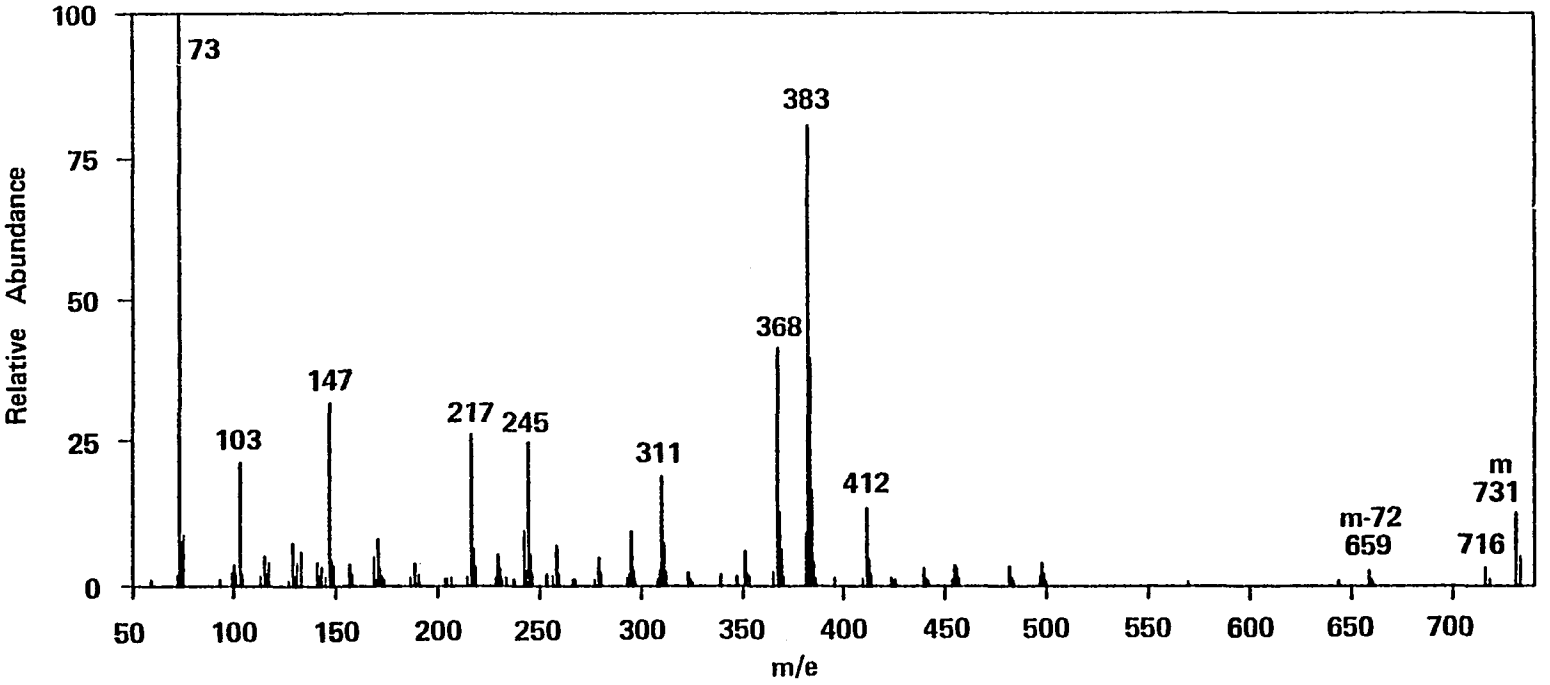

Figure 61. Mass spectrum of the material eluting at 42.17 min in figure 60.

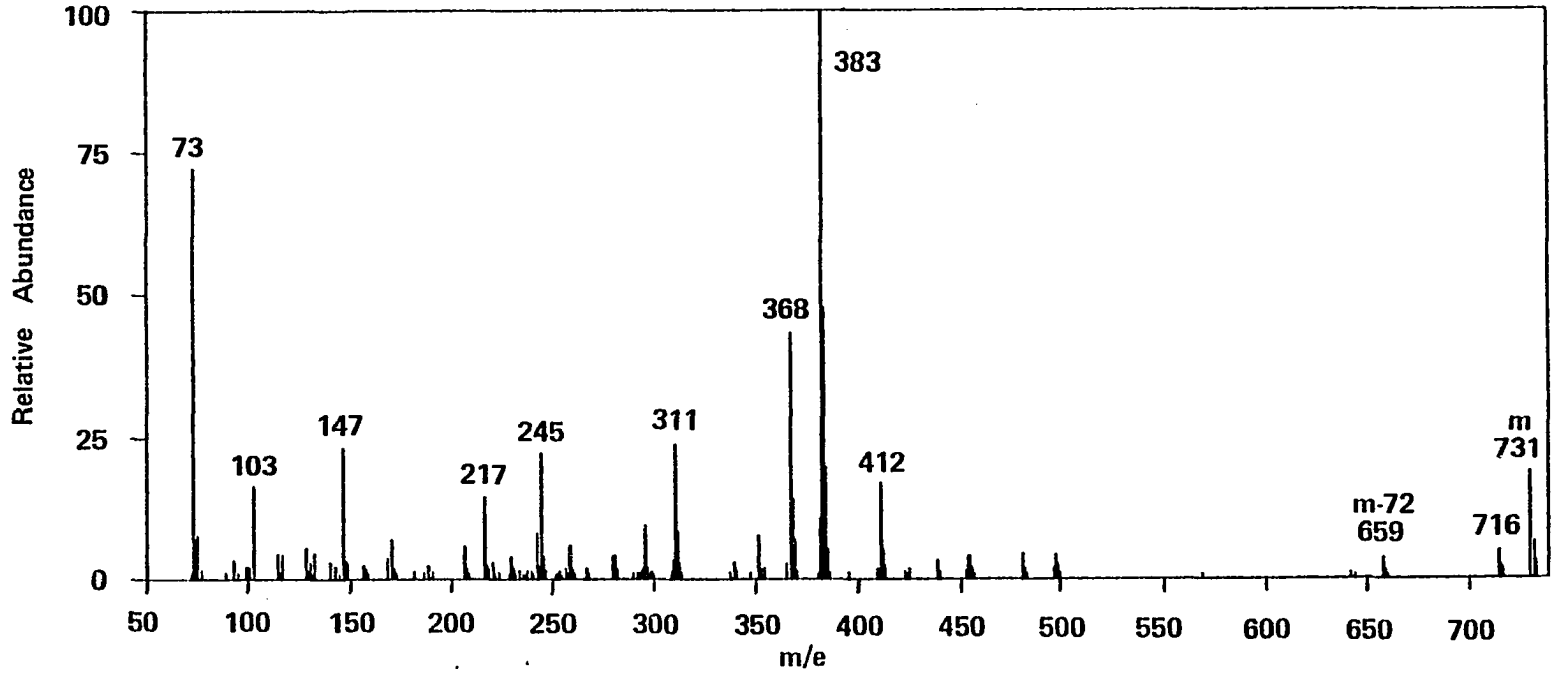

Figure 62. Mass spectrum of authentic silylated 8-hydroxyguanosine.

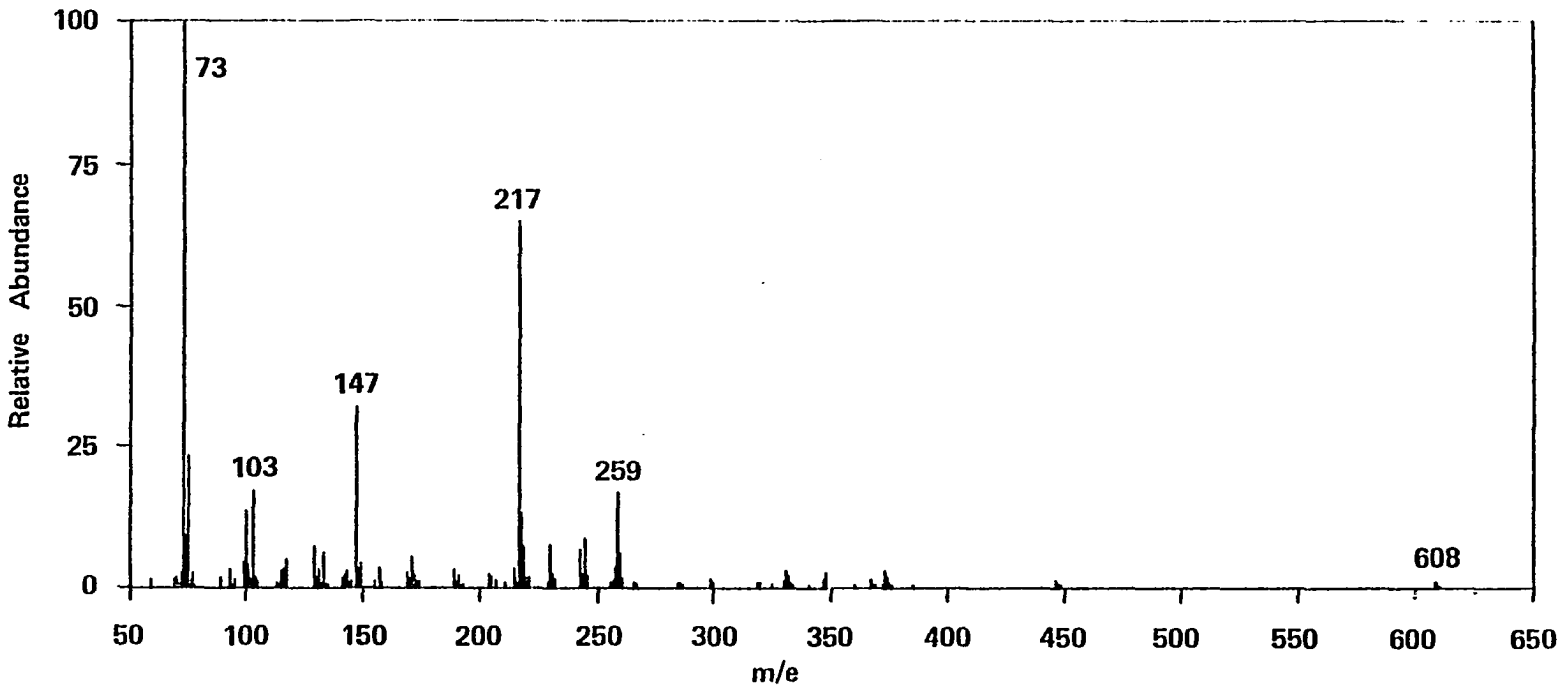

Figure 63. Mass spectrum of material eluting at 38.9 min in figure 60.

were decomposing after being injected onto the GC. The mass spectra of the GC peaks at 36.92, 36.33, and 35.87 minutes are virtually identical to each other and appear similar to the peaks between 38.9 and 41.6 minutes except in the case of the peaks at shorted retention times show smaller masses as the highest observed mass, but the fragmentation patterns are almost identical. The cluster of small peaks around thirty minutes in the gas chromatogram bear no obvious relation to the peaks at longer retention times. They show relatively large amounts of ribose residue largest masses in the mid 300's with no obvious molecular ion peak. The peaks around 26 minutes might be free ribose. The peaks around 26 minutes might be free ribose. The retention times are approximately correct, but the peaks are too small to be conclusive.

The gas chromatogram of TL #3 proved to be typical of those samples which showed some peaks not due directly to background. TL #9 showed the same peaks in the gas chromatogram as TL #3. However, in TL #9 the peaks around 36 minutes were quite large and the peaks around 39 minutes too small to obtain good mass spectral data. The mass spectra for the GC peaks around 36 minutes were identical for TL #9 and TL #3. TL #10 showed essentially the same pattern (see figure 64). Most of the peaks either matched exactly with TL #3 or were too small to obtain good mass spectral data. The peak of 39.38 (see figure 65) is quite small and does not give 608 as does the equivalent peak in TL #3, but all the same peaks are present, as though TL #10 were too dilute for the higher masses to show. Further TL #10 GC peak 39.38 matches exactly the mass spectrum presented in figure 54. In

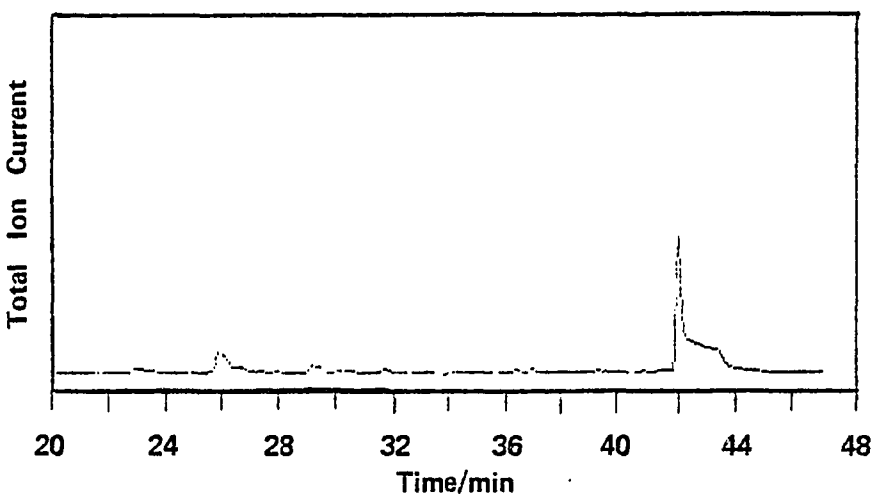

Figure 64. Gas chromatogram for the silylated material of TL #10.

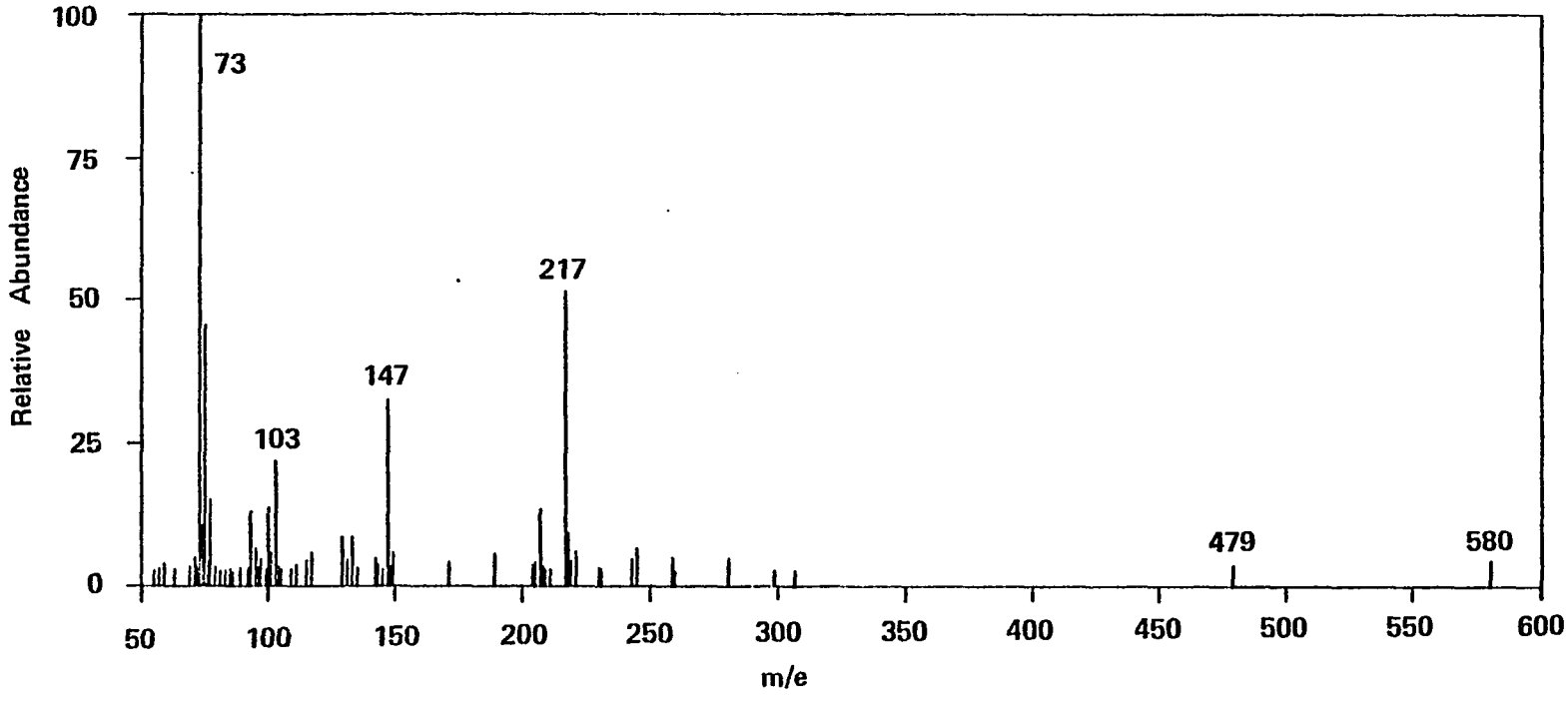

Figure 65. Mass spectrum of the material eluting at 39.38 min in figure 64.

TL #13 the GC peak at 40.73 minutes showed an apparent molecular ion of 706 (see figute 65). No M-15 is present, however, so it is most likely not the molecular ion. In TL #22' a GC peak eluting at 39.9 minutes shows mass 608 again (see figure 67). The retention time and mass spectral data matches quite well with that in figure 63 from TL #3. TL #33 shows an ion at m/e = 580 and while the abudnance is much greater so more peaks occur in the mass spectrum the data for TL #33 in figure 68 is virtually identical to that for TL #10 in figure 65.

In all of these cases where interesting mass spectral data were obtained chemical ionization (CI) mass spectroscopy was attempted in an effort to find the molecular ion. In each case there was insufficient sensitivity in the CI mode to observe the desired peaks.

Electron impact (EI) mass spectroscopy performed at lower ionizing potentials (12 eV rather than 70 eV) produced the same information as those run at 70 eV.

Thus whether one performed large scale electrolyses and various separation schemes or performed thin-layer electrolyses and silylated directly the same results were obtained. Only fragments of some larger species were found with ribose and ions at m/e = 580 and 608 being the most common fragments observed. It was initially believed that oxalyl guanidine riboside would be the major product. Fully silylated oxalyl guanidine riboside would have a mass of 865. It was thought that this molecule was decomposing and many of the procedures attempted had in mind minimizing the decomposition of this molecule. Only later were the coulometric concentration studies per-

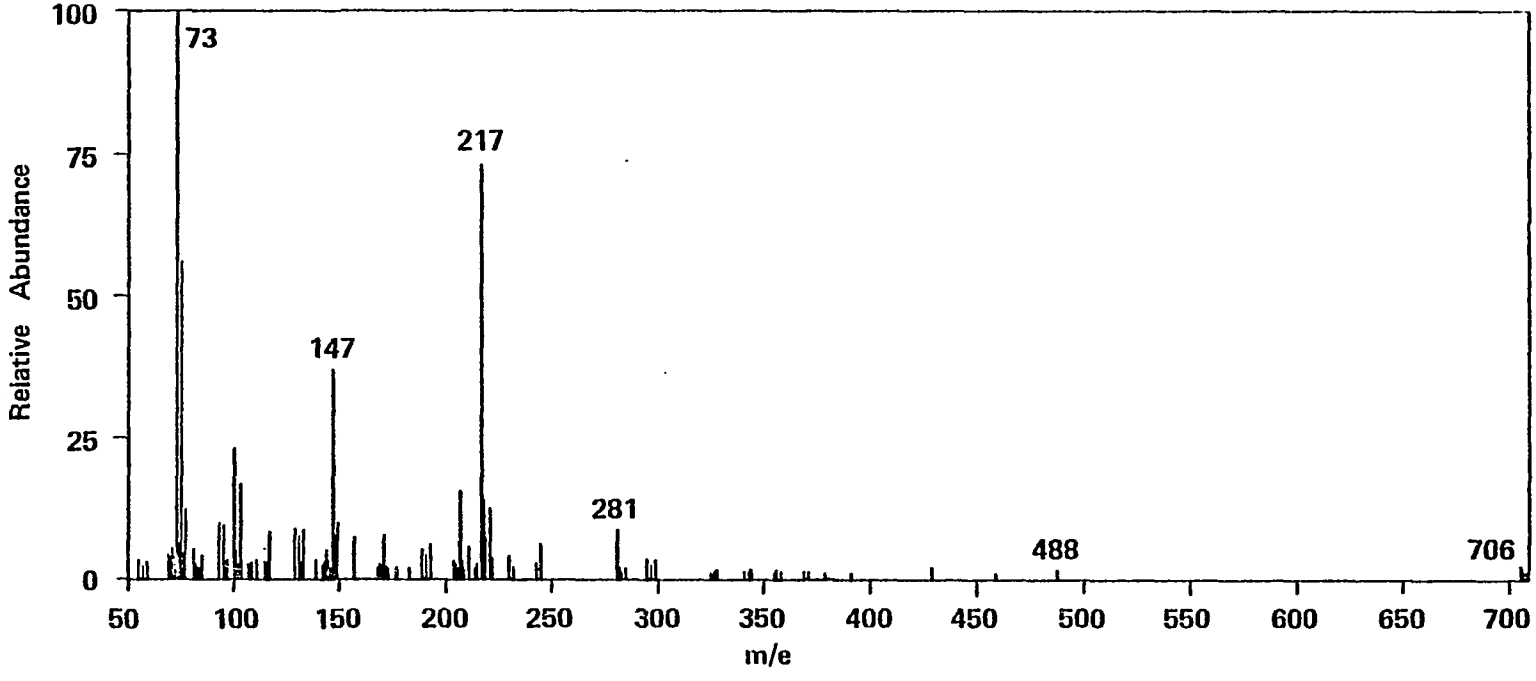

Figure 66. Mass spectrum of the material eluting at 40.73 min in the G.C. of a silylated TL #13.

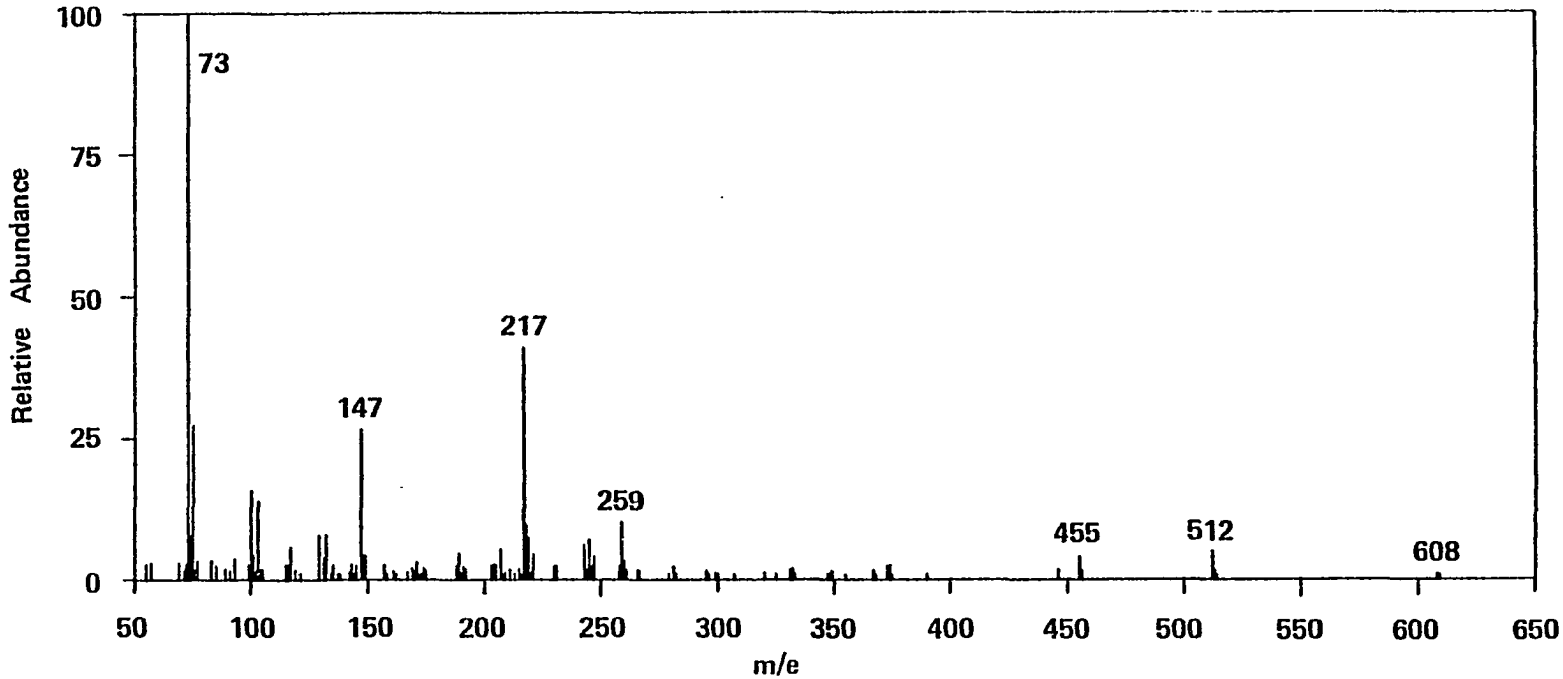

Figure 67. Mass spectrum of the material eluting at 39.9 min in the G.C. of TL #22'.

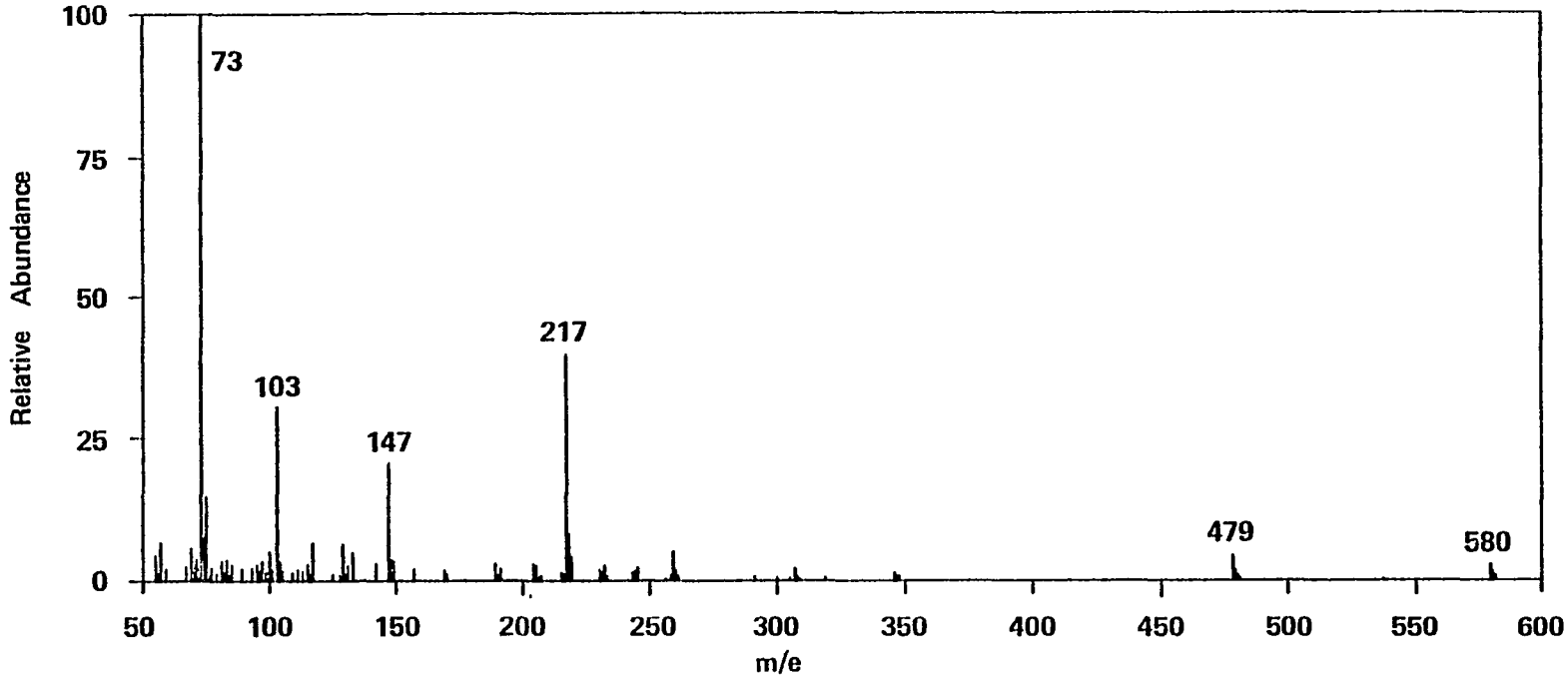

Figure 68. Mass spectrum of the material eluting at 39.18 min in the G.C. of TL #33.

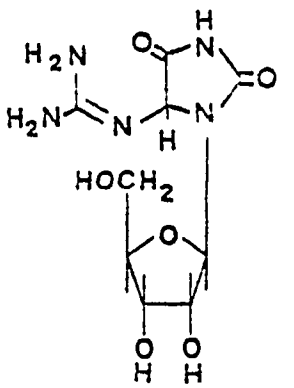

formed which indicated that perhaps a dimer was being formed. The GC/MS data obtained would certainly be consistent with a dimer which is decomposing after introduction to the GC/MS system. One would not observe a molecular ion for a silylated dimer even if it were sufficiently volatile to pass through the GC since the molecular weight would be too large for the mass spectrometer to measure.

DISCUSSION

The data presented in this study yields a complex and somewhat unclear picture of the reactions taking place in the oxidation of guanosine and 8-hydroxyguanosine.

The coulometric concentration studies and the mass spectral data seem to suggest that some non-monomer species is being formed. Whether this species is a dimer, several different dimers, an oligomer, or polymer is uncertain. If the linkage is <u>via</u> an N-N bond as is implied by the apparent similarity of products (since 8-hydroxyguanosine

has no sites available for a C-C linkage) then there are a number of possible sites for a linkage to occur. This makes it quite possible to envision units larger than a dimer being formed. The picture is further complicated by the fact that even though the separations that have been performed indicate that the products from the oxidation of 5 mg of guanosine or 8-hydroxyguanosine at pH 7 and 1.0 V are the same the voltammetry of guanosine still shows an oxidation peak after this electrolysis. If the electrolysis of guanosine is carried out at 1.15 V (peak V_a) until all voltammetric peaks are gone a new product peak appears in the chromatography. This indicates that some process is occurring in the oxidation of guanosine that does not occur in the oxidation of 8-hydroxyguanosine. Another portion of data indicates, however, that any differences must be small. That is as far as one can tell from the thin-layer spectroelectrochemistry and the kinetic studies the electrooxidation of guanosine and 8-hydroxyguanosine produce the same intermediates. It could be that in the case of guanosine some unoxidized guanosine is being incorporated into the product and that as part of this larger unit the guanosine is not oxidized until 1.15 V (peak V_a).

Whatever uncertainties there are in the reaction scheme a good deal of positive information was obtained in the course of these various studies. There is no doubt that in the oxidation of guanosine at least part of the guanosine is oxidized to 8-hydroxyguanosine. This is clearly indicated by the voltammetry. The voltammetry also indicates (though with somewhat less certainty) that a diimine (III, equation 1) and imine-alcohol (IV, equation 1) are formed. It is also clear,

however, from attempted product identification processes that if the products proposed in equation 1 are formed they are very, very minor products.

The thin-layer spectroelectrochemistry and thin-layer kinetics strongly imply that the intermediates formed upon electrooxidation of guanosine and 8-hydroxyguanosine are the same. Finally, there appears to be no doubt as shown by the spectra and kinetics that the electo-oxidation and the enzymic oxidation of 8-hydroxyguanosine over the pH range 4.6-9.3 follow the same reaction scheme.

EXPERIMENTAL

Chemicals

Guanosine was obtained from Calbiochem (San Diego, Cal.). 8-Hydroxyguanosine was synthesized *via* the technique of Holmes and Robins.[67] Catalase and Type VIII horseradish peroxidase were obtained from Sigma (St. Louis, Mo.). All buffers were prepared from reagent grade sodium phosphates and had an ionic strength of 0.5 M with the exception of certain liquid chromatographic (LC) eluants which had ionic strengths of 0.025 M or 0.005 M. Silylating reagents, bis(trimethylsilyl)trifluoro acetamide (BSTFA), N,O-bis(trimethylsilyl)acetamide (BSA), pyridine, and acetonitrile were obtained from Supelco, Inc. (Bellefonte, Pa.). Methanol used as L.C. eluant was reagent grade and was distilled in this lab before use.

Apparatus

The apparatus used for voltammetry was described in Chapter 2. The rapid-scan spectrometer (RSS) was the same as in Chapter 2 with

one exception. The RSS in Chapter 2 was equipped with a xenon arc lamp. For this work the RSS was modified to use a deuterium lamp. This change allowed the spectral region down to 200 nm to be observed. A new thin-layer cell was constructed utilizing Reticulated Vitreous Carbon (RVC) (FLUORO CARBON, Process Systems Div., Anaheim, Cal.) as the working electrode. This is a glassy carbon material with pores of controlled number and size. It is available in several porosities, but the electrode employed in this experiment used RVC having 100 pores/inch. A thin slice (7-9 mm) of RVC approximately 11 mm x 30 mm is obtained and a very fine copper wire attached to one corner by burring away liquid organic silver (Engelhard, East Newark, N.J.). This leaves behind a residue of metallic silver which provides contact between the RVC and the copper wire. The silver is then coated with Tygon paint (Carboline K-63 white paint, Carboline Co., St. Louis, Mo.) to protect it from test solutions when the cell is in use. The RVC is then sandwiched between two quartz microscope slides (1"x2 1/4"x1/16") with RVC flish with the edge of the slides on one side and on the opposite side the corner with the copper wire attached is allowed to protrude approximately 5 mm. The two slides are then fastened together with two small spots of epoxy resin (Epoxi-Patch, The Dexter Corp., Olean, N.Y.). When the epoxy resin has cured a 1 cm length of 2mm I.D. glass tubing is attached to the top of the slides with Duro Super Glue 3 (Woodhill Chemical Sales Corp., Cleveland, Ohio). Next a 1 cm length of 22 gauge copper wire is bent in the middle at a 90° angle and one leg of the L thus formed is soldered to the fine copper wire attached to the RVC. The RVC is then adjusted to be approximately 7 mm above the bottom of

the cell. The L shaped copper wire is then placed on the protruding RVC. The wire is positioned such that one leg is perpendicular to the long axis of the quartz slides. The wire is then epoxied to the protruding RVC while the perpendicular leg is left uncoated so that it may be used later for electrical contact. Once this epoxy resin has cured the RVC is locked into place and the protruding RVC is protected from breakage by the epoxy coating. All edges except the bottom can then be safely sealed with epoxy resin and the resin allowed to cure.

Some gas chromatograms were performed with a Varian Aerograph series 2400 dual column gas chromatograph with flame ionization detectors. For coupled GC-mass spectral experiments a Hewlett-Packard series 5985 GC/MS was utilized.

Coulometric experiments utilized either a Wenking model LT 73 potentiostat or a PAR model 373 potentiostat to maintain a controlled potential. In order to measure the number of coulombs which have passed through the electrochemical cell a Koslow model 541 coulometer or a PAR model 379 digital coulometer was utilized.

Gravity flow liquid chromatographic systems utilized either a 100 cm x 2.5 cm Pharmacia column or a 45 cm x 2.5 cm Pharmacia column. The 100 cm x 2.5 cm columns were generally filled with 90 cm of resin. The resins used were Sephadex G-10, a gel permeation type packing, and Sephadex QAE A-25 anion exchange resin. Both were obtained from Pharmacia. A Gilson Model HM UV-Vis Holochrome detector set at 200 nm was used as the detector. The detector output was recorded on a Fisher Model 5000 stripchart recorder. The eluant

was collected after passing through the detector in 3 ml fractions by an ISCO Fraction Collector Controller Model 328.

High performance liquid chromatography utilized a Waters Associates system consisting of a Milton Roy mini-pump, Waters Associates model U6K injector, a Waters Associates Model 440 absorbance detector, and a Fisher Model 5000 stripchart recorder.

Procedures

Preliminary studies of the enzymatic oxidation of 8-hydroxyguanosine indicated that at the HRP concentrations used for the uric acid studies (i.e., 0.17 μM, see Chapter 3) the oxidation of 8-hydroxyguanosine was too slow at pH 7 or pH 4 to observe any intermediate. It was necessary to use approximately ten times higher HRP concentrations in order to obtain adequate oxidation rates.

The procedure which developed used 0.5 ml of a 15 μM HRP solution and 0.5 ml of 300, 150, or 30 μM 8-hydroxyguanosine solution, both in 0.5 M ionic strength buffer of the desired pH. The oxidation was initiated with 0.5 ml of 600 μM H_2O_2 solution, once again in 0.5 M ionic strength buffer of the desired pH. The oxidation was allowed to proceed for approximately 50 seconds then 1.5 ml of 0.5 M ionic strength buffer of the desired pH containing 0.3 mg of catalase was added to stop the oxidation. The absorbance was then measured as a function of time at 250 and 300 nm. Below pH 5.6 catalase was not sufficiently soluble that it could stop the oxidation. A review of the literature indicated sodium azide (NaN_3) was a good inhibitor of horseradish peroxidase, so it was tried at pH 4.6. The oxidation was

initiated as described previously, but in order to stop the reaction 1.5 ml of 0.5 M ionic strength pH 4.6 phosphate buffer containing 0.039 mg of NaN_3 was added. The rate constants obtained by this method agreed quite well with those obtained at higher pH, and the absorbance versus time curves were much less noisy than those obtained using catalase. At pH 4, however, the absorbance versus time curves suddenly flattened out making it impossible to determine any rate constants.

Test solutions utilized for thin-layer spectroelectrochemical studies ranged from 0.2-2.0 mM. The procedures used in thin-layer spectroelectrochemical studies of guanosine and 8-hydroxyguanosine were essentially the same as those in Chapter 2 except for differences arising from the different working electrode material and due to the use of a deuterium lamp a wider spectral region (200-400 nm) was scanned.

The RVC electrode required somewhat different treatment than the gold minigrid described in Chapter 2. First when a cell was initially assembled there was a problem with bubble formation. It was discovered that by using vacuum to pull approximately 100 ml of double distilled water through the cell all bubbles could be dislodged and the entire electrode surface wetted. Once the entire electrode was wet further bubble formation was uncommon and easily remedied by pulling a few milliliters of solution or water through the cell. The cells were stored wet in double distilled water in order to eliminate the bubble problem.

In early studies of guanosine and 8-hydroxyguanosine with the RVC thin-layer cells there was a severe problem with a lack of

reproducibility. Eventually it was noticed that the first run made after a cell had soaked over night was relatively consistent and each successive run without cleaning the cell gave larger and larger rate constants and smaller and smaller total absorbance changes. A series of cleaning procedures were attempted in which the cell was allowed to soak for various lengths of time from 15 minutes to 12 hrs. Ultimately the best procedure was to rinse the cell with approximately 15 ml of 0.1 M HNO_3 and 15 ml of 0.1 M NaOH. Then 250 ml of water were pulled through the cell and the cell was allowed to soak in water for at least 12 hours.

In the kinetic studies made both a fast and slow step were observed. In order to calculate the rate constant for the fast step it was first necessary to subtract the contribution of the slow step to the absorbance at the times where the fast step occurs. To do this the slope and intercept of the log $|A-A_\infty|$ versus time plot for the slow step are calculated. Knowing these it is possible to calculate the log $|A-A_\infty|$ values for the slow setp at times where the fast step is occurring. By taking the anti-log of the log $|A-A_\infty|$ one obtains the absorbance contribution of the slow step at that time. Then the absorbance due to the slow step is subtracted from the total absorbance to obtain the absorbance arising from the fast step. The log is then taken of this fast step absorbance to obtain log $|A-A_\infty|$ for the fast step. This is done at a series of times to generate a log $|A-A_\infty|$ versus time plot. From the slope of this plot the rate constant is then calculated.

The procedures and electrodes utilized for voltammetric

studies were the same as those discussed in Chapter 2.

In all voltammetric and coulometric studies at least three replicate runs were recorded. In the case of kinetic studies duplicate runs were made. Background runs were carried out for all experiments in exactly the same way except that no guanosine or 8-hydroxyguanosine was included.

SUMMARY

Detailed studies were carried out to investigate the electrochemical oxidation of guanosine and 8-hydroxyguanosine, and the enzymic oxidation of 8-hydroxyguanosine.

From these studies it is clear that the oxidation of guanosine and 8-hydroxyguanosine does not follow the scheme outlined in equation 1, at least not to any great degree. It is also clear, however, that at least to some extent that scheme is followed up to the formation of an imine-alcohol.

It was found that the intermediates which could be observed by u.v.-spectroscopy were the same for guanosine and 8-hydroxyguanosine. Further the RSS and kinetic studies showed the electrochemical and enzyamic oxidation of 8-hydroxyguanosine to proceed via the same process.

CHAPTER 5

REFERENCES

1. C. W. Steele, Opsucula, 2, 73 (1776).

2. R. K. Robins, Heterocyclic Compounds, 8, 162 (1967).

3. Marcet, "An Essay on the Chemical History and Medical Treatment of Calculous Disorders," London, 1817, pp. 95-107 (cited in Robins[2]).

4. E. Fischer, Ber. Dtsch. Chem. Ges., 17, 329 (1884).

5. E. Fischer, Ber. Dtsch. Chem. Ges., 30, 558 (1897).

6. G. Dryhurst, Electrochemistry of Biological Molecules, Academic Press, New York, 1977, pp. 1-5.

7. R. S. Nicholson and I. Shain, Anal. Chem., 36, 706 (1964).

8. J. Pech, Collect. Czech. Chem. Commun., 6, 126 (1934).

9. J. C. Heath, Nature, 158, 23 (1946).

10. D. Hamer, D. M. Waldron, D. L. Woodhouse, Arch. Biochem. Biophys., 47, 272 (1953).

11. D. L. Smith and P. J. Elving, J. Am. Chem. Soc., 84, 1412 (1962).

12. R. N. Adams, Electrochemistry of Solid Electrodes, Marcel Dekker, Inc., New York, 1969, pp. 19-42.

13. A. L. Beilby, W. Brooks, and G. L. Lawrence, Anal. Chem., 36, 22 (1964).

14. F. J. Miller and H. E. Zittel, Anal. Chem., 35, 1866 (1963).

15. L. Chuang, I. Fried, and P. J. Elving, Anal. Chem., 36, 2426 (1964).

16. R. E. Panzer and P. J. Elving, J. Electrochem. Soc., 119, 864 (1972).

17. G. Dryhurst, Anal. Chim. Acta, 57, 137 (1971).

18. D. Keilin and E. F. Hartree, Proc. R. Soc. London, Ser. B, 119, 114 (1936).

19. R. Bentley and A. Neuberger, Biochem. J., 52, 694 (1952).

20. K. Agner, Acta Physiol. Scand., Suppl., 8, 5 (1941).

21. K. Agner, Acta Chem. Scand., 12, 89 (1958).

22. K. C. Paul and Y. Avi-Dor, Acta Chem. Scand., 8, 637 (1954).

23. E. S. Canellakis, A. L. Tuttle, and P. P. Cohen, J. Biol. Chem., 213, 397 (1955).

24. R. R. Howell and J. B. Wyngaarden, J. Biol. Chem., 235, 3544 (1960).

25. G. Soberon and P. P. Cohen, Arch. Biochem. Biophys., 103, 331 (1963).

26. T. Matsuura and I. Saito, Chem. Commun., 693 (1967).

27. T. Matsuura and I. Saito, Tetrahedron, 24, 6609 (1968).

28. M. I. Simon and H. Van Vanukis, Arch. Biochem. Biophys., 105, 197 (1964).

29. K. Zenda, M. Saneyoshi, and G. Chihara, Chem. Pharm. Bull., 13, 1108 (1965).

30. E. C. B. Anmann and V. H. Lynch, Biochem. Biophys. Acta, 120, 181 (1966).

31. J. Holian and W. M. Garrison, J. Phys. Chem., 71, 462 (1967).

32. J. Holian and W. M. Garrison, Chem. Commun., 676 (1967).

33. F. Fichter and W. Kern, Helv. Chim. Acta, 9, 429 (1926).

34. D. L. Smith and P. J. Elving, Anal. Chem., 34, 930 (1962).

35. W. A. Struck and P. J. Elving, Biochemistry, 4, 1343 (1965).

36. G. Dryhurst, J. Electrochem. Soc., 119, 1659 (1972).

37. G. Dryhurst, Electrochemistry of Biological Molecules, Academic Press, New York, 1977, p. 130.

38. G. Dryhurst, Top. Curr. Chem., 34, 47 (1972).

39. G. Dryhurst, J. Electrochem. Soc., 116, 1411 (1969).

40. B. H. Hansen and G. Dryhurst, J. Electroanal. Chem., 30, 417 (1971).

41. R. Brdicka and E. Knoblock, Z. Elektrochem., 47, 721 (1941).

42. J. R. Merkel and W. J. Hickerson, Biochim. Biophys. Acta, 14, 303 (1954).

43. J. J. Lingane and O. L. Davis, J. Biol. Chem., 137, 567 (1941).

44. J. Pinson and J. Armand, Collect. Czech. Chem. Commun., 36, 585 (1971).

45. S. Kwee and H. Lund, Acta Chem. Scand., 25, 1813 (1971).

46. P. Zuman, Chem. Listy, 46, 688 (1952).

47. P. L. Pickard and S. H. Jenkins, J. Am. Chem. Soc., 75, 5899 (1953).

48. L. Holleck and B. Kastening, Z. Elektrochem., 60, 127 (1956).

49. M. I. Simon and H. Van Vanukis, Arch. Biochem. Biophys., 105, 197 (1964).

50. B. M. Visinski and G. Dryhurst, J. Electroanal. Chem., 70, 199 (1976).

51. J. L. Owens and G. Dryhurst, J. Electroanal. Chem., 80, 171 (1977).

52. G. Dryhurst and P. K. De, Anal. Chem. Acta, 58, 183 (1972).

53. W. V. Childs, J. T. Maloy, C. P. Keszthelyi, and A. J. Bard, J. Electrochem. Soc., 118, 874 (1971).

54. R. W. Murray, W. R. Heineman, and G. W. O'Dom, Anal. Chem., 39, 1666 (1967).

55. W. R. Heineman, B. J. Norris, and I. F. Goelz, Anal. Chem., 47, 79 (1975).

56. G. Dryhurst, M. Rosen, and P. J. Elving, Anal. Chem. Acta, 42, 143 (1968).

57. R. N. Adams, Electrochemistry at Solid Electrodes, Marcel Dekker, Inc., New York, 1969, p. 207.

58. G. Dryhurst, Electrochemistry of Biological Molecules, Academic Press, New York, 1977, pp. 71-185.

59. J. L. Owens, H. A. Marsh, and G. Dryhurst, J. Electroanal. Chem., 91, 231 (1978).

60. B. J. Davis, Ann. N.Y. Acad. Sci., 121, 404 (1964).

61. R. H. Wopschall and I. Shain, Analytical Chemistry, 39, 1514 (1967).

62. G. Dryhurst and G. F. Pace, J. Electrochem. Soc., 117, 1259 (1970).

63. M. T. Cleary and G. Dryhurst, submitted for publication.

64. V. E. Norvell and G. Mamantov, Anal. Chem., 49, 1470 (1977).

65. M. T. Cleary and G. Dryhurst, Anal. Chim. Acta, 94, 343 (1977).

66. G. Hunter, Biochem. J., 30, 1183 (1936).

67. R. E. Holmes and R. K. Robins, J. Am. Chem. Soc., 87, 1772 (1965).